KU LEUVEN

FACULTEIT INGENIEURSWETENSCHAPPEN

Onderzoek naar de voordelen van geavanceerd legering-gebaseerd sorteren van aluminiumschroot

Simon Van den Eynde

Thesis voorgedragen tot het behalen van de graad van Master of Science in de ingenieurswetenschappen: werktuigkunde

Promotor:
Prof. Dr. Ir. Joost Duflou

Assessoren:
Ir. Yannick Carette
Dr. Ir. Ann Witvrouw

Begeleiders:
Ir. Ellen Bracquene
Dr. MSc. Ing. Jef Peeters

Academiejaar 2019 – 2020

Preface

There are many people who I should thank for supporting me in writing this thesis. I would like to thank Jonas Petersson, Mélina Gilbert Gatty, Louise Hagesjö, and the other colleagues at Swerim for being kind and helpful during my internship. Without their help and guidance, it would have been impossible to perform the LIBS measurements for my thesis.

I also want to thank Vincent, Dillam, and Sam for helping me clean and measure the samples for the XRF analysis. Without their help, it would have taken me many hours extra to get all the desired measurements. I also owe my thanks to Dillam for reading my thesis and giving me valuable advice on a large number of issues.

Thanks to the employees of Galloo and Norsk Hydro, I was able to assess which output fractions could be valuable to separate from the mixed aluminium scrap in the Twitch fraction of Galloo.

I have of course also great gratitude for Ellen Bracquene and Jef Peeters, who have constantly guided me in the past year and have given up a lot of their time to help me achieve better results. I want to thank them for their clear communication, great advice, and encouragements that enabled me to write this thesis.

Last but not least, I want to thank my friends and family, who always support me in whatever I do. I want to thank them for listening to me when I was talking passionately about scrap. They are a great source of motivation and I appreciate everything they do for me.

To whoever reads this thesis, I hope you find it interesting.

Simon Van den Eynde

Table of Contents

Abstract

This thesis investigates the benefits and the challenges related to alloy-based sorting of aluminium scrap. Significant quality losses are involved in the current recycling method of aluminium. As a result, recycled aluminium typically has a low purity and contains a wide range of alloying and tramp elements. Therefore, recycled aluminium is currently mostly used for the production of cast alloys, which have high tolerances for impurities. For the production of wrought alloys, recycled aluminium can only be used to a very limited extent, since these alloys have much lower tolerances for impurities. Due to the sharp rise in the amount of aluminium scrap that is collected for recycling every year, and the limited demand for low-purity recycled aluminium, it is expected that an aluminium scrap surplus will emerge in the coming decade. This is an amount of collected scrap that cannot be absorbed, neither by the wrought nor the cast alloys.

In this thesis, a global Material Flow Analysis (MFA) model is developed to get a better idea on the size and composition of several global aluminium flows, and how these evolve over time. According to the developed model, an aluminium scrap surplus will emerge in 2023, grow to a size of 5,4 million tons by 2030, and reach a size of 8,7 million tons by 2040, if no additional measures are taken to avoid it.

Since recycling aluminium is significantly less harmful for the environment than the production of primary aluminium, a scrap surplus should be avoided. By applying alloy-based sorting methods, the collected aluminium scrap can be sorted into different scrap categories, resulting in a higher volume of collected scrap that can be used for the production of wrought alloys. By enabling more wrought-to-wrought recycling, alloy-based sorting strategies can significantly reduce the size of the scrap surplus in the future, while lowering the environmental burden of wrought alloy production.

Using alloy-based sorting methods to separate wrought alloys from the rest of the collected aluminium scrap is not only beneficial for the environment but can also be interesting from an economic perspective for recycling companies, since sorted aluminium with a characterised composition can be sold at a significantly higher price than mixed aluminium scrap. In this thesis, several potential sorting strategies are investigated for a Belgian metal recycling facility. The composition of the collected aluminium scrap in this facility is measured using two spectroscopy-based characterisation techniques: X-ray fluorescence (XRF) and Laser Induced Breakdown Spectroscopy (LIBS). Based on the results of the measurements, it is estimated that up to 50% of the investigated scrap could be separated for the production of wrought alloys. According to the developed MFA model, separating 14,7% of the globally collected aluminium scrap for the production of wrought alloys would be enough to avoid a scrap surplus in 2030. In 2040, it would be necessary to separate 17,6% of the globally collected scrap.

Alloy-based sorting can yield large benefits but there are also some difficulties due to which these enhanced sorting methods are not yet commonly implemented in existing recycling facilities. This thesis explains which problems are encountered during the XRF and LIBS measurements and offers some possible solutions to overcome these problems.

Samenvatting

Deze thesis onderzoekt de voordelen en uitdagingen gerelateerd aan het legering-gebaseerd sorteren van aluminiumschroot. De huidige recyclagemethode van aluminium gaat gepaard met aanzienlijke kwaliteitsverliezen. Hierdoor heeft gerecycleerd aluminium vaak een lage zuiverheid en bevat het veel verschillende legeringselementen en andere onzuiverheden. Daarom wordt gerecycleerd aluminium tegenwoordig vooral gebruikt voor de productie van gietlegeringen, die een hoge tolerantie hebben voor onzuiverheden. Voor de productie van kneedlegeringen kan gerecycleerd aluminium maar in zeer beperkte mate gebruikt worden, aangezien deze legeringen veel lagere limieten hebben voor onzuiverheden. Door de snelle toename van de hoeveelheid aluminiumschroot die jaarlijks ingezameld wordt voor recyclage en de beperkte vraag naar gerecyleerd aluminium met een lage zuiverheid, wordt verwacht dat het komende decennium een schrootoverschot ontstaat. Dit is een hoeveelheid ingezameld schroot die noch door de gietlegeringen, noch door de kneedlegeringen geabsorbeerd kan worden.

In deze thesis is een MFA model ontwikkeld om een beter idee te krijgen van de grootte en de samenstelling van verschillende globale aluminiumstromen en hoe deze evolueren doorheen de tijd. Volgens het ontwikkelde model zal een schrootoverschot zich voor het eerst voordoen in 2023, waarna het groeit tot een grootte van 5,4 miljoen ton in 2030 en 8,7 miljoen ton in 2040, tenzij bijkomende maatregelen genomen worden om het te vermijden.

Aangezien het recycleren van aluminium aanzienlijk minder schadelijk is voor het milieu dan de productie van primair aluminium, is het beter een schrootoverschot te vermijden. Door legering-gebaseerde sorteermethodes toe te passen, kan het ingezamelde aluminiumschroot zodanig gesorteerd worden dat meer schroot gebruikt kan worden voor de productie van kneedlegeringen. Door een deel van het schroot te gebruiken voor de productie van kneedlegeringen, kan in de toekomst de grootte van het schrootoverschot aanzienlijk verkleind worden.

Legering-gebaseerde sorteermethodes gebruiken om kneedlegeringen te scheiden van de rest van het ingezamelde schroot is niet enkel voordelig voor het milieu. Het kan ook vanuit een economisch perspectief interessant zijn voor de recyclagebedrijven, aangezien zinvol gesorteerd aluminium verkocht kan worden aan een aanzienlijk hogere prijs dan ongesorteerd aluminiumschroot. In deze thesis worden verschillende potentiële sorteerstrategieën onderzocht voor een Belgisch recyclagebedrijf. De samenstelling van het ingezamelde schroot in dit bedrijf is gemeten met twee spectroscopische karakterisatiemethodes: XRF en LIBS. Gebaseerd op de resultaten van deze metingen wordt geschat dat 50% van het onderzochte schroot uitgesorteerd zou kunnen worden voor de productie van kneedlegeringen. Volgens het ontwikkelde MFA model zou 14,7% van het wereldwijd ingezamlede schroot uitgesorteerd moeten worden voor de productie van kneedlegeringen om een schrootoverschot in 2030 te vermijden. In 2040 zou 17,6% van het wereldwijd ingezamelde schroot moeten worden uitgesorteerd.

Legering-gebaseerd sorteren kan grote voordelen opleveren, maar er zijn ook moeilijkheden mee gemoeid, die verklaren waarom deze sorteermethodes nog niet zijn doorgedrongen in de meeste recyclagebedrijven. Deze thesis legt de problemen uit waar metingen met XRF en LIBS momenteel mee kampen, en geeft enkele mogelijke oplosingen voor deze problemen.

List of Figures

List of Tables

Nomenclature

ABAL	Brazilian Aluminum Association
ABRALATAS	Brazilian Association of Highly Recyclable Cans Manufacturers
ANSI	American National Standards Institute
CAIAMA	Argentine Chamber of the Aluminum and Related Metals Industry
CCD	Charge Coupled Device
CMI	Can Manufacturers Institute
EAA	European Aluminium Association
ELV	End-of-Life Vehicles
EMS	Electromagnetic Sensors
EOL	End-of-Life
EPA	Environmental Protection Agency
EV	Electric Vehicles
FWHM	Full Width at Half Maximum
HEV	Hybrid Electric Vehicles
HPA	High Purity Aluminium
IAI	International Aluminium Association
ICEV	Internal Combustion Engine Vehicles
IEA	International Energy Agency
LCA	Life Cycle Assessment
LCC	Life Cycle Costing
LIBS	Laser Induced Breakdown Spectroscopy
MFA	Material Flow Analysis
NIST	National Institute for Standards and Technology
OEA	Organisation of European Aluminium Refiners and Remelters
OPGW	Optical Ground Wire
PAH	Polycyclic Aromatic Hydrocarbons
PCB	Printed Circuit Boards
PGNAA	Prompt Gamma Neutron Activation Analysis
UBC	Used Beverage Cans
UN	United Nations
WEEE	Waste Electric and Electronic Equipment
XRF	X-Ray Fluorescence
XRT	X-Ray Transmission

1 Introduction

1.1 Context

Public concerns about the sustainability of the world's rapid economic development have been growing for decades. Since the earliest estimates of the United Nations in 1950, the global population has more than doubled from less than 3 billion people to 7,7 billion people in 2019 [1]. In the same period, global GDP has skyrocketed due to rapid economic development and increased industrialisation. Although this development has drastically improved living conditions in most parts of the world, there are also negative effects that can be linked to it. Increased demand for goods and services, such as food, housing and mobility has led to the exploitation of the planet's natural resources at a pace that threatens to endanger the quality of life of future generations.

As a reaction to the growing public concerns, governments from around the globe have pledged in the Paris Agreement to increase their efforts in the fight against global warming [2]. With the European Green Deal, the countries of the European Union even agreed upon a strategy for the transition towards a competitive, fair and circular economy that should become climate neutral by 2050 [3]. In the communication report of the European Green Deal, there is a strong focus on the way that materials are currently managed in the European economy. The reason for this specific focus is explained by the report itself; stating that about half of total greenhouse gas emissions and more than 90% of biodiversity loss and water stress come from resource extraction, processing of materials and the production of fuels and food.

In order to achieve the ecological goals of the European Commission, it is clear from these statistics that a serious change is needed in the way materials are managed. To boost the market of secondary raw materials, the European Commission is considering legal requirements, such as mandatory limits of recycled content in the composition of certain materials. In addition, the commission is looking for new waste collection models and is revisiting rules on waste shipments to countries outside Europe. The objective of these measures is to contribute to the establishment of a more circular European economy. Apart from the ecological benefits of these measures, the European Commission also sees strategic opportunities in exporting less and recycling more waste, as well as in the valorisation outside of Europe of the technologies developed for this purpose. This new method of managing materials could ensure the supply of sustainable raw materials, in particular of critical raw materials necessary for clean technologies in digital, transportation, construction, energy, space and defence applications.

One of the crucial bottlenecks in the transition towards a circular economy is the limited ability of current state-of-the-art recycling technologies to convert waste into high value materials. The recycling of metals and plastics is at the moment characterised by substantial quality losses due to a decrease in purity and a degradation of the material properties during the recycling process. In order to minimise these quality losses, new recycling and sorting technologies are being developed for the most relevant waste streams.

This thesis focusses on recycling aluminium, a non-ferrous metal that is already collected and recycled intensively because of its high value. Recycling aluminium offers large opportunities, both environmentally and economically, but it also involves some serious challenges. This thesis explores the most critical challenges and looks for possible solutions, to help pave the way to a more sustainable use of aluminium.

1.2 Rationale for Recycling

The demand for aluminium has increased drastically since the middle of the previous century. As the global population has grown and the standard of living has risen significantly, companies worldwide

have increasingly made use of aluminium to manufacture their products. At the moment, aluminium is the second most produced metal, only preceded by steel. It is produced even more than all other non-ferrous metals combined [4]. Its light weight, high strength, good corrosion resistance and high conductivity make aluminium an attractive choice for many products, including food packaging, car parts, airplane components and building features. The good strength-to-weight ratio of aluminium has led to significant weight reductions in the automotive and aerospace sector. This way, aluminium saves large amounts of fuel in the use phase of cars, trucks, and planes [5]. However, aluminium production itself remains extremely harmful for the environment. In 2013, primary aluminium production was responsible for 3,5% of the total electricity consumption worldwide and 1% of the global CO_2 emissions [4]. Since then, the use of aluminium has only increased. In the past two decades, the demand for aluminium has grown faster than that for any other popular metal, growing at a significantly faster rate than the global GDP (see Figure 1.1) [6]. In order to reduce the ecologic impact of the aluminium industry, companies and policy makers increasingly focus on recycling as a potential solution.

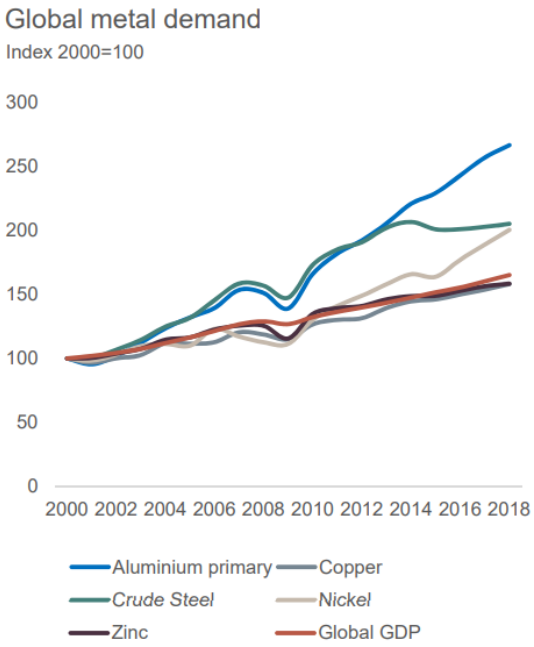

Figure 1.1: Global Metal Demand [6]

While recycling is generally regarded as ecologically beneficial, the possible energy savings by recycling are particularly high for aluminium, when compared to other common metals and plastics. A simple eco audit in CES Edupack, a software package that holds an extensive materials database, shows that the primary production of aluminium requires significantly more energy than other common metals and plastics such as copper, low carbon steel, polyethylene, polypropylene, polyamide, and polylactide (see Figure 1.2) [7]. At the same time, the recycling process of aluminium has an embodied energy that is very similar to that of other that of other common materials. The reported energy savings of recycling aluminium differ from source to source, but some put the required energy of aluminium recycling as low as 5% of the energy needed to produce the same amount of primary aluminium [8] [9].

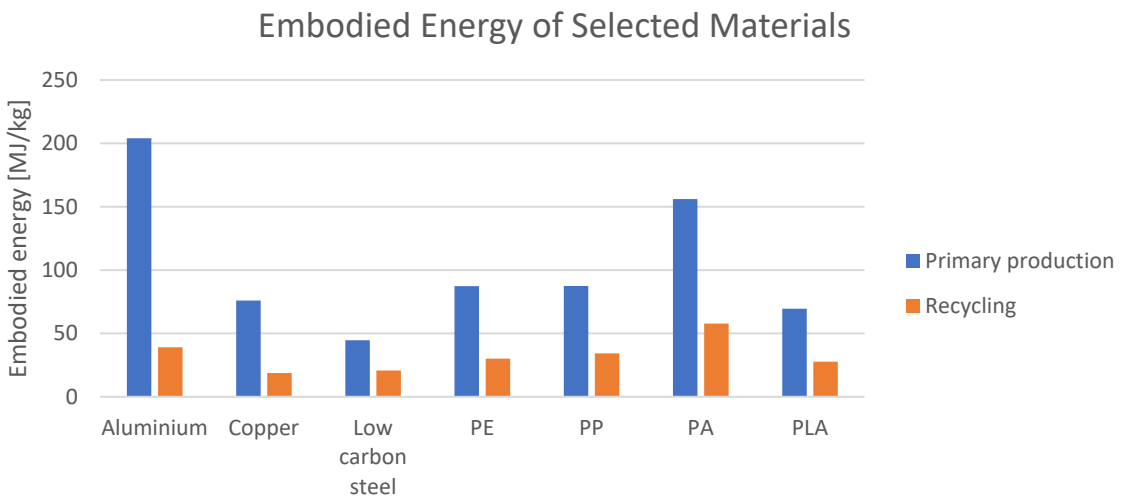

Figure 1.2: Embodied Energy of Selected Materials [7]

Recycled, or "secondary", aluminium also has a significantly lower impact than primary aluminium when it comes to environmental issues such as toxicity, acidification, greenhouse gas emissions and resource depletion [9] [10]. Compared to the primary production process, recycling leads to 85% less solid waste, 95% less CO_2 emissions, 99% less CO emissions and almost eliminates the emissions of polycyclic aromatic hydrocarbons (PAH). Figure 1.3 gives a graphical overview of some of the largest differences in the environmental impact of primary and secondary aluminium.

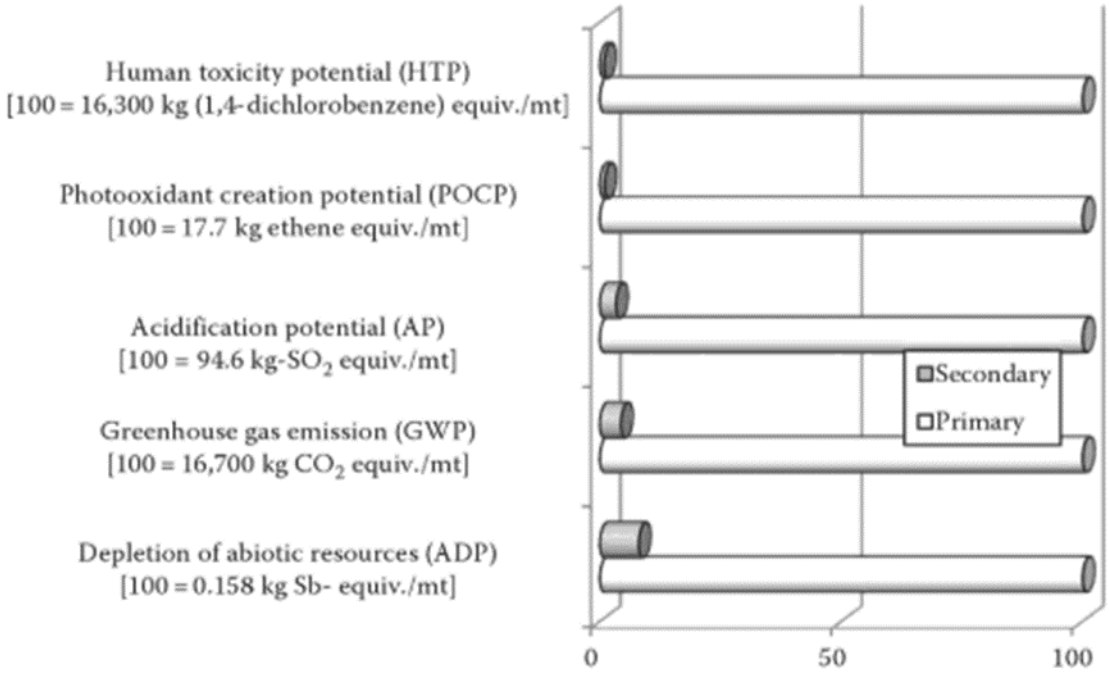

Figure 1.3: Environmental Impact of Primary and Secondary Aluminium [10]

In addition, aluminium mining activities are responsible for considerable biodiversity loss and water stress. The extraction is even more harmful than for most other metals since it involves significant amounts of waste. Aluminium only occurs in nature in the form of bauxite, an ore that consists of

aluminum oxide compounds, silica, iron oxides and titanium dioxide [11]. To produce 1 kg of aluminium, approximately 5,5 kg of bauxite has to be mined [12]. In order to convert bauxite into aluminium, the material must undergo chemical refinement and a Hall-Héroult electrolytic reduction process. These steps are characterised by a high energy consumption and the generation of high amounts of waste products. Numbers of the IAI shed light on the exact amounts of generated waste (see Figure 1.4): in 2018, 337 million tons of bauxite had to be extracted to produce only 66 million tons of primary aluminium [13]. Consequentially, 209 million tons of bauxite residue and wastewater were generated, resulting in substantial damage to the local ecosystems and the environment.

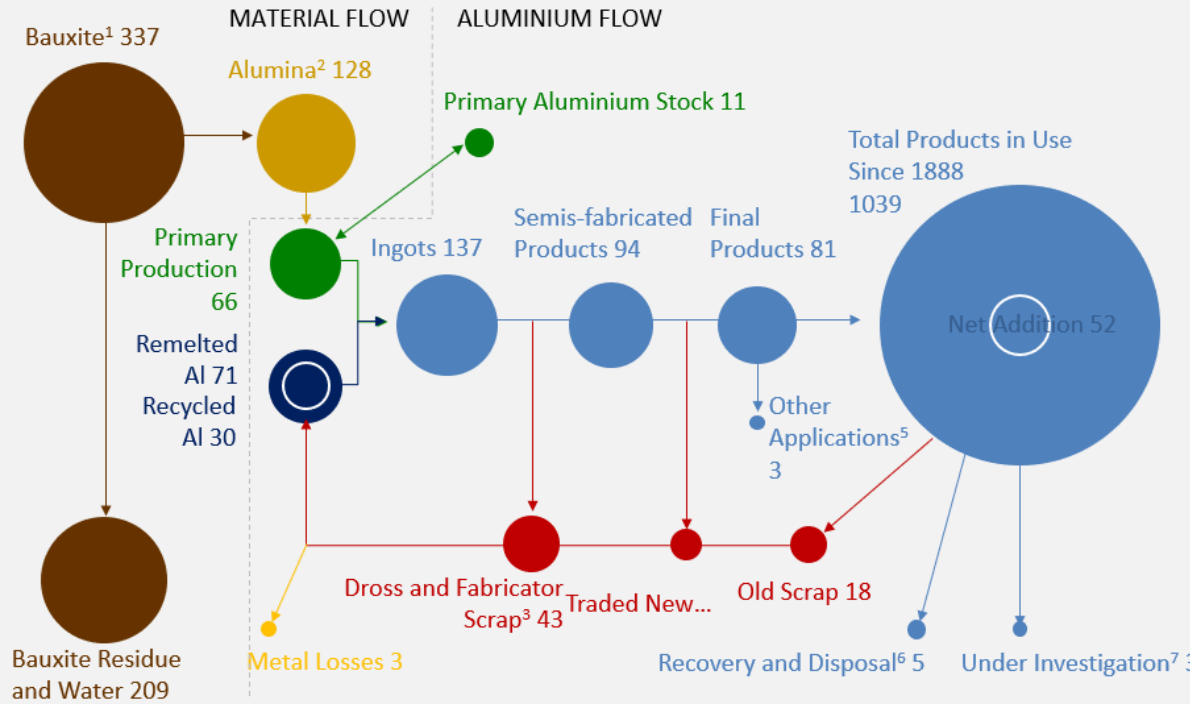

Figure 1.4: Material Flows Involved in the Production of Aluminium [13]

The combination of all the environmental issues related to the extraction and production of primary aluminium justifies the prominent position of aluminium in the research field of sustainable materials management. The particularly large environmental benefits of aluminium recycling have given researchers and policy makers major incentives to thoroughly investigate both technological and legislative methods to boost the use of secondary aluminium.

The European Aluminium Association (EAA), the organisation that represents the European aluminium industry, forecasts a rise in the share of recycled aluminium in European end-use products from 26% in 2000 to 49% in 2050 (see Figure 1.5) [14]. In its “VISION 2050” report, the EAA explains that this is an ambitious but realistic evolution that will result in a large contribution from the aluminium industry to the European efforts to decarbonise the economy. The largest obstacle to achieve such high recycled content for aluminium products is not the availability of aluminium scrap, according to the EAA. Rather, the main issue is the need for improved collection and sorting infrastructure to ensure that the large amounts of aluminium in end-use products do not go to landfill.

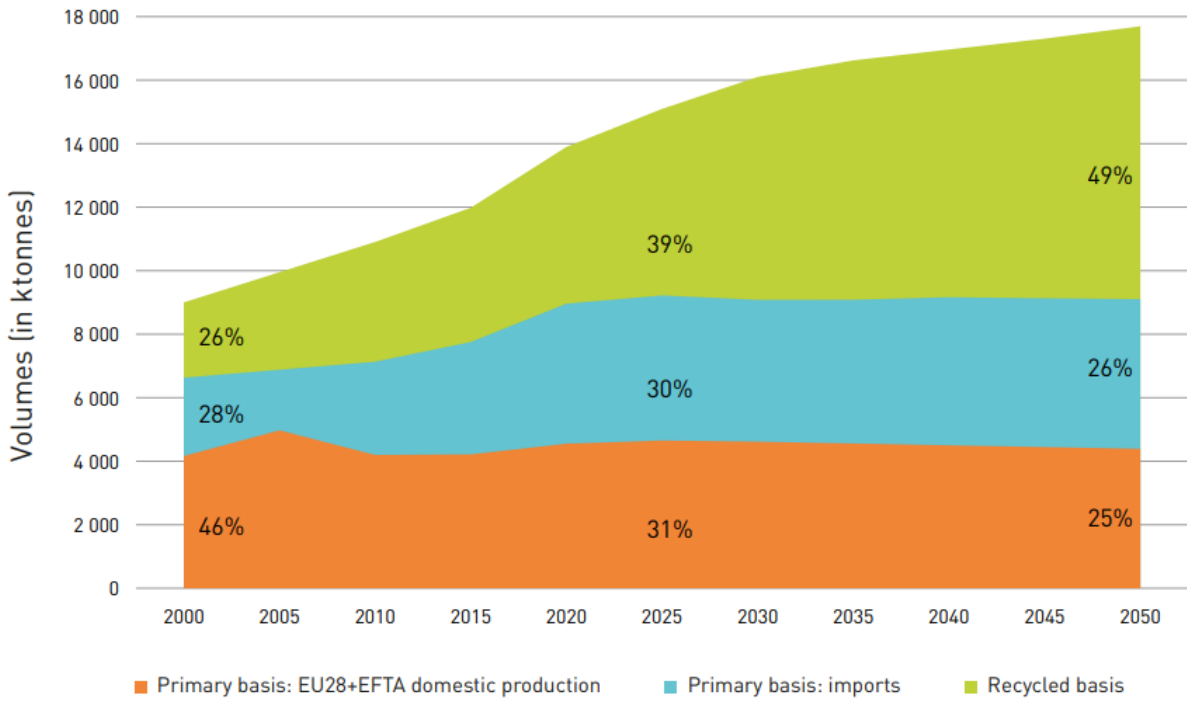

Figure 1.5: Share of Recycled Aluminium in European End-Use Applications [14]

1.3 Wrought and Cast Alloys

While recycling aluminium clearly is an excellent way to curb emissions, technological and economic constraints still limit the potential to reduce the global dependency on primary aluminium. The limited purity of recycled aluminium, due to the complex inclusion of a variety of alloying and tramp elements, is a serious obstacle in the production of new aluminium alloys. The most important alloying elements in aluminium alloys are magnesium, manganese, zinc, copper, and silicon. These elements provide the aluminium with desirable properties like stiffness, strength, and corrosion resistance. Iron is also often present in aluminium alloys, but this is mostly as a tramp element. A tramp element is a contaminant that does not contribute to the desirable qualities of a material. The tolerance for iron and other tramp elements varies significantly between the different aluminium alloys.

Two major categories of aluminium alloys exist: wrought alloys and cast alloys. While alloying elements and tramp elements can constitute up to 20% of the mass of a cast alloy, their presence is usually restricted to 10% of the total mass for wrought alloys [15]. Both categories are further divided into alloy series. The series number of an aluminium alloy indicates the most important alloying element(s) for that specific alloy. For wrought alloys, there are eight different alloy series with each their typical alloying elements. As demonstrated in Figure 1.6, the typical alloying elements are copper for the 2000 series, manganese for the 3000 series, silicon for the 4000 series, magnesium for the 5000 series, both silicon and magnesium for the 6000 series and zinc for the 7000 series. The 1000 series alloys consist almost entirely of aluminium and the 8000 series is a collection of miscellaneous alloys. For cast alloys, there is a similar division in different alloy series but since the tolerances for impurities are much higher for these alloys and since only a handful of cast alloys is actually produced intensively, this division is less relevant for sorting.

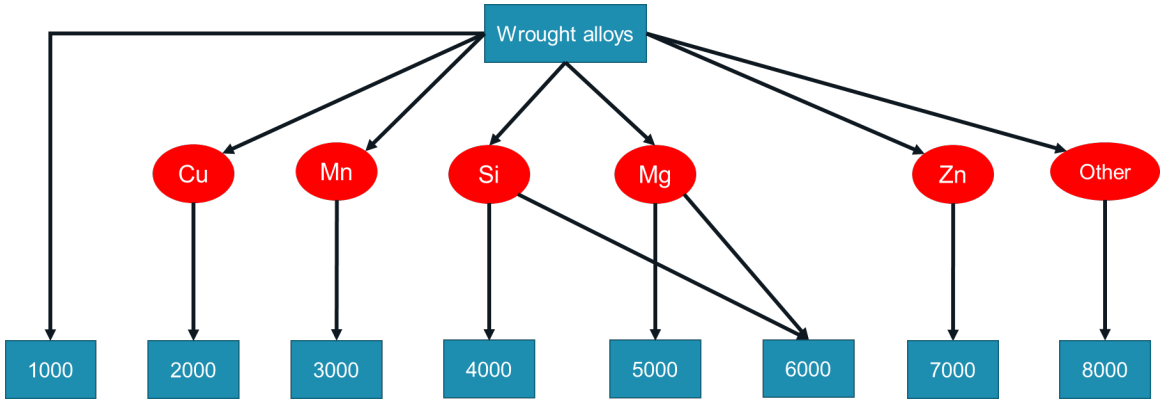

Figure 1.6: Wrought Alloy Series and Main Alloying Elements

As different alloys from different end-use products often arrive at recycling facilities unseparated, the collected aluminium scrap contains high concentrations of all alloying elements and tramp elements. Therefore, aluminium scrap cannot be used directly for the production of wrought alloys. The only way to make wrought aluminium products from recycled aluminium is to upgrade the quality of the collected aluminium scrap by diluting it with primary aluminium and adding the desired alloying elements (see Figure 1.7) [15].

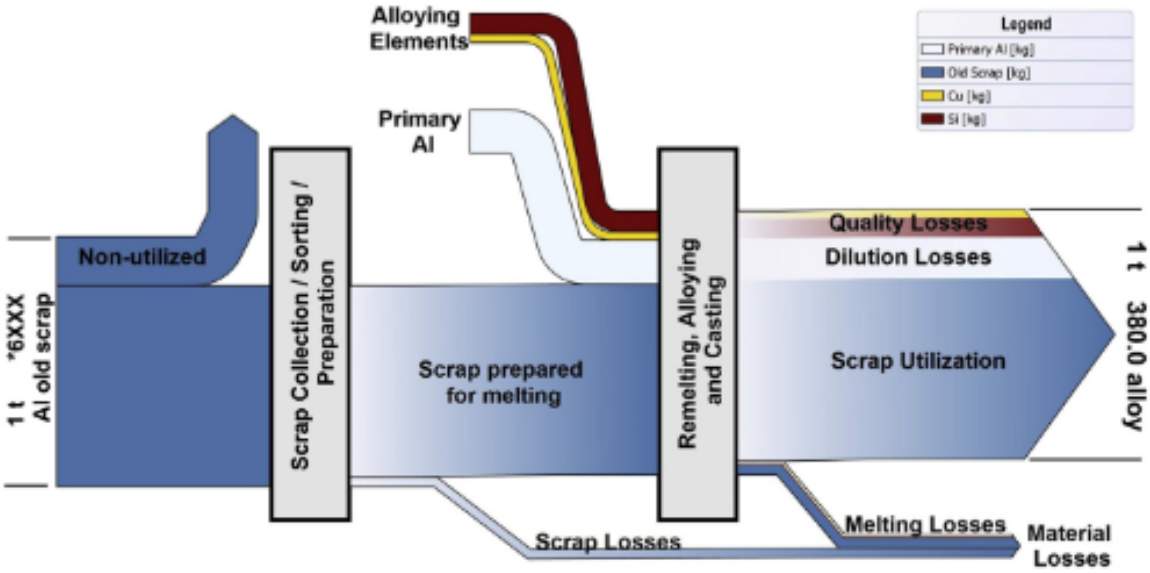

Figure 1.7: Aluminium Dilution Process and Associated Losses [15]

As an alternative to diluting, an electrolytic process, commonly referred to as the Hoopes process, is used in very specific cases to purify aluminium by removing magnesium, manganese, silicon, iron, zinc, copper, and chromium. However, since this process requires even more energy than the primary production process of aluminium (17-18 kWh/kg compared to 14 kWh/kg), it is not a possible large scale solution for the challenges in the recycling industry [8].

At the moment, only a limited amount of recycled aluminium is diluted for the production of wrought alloys. Using recycled aluminium for the production of cast alloys is more convenient since recycled scrap can constitute 99,3wt% of these alloys, requiring only 0,7wt% of primary aluminium and alloying elements [15]. Typical cast alloy applications include engine blocks and cylinder heads for combustion engines [16]. Outside the transportation sector, the number of applications for cast alloys is quite limited [17]. Since there is a clear quality loss involved in the recycling process of aluminium products,

often the term “downcycling” is used instead of “recycling”. The cascading nature of the current way of recycling aluminium, is illustrated in Figure 1.8 [15].

Figure 1.8: Cascading Recycling Chain of Aluminium [15]

This aluminium recycling scheme is under pressure though, as the balance between supply and demand of secondary aluminium is at a tipping point. The amount of collected scrap increases year by year, almost everywhere in the world, while the demand for cast alloys will likely stagnate in the nearby future (see Figure 1.9) [16] [18] [19] [20] [21]. The reason for the stagnating demand for cast alloys is the forecasted rise in the share of electric vehicles in the global car fleet.

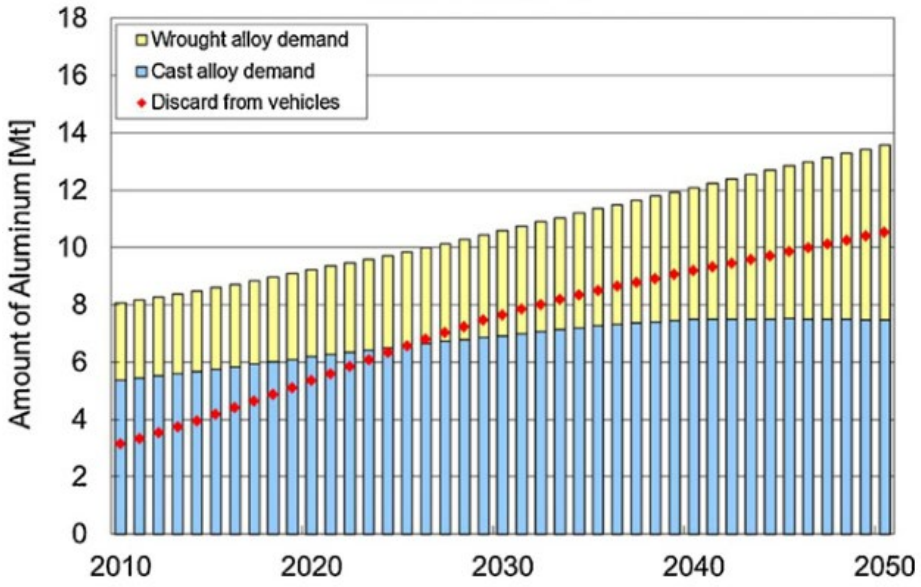

Figure 1.9: Evolution of the Demand for Wrought and Cast Alloys in Passenger Cars [20]

The expectation that hybrid electric vehicles (HEV) and electric vehicles (EV) will quickly replace vehicles with internal combustion engines (ICEV) in the United States, Europe and Japan, exists already quite some time [20]. More recent sources indicate that the rapid penetration of electric vehicles will not only take place in the mentioned developed countries, but also in China and the rest of the world (see Figure 1.10) [22]. In hybrid vehicles, both wrought and cast alloys are used intensively for the production of the same components as in conventional vehicles. In electric vehicles on the other hand, cast alloys are used to a much lesser extent since they have no internal combustion engine. The use of cast alloys in electric vehicles might even be only 50% of what is used in today's typical gasoline cars [23]. Instead, electric vehicles have a power-supply box that is partly made from wrought aluminium alloys, as such increasing their share in the total mass of the car. In addition, wrought alloys are expected to be used in increasing amounts to produce lighter frames for passenger cars. So, in the new generations of cars, the use of wrought alloys will increase while the use of cast alloys will fall.

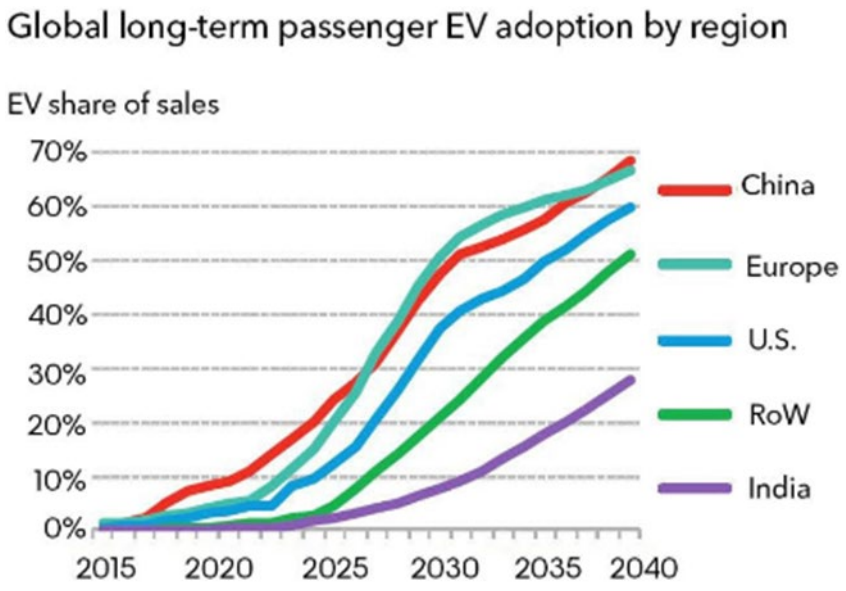

Figure 1.10: Global Long-Term Passenger EV Adoption by Region [22]

This evolution will soon result in a situation where the transportation sector is a net producer of secondary aluminium, rather than a net consumer, as it is today. Aluminium scrap from other sectors will therefore no longer be absorbed by automotive castings. Given the fact that at the moment, the transportation sector overwhelmingly dominates the market demand for cast alloys (73% of all cast aluminium is used in the transportation sector in Western Europe), the number of alternative destinations for low-purity recycled aluminium is very limited [15].

Since the amount of collected aluminium scrap will keep increasing rapidly in the near future and the demand for cast aluminium alloys will not grow accordingly, multiple sources indicate that a scrap surplus of aluminium will soon emerge. This is an amount of scrap that cannot be absorbed by cast alloys due to an oversupply, and that cannot be accepted for the production of wrought alloys based on quality concerns. As such, the aluminium becomes unrecyclable. Without measures to increase the quality of the recycled aluminium, a global scrap surplus is projected to emerge in the coming decade [16]. The two research groups that have investigated this possibility most thoroughly are the Norwegian research group of Modaresi et al. and the Japanese research group of Hatayama et al. According to Modaresi et al., the global scrap surplus will already amount to 4,2 million tons in 2030 [16]. Hatayama et al. put the estimated size of the global scrap surplus on 6,1 million tons in 2030 [20].

In some countries, like Spain, scrap surpluses are already emerging. Spain has recently become a net exporter of aluminium scrap and according to forecasts, the amount of exported scrap will steadily increase in the near future [24]. While most Spanish scrap used to be exported to European countries (88% in 1995), the country now exports its excess scrap mostly to Asian countries. This trend is another indicator that most countries in Europe are dealing with a (near) scrap surplus already. While Spain exports its excess aluminium scrap, imports of primary aluminium into Spain are increasing. This paradoxical situation has arisen, as Spanish manufacturing companies cannot use the locally generated mixed aluminium scrap to make their high quality products. These opposite shipments of primary and secondary aluminium significantly diminish the ecological advantages of recycling and result in a serious economic loss.

An appropriate strategy to avoid scrap surpluses in the future is to recycle aluminium in a way that it can be used to answer the demand for both wrought and cast alloys. Alloy based sorting methods can be a solution to enable wrought-to-wrought recycling. With such methods, it is possible to sort a complex scrap mix of different aluminium alloys into different subcategories of scrap with a more uniform composition. If the aluminium scrap is sorted in strategically chosen categories that each contain only a small variety of alloying elements, it is possible to use recycled aluminium to a much larger extent for the production of wrought alloys. As such, enhanced alloy based sorting can eliminate the threat of a scrap surplus and significantly raise the value of recycled aluminium.

1.4 Sorting Capabilities of State-of-the-Art Recycling Facilities

Currently, in state-of-the-art industrial aluminium recycling processes, the first step after product-specific pre-treatment of the incoming waste is size reduction by shredding. All waste that enters the recycling facility and is not dismantled or separated for direct reuse, undergoes this size reduction to facilitate the further sorting steps and involved logistics. The next step is the removal of iron by magnetic separation. In subsequent sink-float separation steps, first non-metallic materials, such as plastics, wood and rubber are removed, followed by heavy metals and some steels. The final step in many recycling facilities is now an eddy current separation process that separates the aluminium from all leftover non-metallic materials. In recent years, sorting methods based on computer vision and spectroscopic techniques have been gradually integrated in the recycling process. One example is the separation of Printed Circuit Boards (PCB) and some plastics based on their colour. X-ray Fluorescence (XRF) spectrometry is sometimes used to separate stainless steel and other types of metal from the rest of the non-ferrous waste.

These methods succeed in separating aluminium from all other waste materials with fairly good accuracy. However, the aluminium itself remains a mix of many different alloys. To increase the value of their aluminium scrap, recycling companies are currently experimenting with new technologies to enhance their sorting systems [25]. One of the most promising new technological developments is the integration of Laser Induced Breakdown Spectroscopy (LIBS) in existing sorting systems [12] [26] [27]. LIBS is a spectroscopy based technology that can be used to characterise and sort aluminium on an alloy level. It outperforms other spectroscopic techniques, such as X-ray Fluorescence, for the detection of light elements [28]. With LIBS, the aluminium output stream can be further divided in smaller streams with a more uniform composition. The International Aluminium Institute (IAI) suggests that the ideal place to integrate LIBS into the sorting process is at the very end of the process chain [29]. This allows a very good control of the final output streams since LIBS characterisation can give an accurate indication of the composition of the sorted scrap.

1.5 Objectives

This introduction has identified three important issues that put the current way of aluminium recycling under pressure. First of all, the amount of recycled aluminium is expected to rise significantly in the near future, driven by the large availability of aluminium scrap and the desire to reduce the environmental impact of aluminium use. Secondly, the demand for cast alloys, the most convenient sink for recycled aluminium, will probably start to stagnate due to changes in vehicle design. And finally, recycling companies are still struggling to enable more wrought-to-wrought aluminium recycling.

To avoid as much as possible the imminent emergence of a scrap surplus, it is up to recycling companies to enhance their recycling capabilities. Alloy based sorting with, for example, LIBS is one of the most promising options to avoid quality losses during recycling. However, it is at the moment not clear how recycling companies should apply alloy based sorting methods, when the techniques become more mature. In order to maximise the financial benefits of alloy based sorting, and to make appropriate choices during the design of the sorting system, recycling companies need to determine optimal sorting targets. Which alloys should be separated from the rest of the aluminium scrap, depends on both the composition of the input scrap and on the value of the possible sorting outputs. At the moment, recycling companies have no clear view on either one of these aspects. Without sufficient knowledge about the sorting targets, it is impossible to come to an optimal design for the sorting system. Suboptimal sorting will result in lower financial returns and therefore lower incentives for the recycling companies to implement alloy based sorting methods in their recycling facilities. Therefore, a lack of information could seriously delay the penetration of enhanced sorting methods in the recycling industry.

In order to provide recycling companies with the necessary data, the first part of this thesis will fill the crucial gaps in the available global aluminium flow data. The first goal is to make a transparent and highly parametrised model that can calculate the global aluminium flows. Based on the data and projections of global and European aluminium institutes, the model will be able to estimate the demand for specific alloy series and the evolution of the size of the scrap surplus. Furthermore, it will allow to estimate the composition of collected scrap, based on its origin. These results will be visualised in a comprehensive way to facilitate the communication of the results with the recycling companies and the broader public.

The second goal is to determine optimal sorting targets for alloy based sorting methods. A LIBS sensor and an XRF sensor are used to analyse the composition of aluminium scrap, gathered at a Belgian recycling facility. The measured composition of the collected scrap is compared to the predicted composition by the developed model. Based on the comparison between the predicted composition and the results of the two measuring campaigns, it is possible to estimate the actual composition of the collected scrap at the recycling facility. Furthermore, it is possible to explain the differences between the results of the two measuring methods and the predictions of the model. Based on the composition of the collected aluminium scrap, and the information on the demand for the specific alloys, as calculated by the developed model, it is possible to suggest different options for enhanced sorting. The suggested sorting scenarios will be an important input for the design of new sorting systems that integrate spectroscopic characterisation technologies such as LIBS.

2 Material Flow Analysis for Global Aluminium Flows

2.1 Introduction

The IAI has a long record of keeping track of the global demand for aluminium in different sectors. In addition, the organisation publishes annual data on the volumes of aluminium scrap that are collected and recycled worldwide. In 2000, the IAI started to combine the data from different studies and surveys in one model. This effort resulted in the first global flow model for aluminium, published in 2009 by Bertram et al. [30]. Preliminary results were published between 2004 and 2009 [31] [32] [33] [34] [35]. The current version of the global aluminium flow model of the IAI gets updated annually, with the support of researchers from the NTNU and the TU Wien [36]. The Microsoft Excel workbook, on which the global aluminium flow model is based, exists since 2006 and the updated version is made available for the public every year by the IAI. This global aluminium Material Flow Analysis (MFA) model has since proven to be a powerful tool for communication, education, strategic planning, environmental impact analysis and lobbying [30] [36]. Many players in the aluminium industry often refer to the model, that is freely accessable on the website of the IAI (see Figure 2.1) [37].

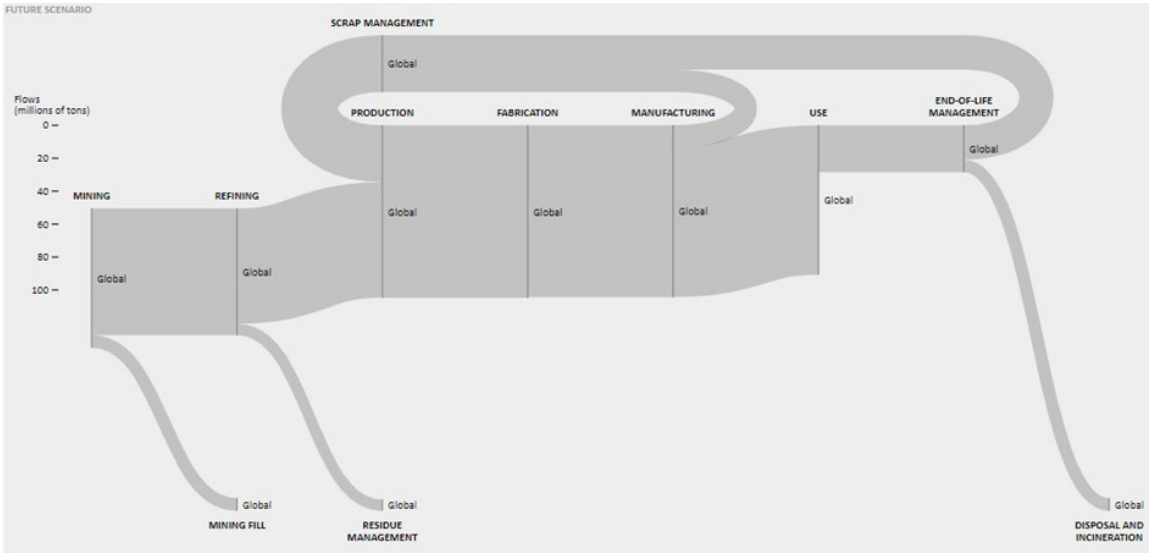

Figure 2.1: Global Flow Model of the International Aluminium Institute [37]

Because the IAI has access to extensive databases from reliable sources all over the world, the accuracy of their model is unparallelled. No other material industry has so far succeeded in quantitatively modeling global material flows on a similar level of accuracy [30]. However, the major drawback of this model is that the aluminium is treated as a single, uniform material, that seems unaltered when it goes from one stage in the life cycle to the next. In reality, the aluminium undergoes significant compositional changes when it goes from mining to refining, to production, to fabrication, to manufacturing, to the use phase, to end-of-life management, to scrap management and back to production. To suggest solutions for the described recycling challenges, the data that is included in the global flow model of the IAI is not detailed enough. In addittion to the total volume of aluminium at each stage of the life cycle, it is equally important to know the composition of the aluminium at the different stages. It is the composition of the collected aluminium scrap and the required composition for the production of the different aluminium alloys that will in the end determine the optimal way of sorting for the recycling companies.

A good estimate of the scrap composition and the demand for the different alloy series is particularly important for alloy based sorting methods such as LIBS. While integrating LIBS in their recycling processes, recycling companies need to decide how they need to further sort their collected

aluminium scrap. In order to maximise profits, the specific scrap input of the recycling companies needs to be sorted in a way that results in output streams that are as valuable as possible. The value of sorted aluminium depends on how good it matches the composition of a specific aluminium alloy. Therefore, the key to maximising profit is to strategically select specific target compositions for the different output fractions of the alloy based sorting process.

Hannula et al. have demonstrated the importance of optimising the sorting parameters and strategically choosing the target alloys in function of the composition of the input waste [38]. They started from a copper-rich batch of aluminium scrap to produce two different 2000 series alloys (that have a high tolerance for copper) and a 6000 series alloy. They proved that a slight change in the settings of the sorting system could significantly reduce the need for primary aluminium to produce the three alloys, leading to a reduction of carbon emissions of almost 75%. With the optimal sorting parameters, the produced 2017A alloy, 2014A alloy and 6024 alloy reached an impressive recyled content of 72%, 56% and 87%, respectively. This experiment proves that strategically choosing the targeted compositions of the output streams, combined with matching sorting parameters, can dramatcially improve the economic value of the processed scrap and reduce the need for primary aluminium for the production of wrought alloys, even with less advanced sorting processes. In a similar way, recycling companies should use LIBS to achieve output fractions that need as little dilution with primary aluminium as possible to produce wrought aluminium alloys that are high in demand. Figure 2.2 gives an overview of the aluminium flows in the experiment. Furthermore, it illustrates quite clearly how collected scrap in general is converted into new alloys, and what the typical inputs and outputs are in the remelting and alloying furnaces.

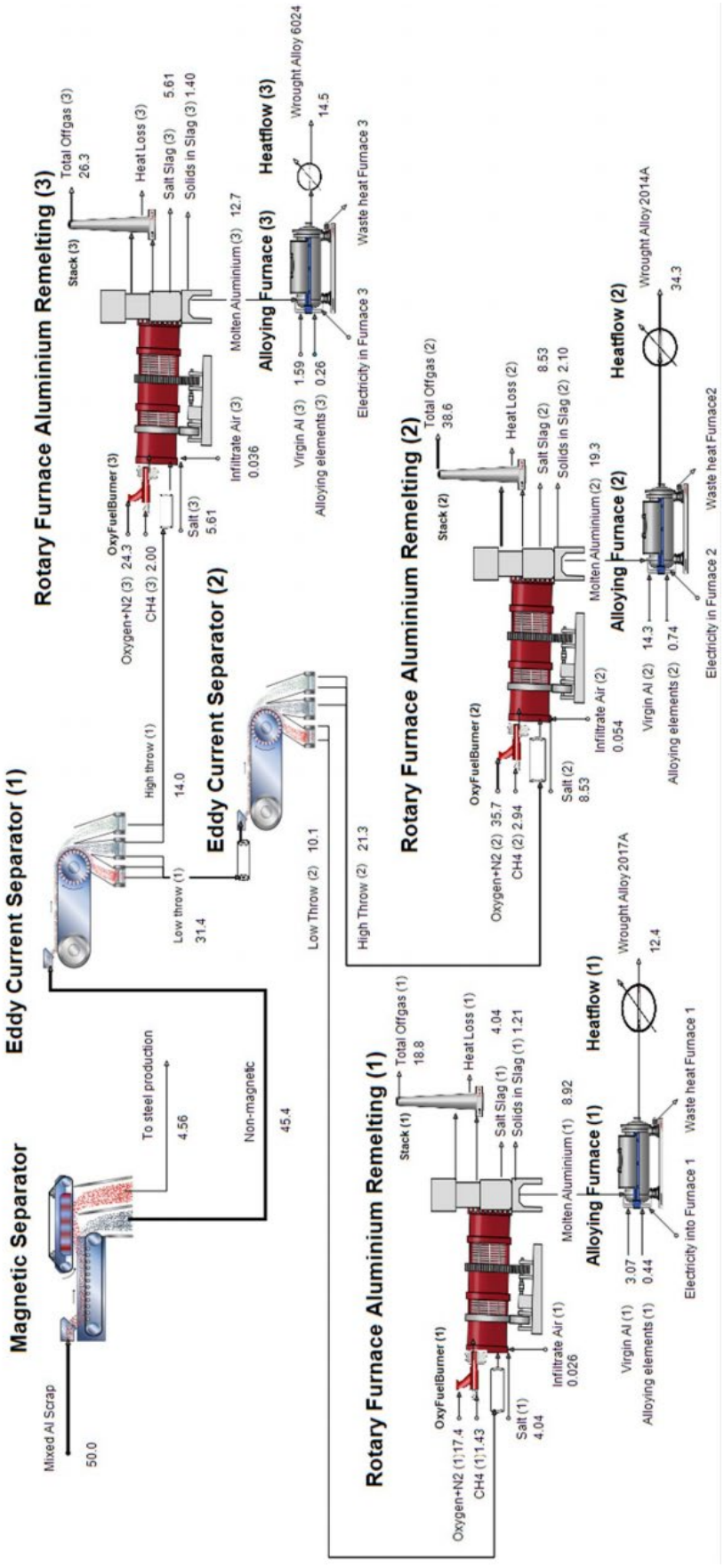

Figure 2.2: Aluminium Remelting Flowsheet [38]

The model that is developed in this chapter gives a good idea of which aluminium alloys can be expected in the aluminium scrap of different origins, such as demolition scrap, ELV, WEEE and consumer durables. Since recycling companies often know the origin of their collected scrap, this additional information will be very helpful to decide which target alloys should be selected. Furthermore, the model indicates for which alloy series and for which sectors the demand is highest. All this information can assist recycling companies in designing new sorting processes and developing new business models. The developed MFA model covers a time span ranging from 1950 to 2040 to demonstrate the evolution of some material flows and to have some useful data for the future.

The developed MFA model has a global scope. Some researchers have made MFA analyses on national or regional levels and have made estimates for the size of local scrap surpluses [36] [39] [40] [41]. However, since aluminium is traded intensively worldwide, local scrap surpluses can be absorbed immediately by other regions, if there is demand for aluminium scrap elsewhere [41] [42]. Since even aluminium scrap is shipped transcontinentally, only a global scope is suitable to investigate the future of aluminium recycling [42].

2.2 Materials

Since the IAI has no information on the demand for specific aluminium alloy series, this data must be collected from different sources in order to build the MFA model. The sections below mention the assumptions and sources that lead to the given estimates for the demand for the different alloy series. Each section focuses on a specific sector that is important for the aluminium industry. The sectors in this chapter correspond to the sectors that are defined in the global flow model of the IAI. That way, the model that is developed in this chapter can rely on the accurate data of the IAI for the total demand for aluminium in each sector, which leaves only the task of determining the share of each alloy series in the total demand per sector. In each section, two graphs are added to illustrate relevant data about the corresponding sector. One graph shows the estimated share of the different alloy series in the total demand for aluminium in that sector for the year 2020. The other graph shows the evolution of the global aluminium demand of the sector up to 2020 (see Figure 2.4 and Figure 2.6 to Figure 2.16).

The IAI defines the following sectors: (1) “Building & Construction”, (2) “Transportation – Auto & Light Truck”, (3) “Transportation – Aerospace”, (4) “Transportation – Other”, (5) “Packaging – Cans”, (6) “Packaging – Other (Foil)”, (7) “Machinery & Equipment”, (8) “Electrical – Cable”, (9) “Electrical – Other”, (10) “Consumer Durables”, (11) “Other (except Destructive Uses)” and (12) “Destructive Uses”. The share of each sector in the total demand for aluminium varies slightly over time. Figure 2.3 shows the situation in the year 2020. The demand for aluminium is clearly dominated by the construction sector and the transportation sector. The shares of the other sectors are relatively limited.

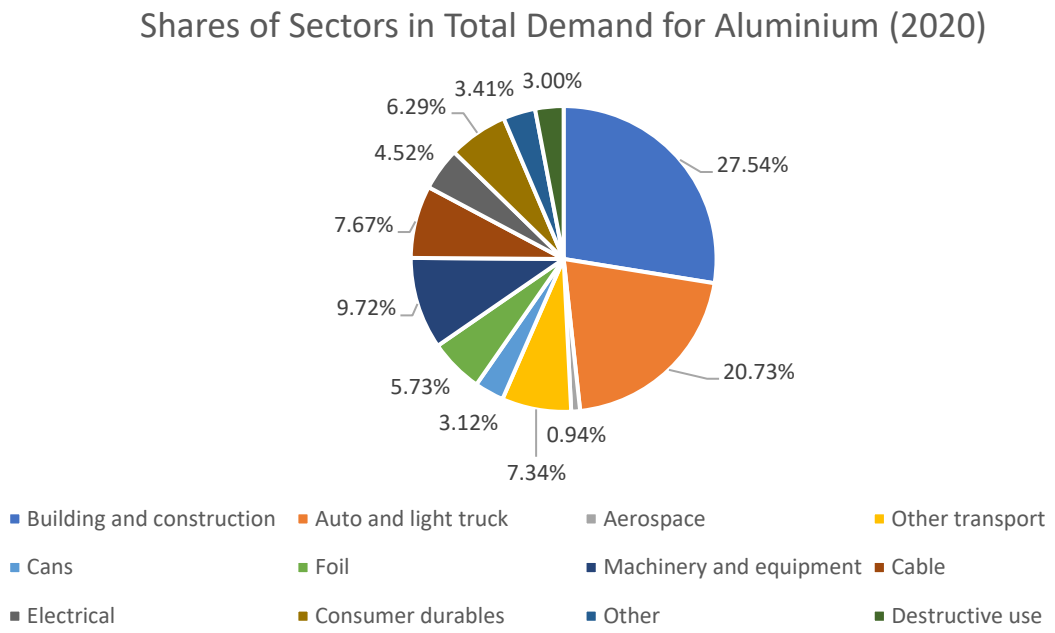

Figure 2.3: Shares of Sectors in Total Demand for Aluminium in 2020

2.2.1 Building & Construction

Based on the Aluminum Statistical Review for 2008 of the American Aluminum Association, Allwood and Cullen come up with the following data about aluminum in the building and construction sector [4]; of the aluminum used for structural applications in buildings, 56% is used for sheets and plates and 44% is used for extruded shapes; of the aluminum used for non-structural applications in buildings, 60% is used for extruded shapes, 39% is used for sheets and plates and 1% is used for wire; of the aluminum used for infrastructure, 48% is used for sheets and plates, 23% is used for extruded shapes, 16% is used for castings and 13% is used for pipes and tubes. According to Allwood and Cullen, 4,8 million tonnes of aluminum were used in structural applications in buildings, 5,2 million tonnes were used in non-structural applications in buildings and 0,9 million tonnes were used in infrastructure in 2007.

In structural applications, extrusions are almost exclusively made from alloys of the 6000 series and sheets and plates are almost exclusively made from alloys of the 5000 series [43]. For the calculations in this chapter, it is assumed that 100% of the structural extrusions is made from 6000 series alloys and 100% of the structural sheets and plates is made from 5000 series alloys. This simplification deviates only slightly from the actual situation.

For non-structural, extruded components like window frames, door frames and curtain walls, the 6060 and 6063 grades are most often used [44]. These alloys have a good strength-to-weight ratio, are durable and stiff. In this chapter it is assumed that 100% of the non-structural extrusions are made of 6000 series alloys. Since the overwhelming majority of the non-structural, extruded components are made from these two alloys, the error that results from this simplification will be very limited. The second group of non-structural aluminium components, after the extrusions, consists of cold rolled sheets for roofing and cladding. These components must be light and aesthetic and need to protect the building from all types of weather. Literature suggests that the most appropriate alloys for this type of application are the 3003 grade and the 5005 grade [44]. Also considering other data, it seems reasonable to assume that 20% of the alloys for this type of application is from the 3000 series and 80% is from the 5000 series [4] [43] [45]. The wires in non-structural applications are assumed to be

entirely made from alloys of the 1000 series. The AA1350-H19 alloy is by far the most used alloy for aluminium wires and cables, and the most common alternative alloys for building wires are from the 1000 series as well [44].

For aluminium extrusions, sheets and plates in infrastructure, the same assumptions are made as for their structural applications in buildings. The extrusions are entirely made from alloys of the 6000 series and the sheets and plates are entirely made from alloys of the 5000 series. In addition, this it is assumed that only cast alloys are used for castings in infrastructure and that the pipes and tubes consist entirely of alloys of the 3000 series [4].

The combination of these numbers leads to the following estimated proportions of the different alloy series in the total use of aluminium in the building and construction sector. About 0,5% of the used aluminium is from the 1000 series, 4,8% is from the 3000 series, 43,5% is from the 5000 series, 49,9% is from the 6000 series and 1,3% is made from cast alloys. Multiple sources indicate that these shares are very stable over time [4] [43] [46]. Therefore, it is assumed that these shares will remain constant in the nearby future, while the total demand for aluminium in the construction sector keeps growing.

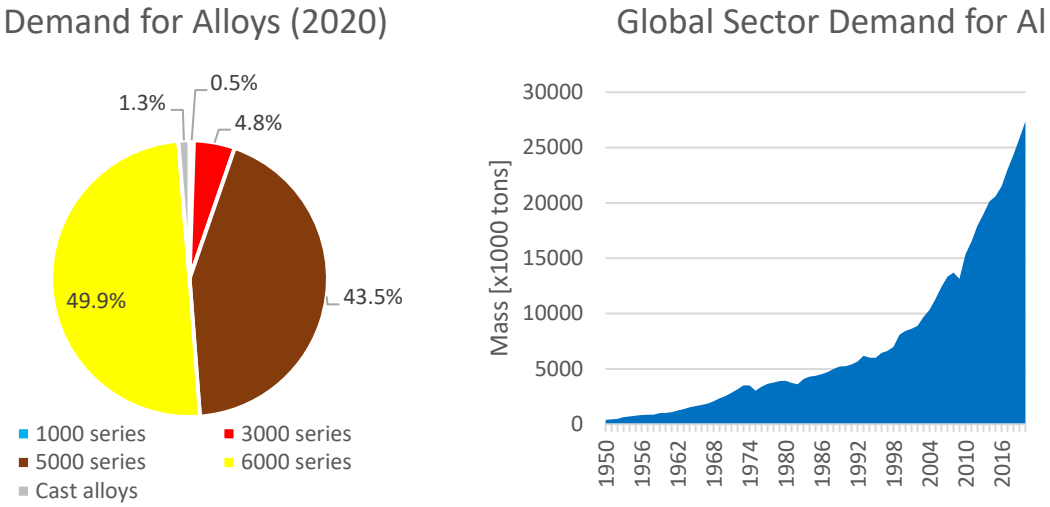

Figure 2.4: Building & Construction: Demand for Alloys in 2020 and Evolution of Sector Demand for Aluminium

2.2.2 Transportation – Auto & Light Truck

The automotive sector is the second most important one, after the construction sector. The demand for the specific aluminium alloy series in this category are estimated based on research conducted by Modaresi et al. [16]. Their research provides historical data on the use of the different alloy series in the automotive sector, starting from the year 1950, and makes forecasts up until 2050. Since Modaresi et al. had the support of the IAI, the EAA, the Norwegian renewable energy and aluminium concern Norsk Hydro, and the professional market research company Ducker to collect the required data, their results are assumed to be accurate. Furthermore, the researchers explicitly mention that the purpose of their research was to provide the necessary data to build alloy-specific models and to investigate solutions for the looming scrap surplus in the aluminium industry. This confirms that their data is especially suitable for the calculations in this chapter. With the input of Ducker, that has a tradition of tracking the aluminium content in passenger cars, it was even possible for the researchers to estimate the use of aluminium alloys on the level of the different car components (see Figure 2.5) [47] [48] [49]

[50]. This additional information can be very useful for companies that recycle ELV to dismantle the cars in a more strategic way.

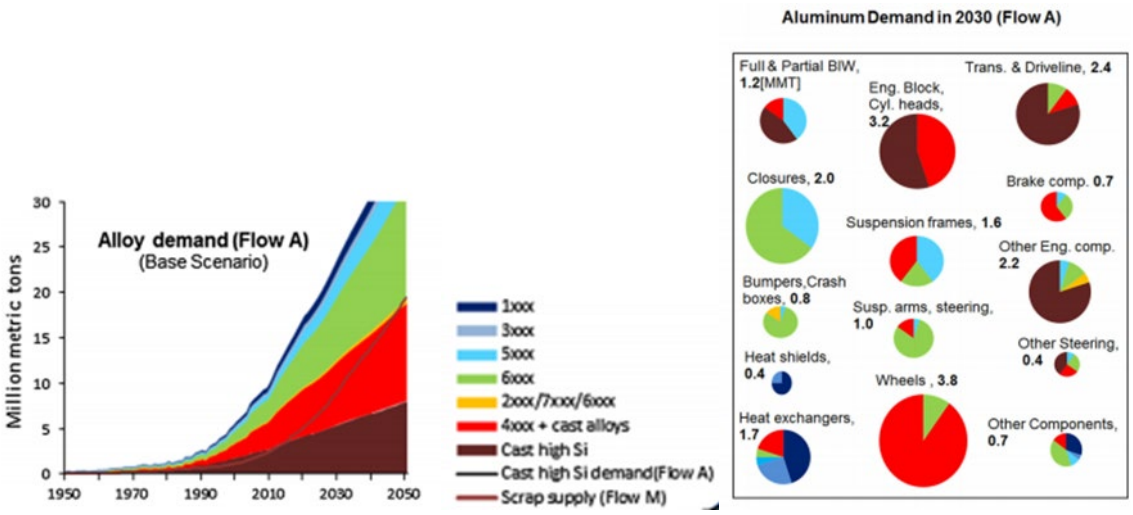

Figure 2.5: Forecast of Demand for Aluminium Alloys in Passenger Cars [16]

For the year 2020, cast alloys represent an estimated 57,9% of the used aluminum in this sector. The 6000 series alloys have a share of 21,2%, the 5000 series alloys have a share of 12,7%, the 1000 series alloys have a share of 3,7%, the 3000 series alloys have a share of 1,7%, the 4000 series alloys have a share of 1,5% and the 2000 and 7000 series alloys both have a share of 0,6%.

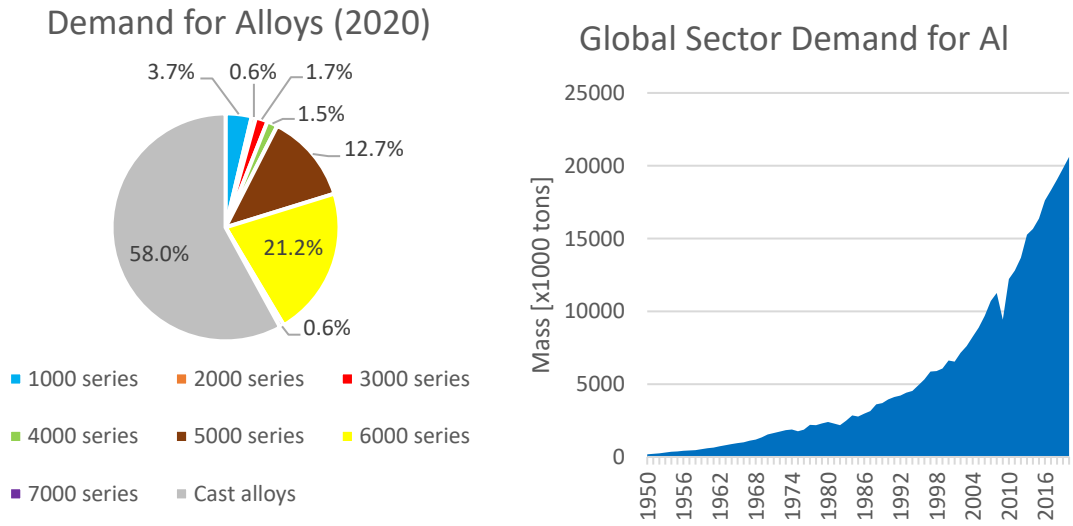

Figure 2.6: Transportation – Auto & Light Truck: Demand for Alloys in 2020 and Evolution of Sector Demand for Aluminium

2.2.3 Transportation – Aerospace

The aerospace sector primarily demands aluminium alloys of the 2000 and 7000 series [51]. The 2000 series alloys are typically used in lower wing skins and fuselage structures of commercial airplanes, where damage tolerance is important, while the high strength 7000 series alloys are typically used for upper wing skins [52]. In addition, the aerospace sector uses 6000 series alloys, and to a lesser extent 8000, 1000 and 4000 series alloys for various light weight components [53]. Based on this information, the estimated shares of the different aluminium alloy series in the total demand of the aerospace sector are the following. The 2000 series alloys have a share of 43,0%, the 7000 series alloys have a

share of 33,0%, the 6000 series alloys have a share of 15,0% and the 1000 series alloys, the 4000 series alloys and the 8000 series alloys each have a share of 3,0%.

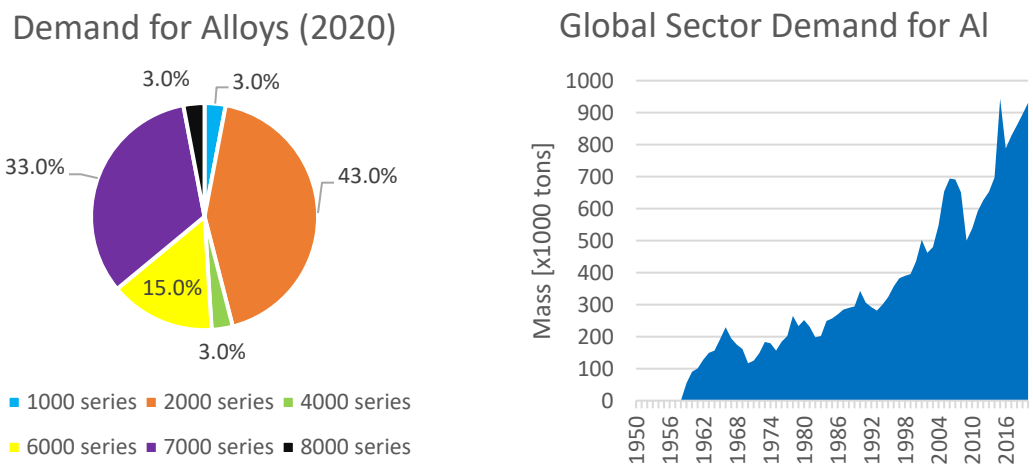

Figure 2.7: Transportation – Aerospace: Demand for Alloys in 2020 and Evolution of Sector Demand for Aluminium

2.2.4 Transportation – Other

Based on data from several sources, an estimated 16,2% of the aluminum in this category is used for rail applications and another 16,2% is used for marine applications [4] [54] [55]. That leaves 67,6% of the aluminum in this category for trucks, buses, trailers, and other vehicles. In rail applications, half of the used aluminum goes to sheets and plates and half of the aluminum goes to extruded shapes [55]. The sheets and plates consist almost entirely of aluminum alloys of the 5000 series and the extrusions consist almost entirely of alloys of the 6000 series [55]. In marine applications, 80% of the aluminum is used for sheets and plates and 20% of the aluminum is used for extruded shapes. Also for marine applications, the sheets and plates consist almost entirely of alloys of the 5000 series and the extrusions consist almost entirely of alloys of the 6000 series [54]. The proportions of the used aluminum series in trucks, buses, trailers, and other vehicles are assumed the same as those for cars. These assumptions lead to the following shares for the different aluminum series used in this category for the year 2020. Cast alloys have a share of 39,1%, the 5000 series alloys have a share of 29,7%, the 6000 series alloys have a share of 25,7%, the 1000 series alloys have a share of 2,5%, the 3000 series alloys have a share of 1,2%, the 4000 series alloys have a share of 1,0% and both the 2000 and the 7000 series alloys have a share of 0,4%.

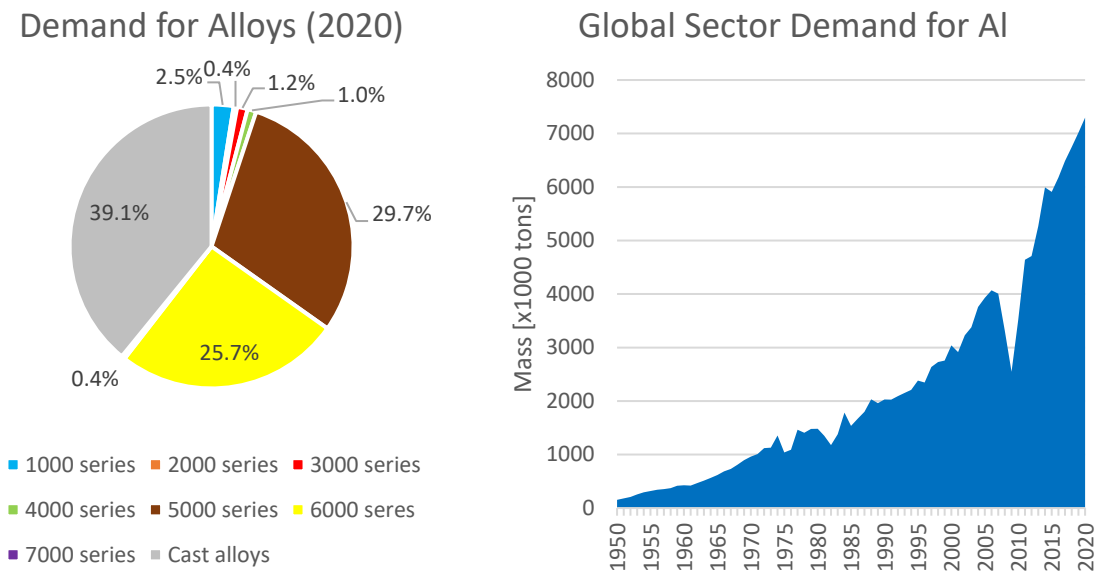

Figure 2.8: Transportation – Other: Demand for Alloys in 2020 and Evolution of Sector Demand for Aluminium

2.2.5 Packaging – Cans

The body of an aluminium can, which typically consists of a 3000 series alloy (3004), constitutes 75% of the total weight of the can [38]. The lid, which typically consists of a 5000 series alloy (5182), constitutes 25% of the total weight [56].

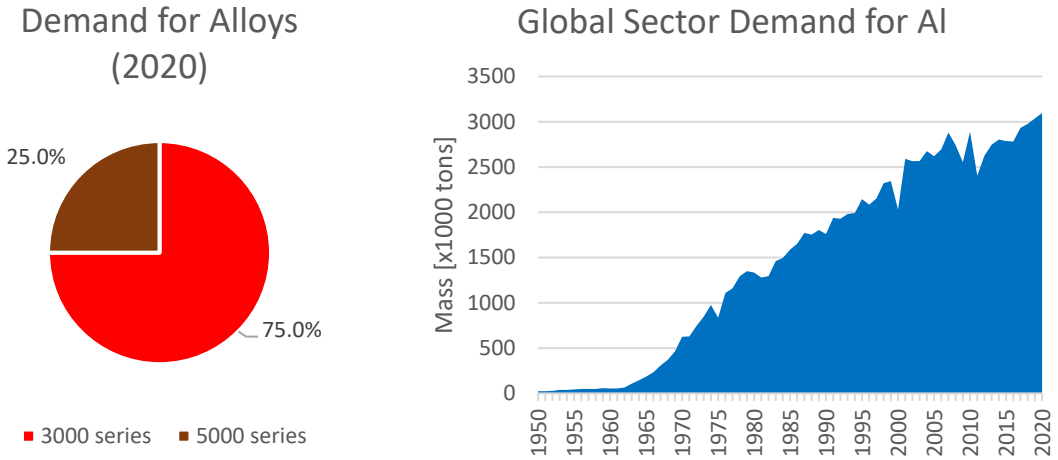

Figure 2.9: Packaging – Cans: Demand for Alloys in 2020 and Evolution of Sector Demand for Aluminium

2.2.6 Packaging – Other (Foil)

According to Allwood and Cullen, 83% of all packaging foil is standard aluminum foil and 17% is actually cold rolled sheet [4]. The first type of foil is assumed to consist entirely of 1000 series alloys. The second type of foil, the high strength foil, is assumed to consist entirely of 3000 series alloys.

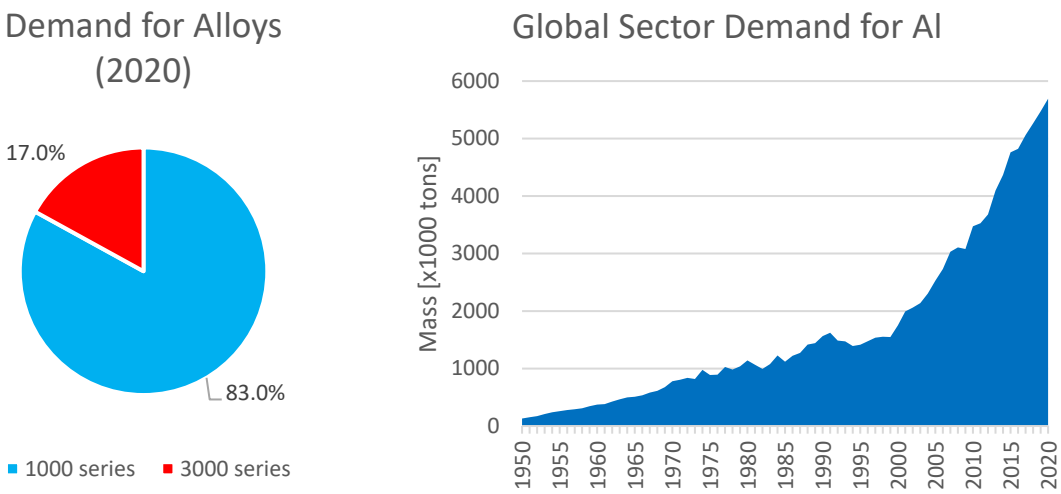

Figure 2.10: Packaging – Other (Foil): Demand for Alloys in 2020 and Evolution of Sector Demand for Aluminium

2.2.7 Machinery & Equipment

Machinery is a category that encompasses a wide variety of industrial machines. According to multiple sources, the machinery sector uses predominantly alloys of the 6000 series and the cast series [46] [57]. For heat exchangers, that also fall into this category, aluminium is a very popular material because of its high thermal conductivity, good corrosion resistance and low cost. The typical alloys used for this application are from the 1000 and 3000 series [16] [44]. A combination of the data from the mentioned sources gives the following estimations for the proportions of the used aluminium alloys in this sector: 15% of the used alloys are from the 1000 series, 10% are from the 3000 series, 5% are from the 5000 series, 20% are from the 6000 series and 50% are cast alloys. These numbers are assumed to be constant over time since no major changes are expected in the types of alloys that are used for most machinery, including heat exchangers, by far the most prominent homogeneous group of products in this category. The European Aluminium Association confirms in its *"Aluminium Automotive Manual"* that while further design improvements of heat exchangers are expected in the future, this will probably have no significant impact on the use of aluminium [58].

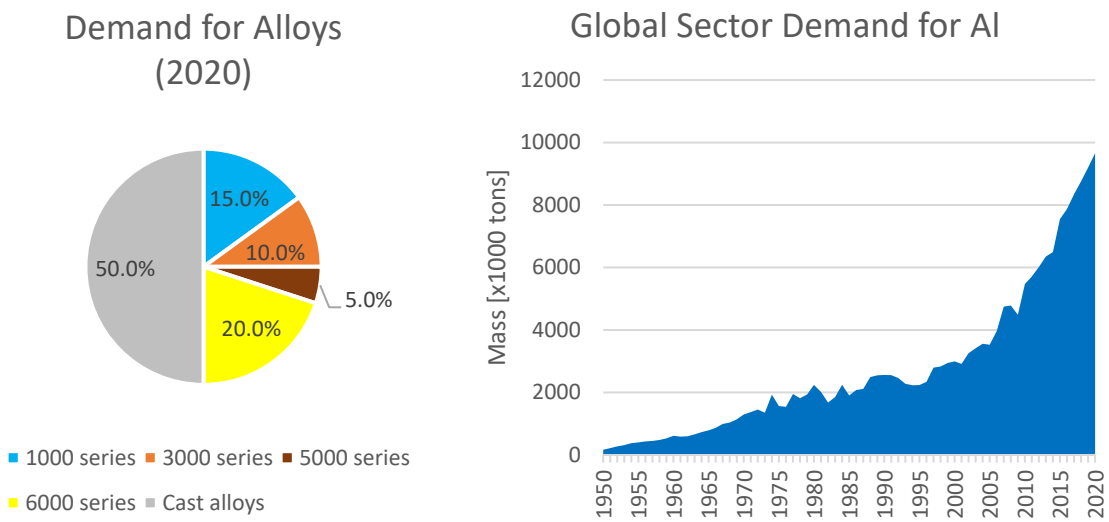

Figure 2.11: Machinery & Equipment: Demand for Alloys in 2020 and Evolution of Sector Demand for Aluminium

2.2.8 Electrical – Cable

Literature suggests that AA1350-H19 is by far the most common alloy for the production of aluminium cables [44]. The alloy has a conductivity that is 60% of that of copper, while being lighter and cheaper. On the websites of Southwire and Lamifil, two big producers of aluminium wire, the 1350 alloy is also the most prominent one, followed by other 1000 series alloys, some alloys of the 5000 series, 6000 series and 8000 series [59] [60] [61]. Especially for high voltage applications, where aluminium-conductor steel-reinforced cable is used, the 1350 alloy seems to be the standard [62]. This is also confirmed by the American Aluminum Association [63]. However, since 1970, the 1000 series alloys have lost some applications to the newly developed 8000 series alloys, especially for cables for lower voltage applications [64]. The 8000 series alloys have a higher yield strength and are a safer choice for some types of cable. The 5000 series and 6000 series alloys are used less frequently, for example in specific applications, such as optical ground wire (OPGW). The estimated proportions for this sector are 5% for the 5000 series, 10% for the 6000 series and 85% for the 1000 series, while the share of the 8000 series rises from 0% in 1970 to 30% in 2040 at the expense of the 1000 series.

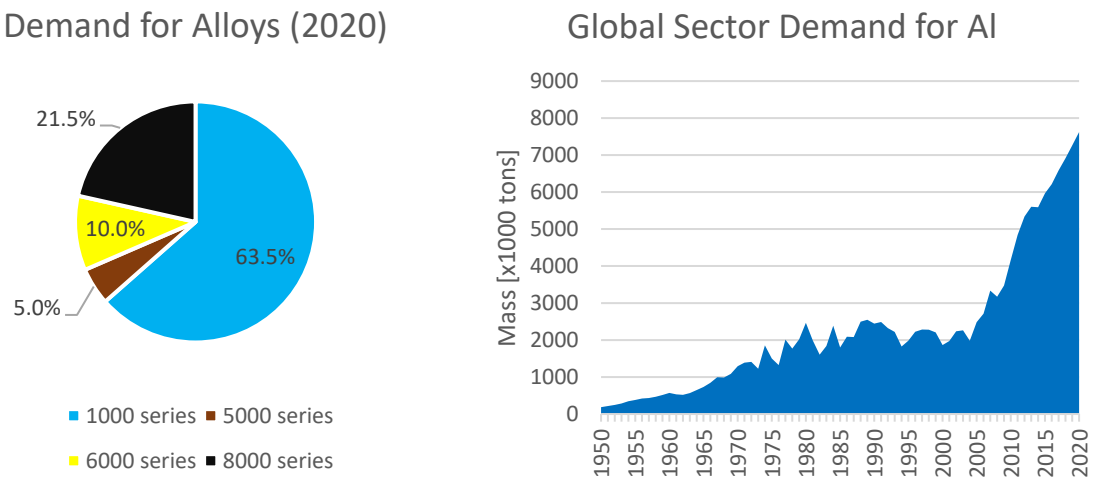

Figure 2.12 Electrical – Cable: Demand for Alloys in 2020 and Evolution of Sector Demand for Aluminium

2.2.9 Electrical – Other

The proportions of the used aluminium alloys in this category are estimated based on slightly conflicting data of different sources [4] [44] [46] [57] [65]. Since information on the use of aluminium alloys for electrical equipment on a global level is scarce, it is necessary to combine and extrapolate data from regional studies. However, for electrical equipment there are more outspoken regional differences in the use of aluminium than for most other sectors. The United States, Europe, and Japan, the three regions that report most clearly about their use of aluminium, each have a unique electrical and electronics industry that focuses on different products, and this reflects in their use of aluminium. Due to these more outspoken differences, making a global average is somewhat more complicated than for most other sectors. However, since the demand for aluminium from this sector is an order of magnitude smaller than the demand from the building and transportation sector, errors in these estimates will not weigh heavily on the overall results. The estimated share of both the 1000 and the 5000 series alloys in the total use of aluminum for this sector is 24,0%, the share of cast alloys is 20,0% and the share of both the 3000 and 6000 series alloys is 16,0%. The 1000 series alloys are mainly used for bus bars, while the 5000 series alloys are used for sheathing and the 6000 series alloys for conduits. The 3000 series alloys and cast alloys are used in various applications.

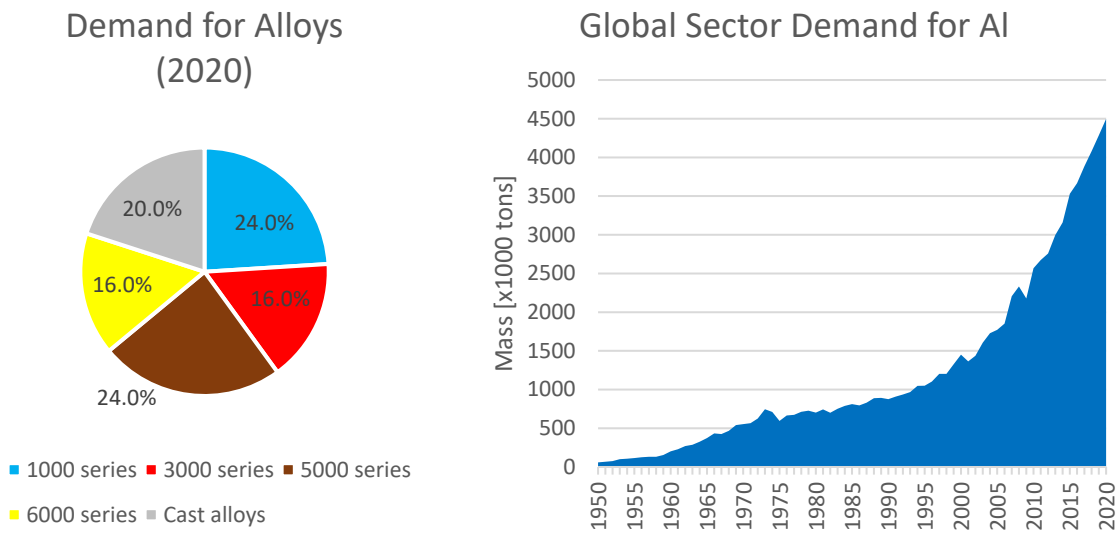

Figure 2.13: Electrical – Other: Demand for Alloys in 2020 and Evolution of Sector Demand for Aluminium

2.2.10 Consumer durables

According to Allwood and Cullen, 27% of the aluminum in this category is present in castings, 13% in extrusions and 60% in sheets and plates [4]. According to other sources, the extrusions in this sector consist almost entirely of 6000 series alloys and the sheets and plates consist of 3000 series alloys (mainly 3003 and 3103), 5000 series alloys (mainly 5754) and 7000 series alloys in equal proportions [44] [46]. Following from these assumptions, the estimated share of the cast alloys is 27,0%, the share of the 3000 series alloys is 20,0%, the share of the 5000 series alloys is 20,0%, the share of the 7000 series alloys is 20,0% and the share of the 6000 series alloys is 13,0%.

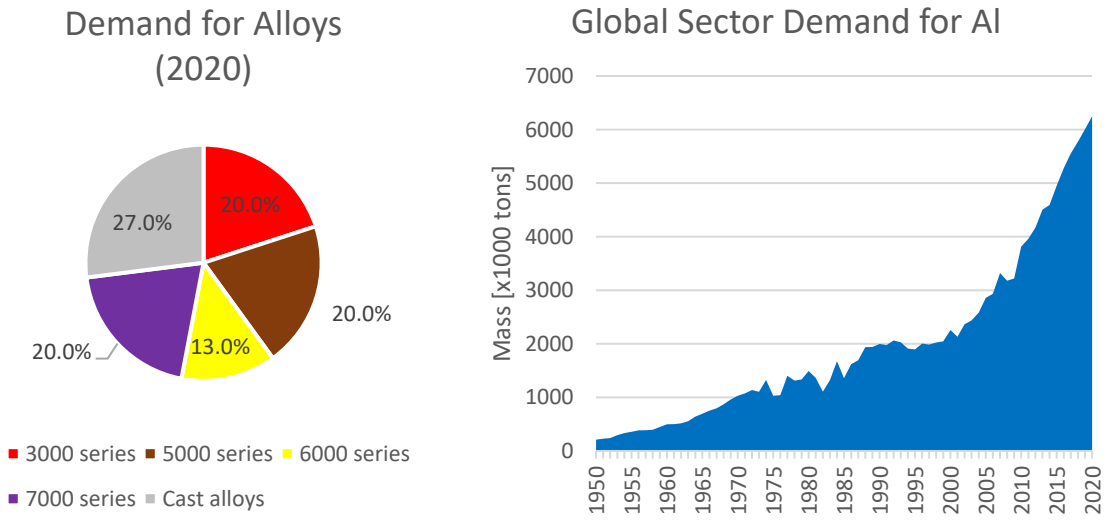

Figure 2.14: Consumer Durables: Demand for Alloys in 2020 and Evolution of Sector Demand for Aluminium

2.2.11 Other (Except Destructive Uses)

Allwood and Cullen estimate that 53% of the aluminum in this category is present in the form of cast alloys [4]. The remaining 47% is spread equally over the 3000, 5000 and 6000 series alloys.

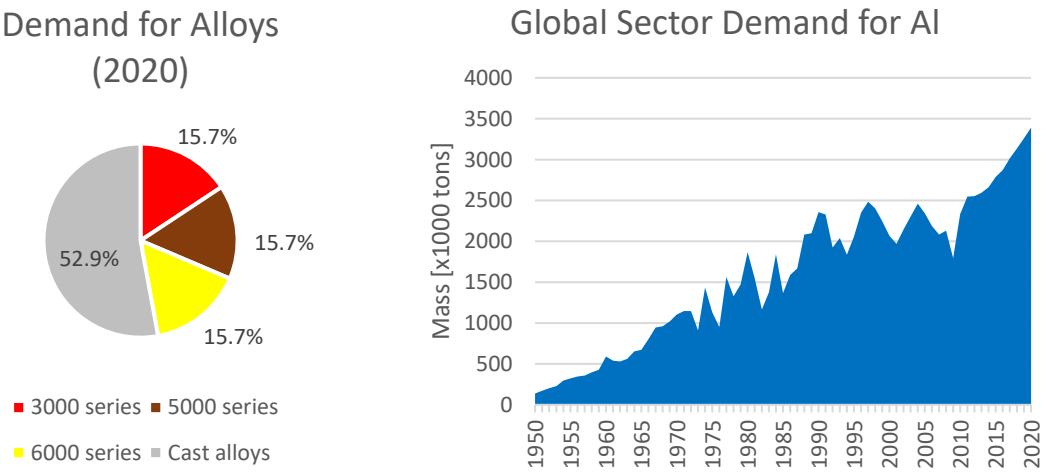

Figure 2.15: Other (Except Destructive Uses): Demand for Alloys in 2020 and Evolution of Sector Demand for Aluminium

2.2.12 Destructive uses

The aluminium in this sector is used to deoxidise steel, as an alloying element for other metals, for explosives and for pyrotechnic purposes [66]. It is assumed that only 1000 series alloys are used in this category since the applications in this category require pure aluminium and do not benefit from the properties that come with the addition of alloying elements.

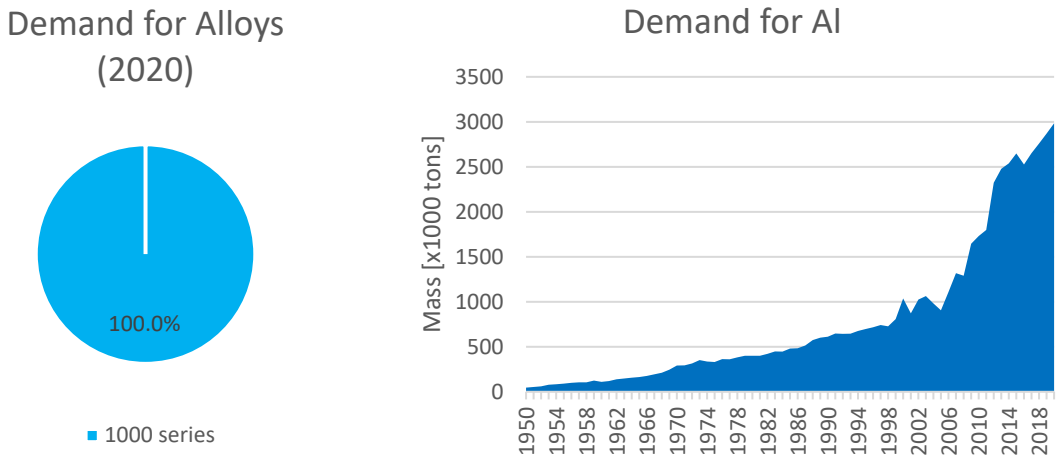

Figure 2.16: Destructive Uses: Demand for Alloys in 2020 and Evolution of Sector Demand for Aluminium

2.3 Methodology

The developed MFA model is visualised with a Sankey diagram, where the different nodes in the diagram represent the different lifecycle stages of specific aluminium streams. As in traditional Sankey diagrams, the width of the arrows between the nodes is proportional to the volumes of material that flow from one node to the next. The popularity of Sankey diagrams as a means of representing energy and material flows has grown in recent years due to the increased focus on process efficiencies in

various industries [67] [68]. Among academics and companies, Sankey diagrams have become particularly common for representing aluminium and steel flows [4] [69] [70] [71] [72] [73]. This is also demonstrated by the fact that the IAI uses a Sankey diagram to visualise its global aluminium flow model on its website [37]. Therefore, the structure of a Sankey diagram seems also most appropriate for the development of the MFA model in this thesis.

Figure 2.17 gives the basic structure of the developed Sankey diagram. Starting from the left of the diagram, primary and recycled aluminium flow to the manufacturing phase. In the manufacturing phase, most of the aluminium from the incoming flows is converted into products. However, some of the aluminium is converted into manufacturing scrap due to process inefficiencies. This manufacturing scrap is sometimes called pre-consumer scrap or "new" scrap. For the manufactured products, the next phase in the life cycle of the aluminium is the use phase. The IAI subdivides the aluminium flows in the manufacturing phase and use phase into 12 sectors. These sectors are the ones mentioned in the *Materials* section. In the developed model, the aluminium flows are subdivided according to these same sectors and are visualised separately. After the use phase, when the aluminium products reach the end of their lifetime, they are either collected for recycling or not. In the latter case, the aluminium ends up in incinerators or in landfill. Collected aluminium from End-of-Life products is called post-consumer scrap or "old" scrap. It can be recycled to make new aluminium products.

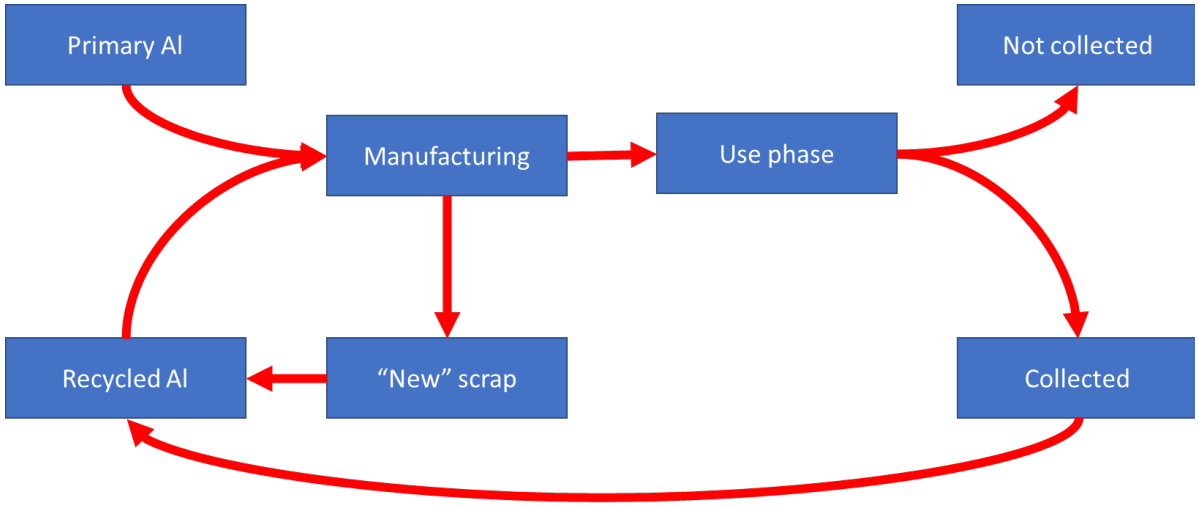

Figure 2.17: Basic Structure Sankey Diagram

2.3.1 Adoption of Sufficiently Detailed IAI Data

The development of the model happens in several steps. In a first step, the flows are modelled for which the IAI provides sufficiently detailed data. In fact, the global aluminium flow data of the IAI, which are freely accessible on its website, provide most of the information that is needed in this model [13]. The total amount of aluminium that flows to the "manufacturing" node is reported by the IAI per sector since 1950, and projections are made for these flows until the year 2040. Numbers are available on the amount of new scrap that is generated yearly in the manufacturing phase, together with the amounts of aluminium that enter the use phase in the different sectors. The IAI keeps track of the annual amount of aluminium that is collected (and not collected) from End-of-Life (EOL) products as well. Finally, the IAI holds data on the pre-melting and melting losses involved in the recycling process of old and new scrap. Due to these losses, the amount of aluminium that can be recycled is slightly lower than the amount of collected old and new scrap. According to the IAI, old scrap pre-melting recovery rates are consistently higher than 97% for any sector in any year, while melting recovery rates go as low as 85% for aluminium foil in the earlier years of the investigated time frame. For new

scrap, pre-melting losses are neglected, and the melting recovery rate is estimated at 98% for each sector and each year.

In the developed MFA model, the aluminium from the twelve sectors that is not collected for recycling is bundled in one node. The aluminium that is collected for recycling is bundled for all sectors except "Packaging – Cans". The aluminium from collected aluminium cans flows to a separate node in the Sankey diagram because globally, there is a different approach to recycling aluminium cans as compared to other collected scrap. The researchers that contributed to the global flow model of the IAI indicate that used beverage cans (UBC) reach cast houses mostly separately from casting scrap, extruded scrap, rolled scrap and other scrap from different sources [36]. To represent this fact in the Sankey diagram of the developed MFA model, the flow of UBC is kept separate from the rest of the collected aluminium scrap.

Based on the data that the IAI provides, most flows of the MFA model can be modelled with a satisfying level of detail. Therefore, this first step of the development process results already in a large part of the complete model, as can be seen in Figure 2.18. Only the flows of primary and secondary aluminium to the manufacturing phase do not rely on IAI data.

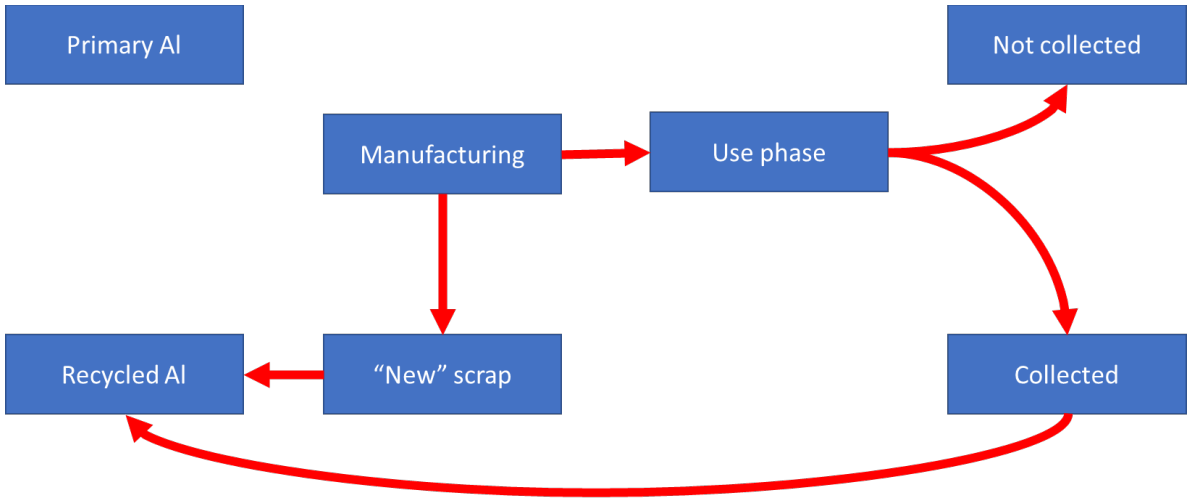

Figure 2.18: Part of the Model that Relies on IAI Data

Although the IAI does provide numbers for past and future amounts of primary and secondary aluminium flows to the manufacturing phase, these numbers are not deemed appropriate for the development of the model in this thesis. The data of the IAI only consider the total volumes of primary and secondary aluminium that flow to the manufacturing phase and provide no insight in the composition of these aluminium streams. Furthermore, the IAI assumes in its calculations that all collected scrap can be recycled for the production of new alloys, so that a scrap surplus will not emerge in the investigated time frame. This is a problematic assumption since the emergence of a scrap surplus is highly probable unless drastic measures are taken. Therefore, the flows of primary and secondary aluminium to the manufacturing phase are calculated in a different way in this model.

In the following sections, it is explained how in different steps, the flows of primary and secondary aluminium to the manufacturing phase are modelled in a way that better suits the purpose of this thesis. In the next step, the demand for aluminium is first split up in the demand for specific alloy series. Afterwards, the composition of the collected aluminium scrap is calculated. Then, the tolerance of the different alloy series for impurities is determined. Based on the information about the composition of the scrap and the tolerance for impurities of the alloy series, it is possible to determine how much recycled aluminium can flow to the different alloy series. Finally, it is possible to calculate

the size of the scrap surplus and the amount of primary aluminium that is required to meet the total demand for aluminium. Figure 2.19 summarises this five step plan and shows in which sections each step is explained in more detail. These five steps are the most crucial ones in the development of the model, since they make the difference between this model, and the global flow model developed by the IAI.

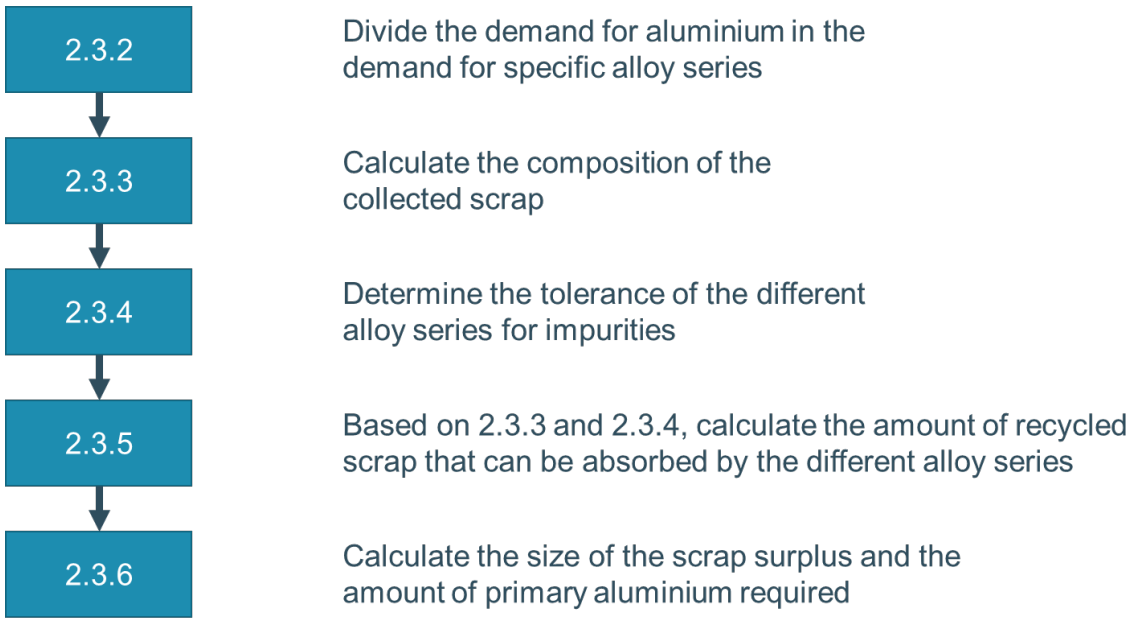

Figure 2.19: Steps to Model the Flows of Primary and Secondary Aluminium to the Manufacturing Phase

2.3.2 Demand for Alloy Series

The calculation of the demand for the different alloy series is based on the assumptions explained in the *Materials* section. In the *Materials* section, estimates have been made for the share of each alloy series in the total demand for aluminium in each sector, throughout the years in the investigated time frame. The demand for aluminium in each sector is divided in the demand for wrought alloys (the 1000 to 8000 series) and cast alloys.

As a result, the demand for each alloy series in a certain sector can be calculated by multiplying the estimated share of the alloy series in the demand for aluminium of that sector, with the total demand for aluminium in that sector, which is given by the IAI. Adding up the results of the twelve sectors allows to determine the total global demand for each individual alloy series.

A part of the demand for aluminium in the "Packaging – Cans" sector can be satisfied directly with aluminium from recycled UBC, which is collected and recycled separately from the rest of the collected aluminium scrap. With this closed-loop recycling method, the amount of aluminium cans that has to be produced in the "conventional" way is reduced by the amount of recycled UBC.

2.3.3 Composition of the Collected Scrap

At this point in the development of the model, it is clear how high the demand is for the different alloy series. The next step is to determine the elemental composition of the collected scrap. This is a necessary step to determine how much recycled scrap can flow to the different alloy series, since each alloy series has certain tolerance limits for impurities. The global flow model of the IAI does not take

the composition of the collected scrap into consideration in its calculations, and assumes that regardless of its composition, all collected scrap can be recycled somehow.

In order to determine the average elemental composition of all the collected scrap, it is first estimated which aluminium alloys can be expected in the scrap from the different sectors. After establishing in which proportions the different alloy series are present in the collected scrap, it is possible to approximate the elemental composition of the scrap by looking at the elemental composition of the present alloys.

For new scrap, it is assumed that the generated scrap consists of the same alloys that enter the manufacturing phase in that year, in the same proportions. For old scrap, estimating which alloys can be expected in the collected scrap is more complex since the products in each sector have lifetimes that can be much longer than one year. Therefore, the alloys that are collected from end-use products are not identical to the ones that entered the use phase that year.

The average time that aluminium remains “in stock” in the use phase of finished products is estimated by the IAI per sector and per region. It varies from one year for packaging to 60 years for aluminium in buildings in Europe, Japan and the United States [36]. The uncertainty and variation in these estimates is considered in the data of the IAI by using a normal distribution on the average lifetime of the products in every sector and every region. The normal distribution has a coefficient of variation equal to 1/3 and considers only whole years.

It is estimated here that the alloy series in the scrap of a sector are present in the same proportions as the alloy series that entered the use phase a certain number of years ago. This number is equal to the average lifetime of the products in that sector. This simplification does not consider the variation in the lifetime of the products within a sector and is therefore not completely accurate. However, since in most sectors, the use of alloys does not change significantly during the lifetime of the products, this approach still yields reasonable approximations.

Based on the estimated amounts of aluminium from the different alloy series in the collected old and new scrap, it is possible to approximate the average elemental composition of all the collected scrap that is available for recycling. To convert the estimated alloy-level composition to an elemental composition, it is necessary to know the approximate elemental composition of the different alloy series. The composition of an alloy series is not something that is strictly specified. All alloys within the same series have the same main alloying element(s), but between them, there are still some limited differences in composition.

In order to come to a generalised composition of each alloy series, the most popular alloys are selected to represent the composition of their alloy series. This is a reasonable way to approximate the composition of the alloy series because the difference in composition between alloys in one series is small and the selected alloys are by far the most popular ones in their series. The selected alloys are the following: 1050, 1100, 1200, 2014, 2024, 2025, 3004, 4043, 5005, 5052, 5083, 6061, 6063, 6082, 7050, 7075, 7475, 8176, 319, 356 and 380. This list includes all standard alloys that are used for atomic emission spectroscopy testing, supplemented with some other popular alloys [74].

Table A.0.1 to Table A.0.9 in Appendix A show the allowable ranges for the presence of alloying elements and contaminants in the selected aluminium alloys. This information is accessible in various material databases [75] [76] [77] [78] [79]. Based on these ranges, a probable composition is determined for each alloy series. The estimated composition of each series is noted in the rightmost column of Table A.0.1 to Table A.0.9 and is summarised in Table 2.1. Combining these compositions

with the estimated shares of the different alloy series in the collected scrap, allows to make an estimate for the elemental composition of the collected scrap.

Table 2.1: Estimated Elemental Composition Alloy Series

	1000	2000	3000	4000	5000	6000	7000	8000	Cast
Al (wt%)	99.34	93	96.65	94.29	96.2	97.2	89.1	98.9	87.7
Cu (wt%)	0.05	4.5	0.1	0.1	0.05	0.2	1.8	0.05	2.5
Fe (wt%)	0.2	0.2	0.5	0.2	0.2	0.3	0.3	0.7	0.6
Mg (wt%)	0.04	1	1.1	0.03	3	1.1	2.4	0.05	0.3
Mn (wt%)	0.02	0.5	1.3	0.03	0.1	0.3	0.1	0.05	0.3
Si (wt%)	0.2	0.6	0.15	5.2	0.25	0.7	0.1	0.1	7.1
Zn (wt%)	0.05	0.1	0.1	0.05	0.1	0.1	6	0.05	1.2
Other (wt%)	0.1	0.1	0.1	0.1	0.1	0.1	0.2	0.1	0.3

2.3.4 Tolerances for Impurities

Besides the composition of the recycled aluminium, it is also necessary to know the tolerance limits of the wrought and cast alloys for the different elements in the scrap in order to determine how much recycled aluminium can be absorbed by each alloy series.

Cast alloys have a very high capacity to absorb recycled material. According to literature, recycled aluminium can constitute 99,3 wt% or even more of the total aluminium mass in typical applications for cast alloys [15] [16]. The small fraction of primary aluminium that has to be added to recycled aluminium for the production of cast alloys, is neglected in this thesis. Modaresi et al. also neglect the required aluminium for diluting cast alloys in their calculations to forecast the emergence of a scrap surplus, since this simplification only has a very small impact on the overall result [16]. The maximum recycled content of cast alloys is therefore 100% in this model.

Wrought alloys on the other hand, have much tighter restrictions on the presence of alloying and tramp elements. The maximum tolerance for alloying elements and other contaminants is also included in Table A.0.1 to Table A.0.9 for all selected representative alloys. The maximum tolerance of each alloy series for each element is determined by taking the most critical limit from the representative alloys in that series. For example, the representative alloys for the 5000 series are the 5005 alloy, the 5052 alloy and the 5083 alloy. The tolerance for manganese of these alloys is 0,2wt%; 0,1wt%; and 0,15wt%; respectively. The tolerance of the 5052 alloy is with 0,1wt% the lowest and therefore most critical value. This value is chosen as the tolerance for manganese for the 5000 series. Choosing the lowest value for the tolerance guarantees that the amount of recycled aluminium that can flow to the 5000 series is not overestimated. The tolerances for each series are mentioned in Table A.0.1 to Table A.0.9, in the column on the left of the one that indicates the composition of the alloy series.

2.3.5 Secondary Aluminium Flows

As such, all the information is present to calculate the amount of recycled aluminium that can flow to the different alloy series. An additional assumption here is that the recycled aluminium still has the same composition as the collected scrap from which it is made, therefore assuming that the recycling process itself does not change the composition of the collected scrap. As mentioned, pre-melting and

melting losses occur during recycling, causing a slight decrease in the amount of recyclable aluminium. So, the assumption here is that these limited losses do not impact the composition of the aluminium scrap.

Table 2.2 shows which limits the elements in the recycled aluminium impose on the recycled content of the different wrought alloy series in 2020. As mentioned, the maximum recycled content of the cast alloys is assumed to be 100%. To be clear, the recycled content is defined here as the portion (mass fraction) of recycled aluminium in the total amount of aluminium that is used for the production of the different alloy series. The limits on the recycled content are calculated by dividing the tolerance of an alloy series for an element by the mass fraction of that element in the collected scrap. For example, the tolerance of the 5000 series for copper is 0,1wt%. Copper constitutes 0,94wt% of the collected scrap in the year 2020. Therefore, the maximum recycled content that copper imposes on the 5000 series in 2020 is 0,1wt% divided by 0,94wt%; which is a little more than 10%. In the table, all calculated values are rounded down to a whole number, again to avoid overestimating the amount of recycled aluminium that can be used for the production of wrought alloys. By rounding down the numbers, they also remain constant between 2020 and 2040, the critical time period for the emergence of the scrap surplus.

Table 2.2: Limits to Recycled Content of Wrought Alloys

	1000	2000	3000	4000	5000	6000	7000	8000
Cu	5%	100%	26%	31%	10%	10%	100%	5%
Fe	100%	100%	100%	100%	93%	93%	32%	100%
Mg	4%	4%	100%	4%	100%	89%	100%	4%
Mn	17%	100%	100%	17%	34%	34%	20%	17%
Si	9%	19%	11%	100%	10%	23%	4%	5%
Zn	8%	42%	42%	16%	16%	16%	10%	16%
Other	36%	90%	90%	90%	90%	90%	90%	90%

The most critical limit for each alloy series is marked in yellow. For the 1000, 2000, 4000 and 8000 series, the recycled content is limited to 4% by the presence of magnesium in the collected scrap. The limit for the recycled content lies on 11% for the 3000 series, with silicon as the most critical element. Both copper and silicon put a limit of 10% on the recycled content of the 5000 series. The limit for the recycled content of the 6000 series lies on 10%, with copper as the most critical element. For the 7000 series, silicon puts a limit of 4% on the recycled content. Since the calculation of these percentages involves a number of uncertainties, a sensitivity analysis is on order to demonstrate the effect of changes in these percentages on the most important results.

What is also apparent from the calculated limits is that some elements put no restrictions at all on the recycled content of some alloy series. This is the case when the tolerance of an alloy series for a certain element is higher than the concentration of that element in the collected scrap. The calculated fraction for the recycled content is then higher than 100%, but since this is not a feasible value for a recycled content, the value is rounded down to 100%. Silicon, for example, puts no limit on the recycled content of the 4000 series. This is because the 4000 series has a tolerance for silicon that is higher than the amount of silicon that is present in the scrap. The combinations of the elements and the alloy series for which this is also the case, are marked in orange.

2.3.6 Primary Aluminium Flows and Scrap Surplus

At this point in the calculations, it is clear how much of the recycled aluminium can flow to the wrought and cast alloys. With this information, the flows of primary aluminium to the different alloy series are also immediately determined. The amount of primary aluminium that flows to the wrought alloy series is the difference between the total demand for wrought aluminium and the amount of recycled aluminium that flows to the wrought alloys.

As long as the flow of recycled aluminium that cannot go to wrought alloys, is smaller than the demand for cast alloys, it can be absorbed entirely by the cast alloys. In that case, the flow of recycled aluminium to the cast alloys is supplemented with primary aluminium to satisfy the total demand for aluminium for cast alloys. However, if the amount of recycled aluminium exceeds the capacity of both wrought and cast alloys to absorb this material, there is no destination left for this flow.

The amount of collected aluminium scrap that cannot flow to either wrought or cast alloys is called the scrap surplus. This scrap is unrecyclable due to a lack in demand for this material. This fraction can not flow to the manufacturing phase and therefore, in the Sankey diagram, this flow stops halfway between the resource phase and the manufacturing phase. With that, all flows in the model are calculated.

2.3.7 Refinement of IAI Future Data

The last step in the development of the model is the adjustment of some future data. In the period between 2030 and 2040, the developed model relies on the projetions of the European Aluminium Institute instead of the IAI for the evolution of the demand for aluminium and the amounts of collected scrap. The projections of the EAA are based on a more recent research and are also somewhat more realistic than what the IAI predicts in this period. In the latest update of the global flow model of the IAI, the demand for aluminium grows sharply in the years 2030, 2031 and 2032. In the period between 2033 and 2040 there is almost no growth. The amount of collected scrap follows a similar trend. The EAA on the other hand, predicts a more constant growth rate (see Figure 2.20) [14]. Since no apparent reason is available for the accelerated growth between 2030 and 2032 and the lack of growth in between 2033 and 2040, the projections of the EAA are preferred as a base for the calculations between 2030 and 2040.

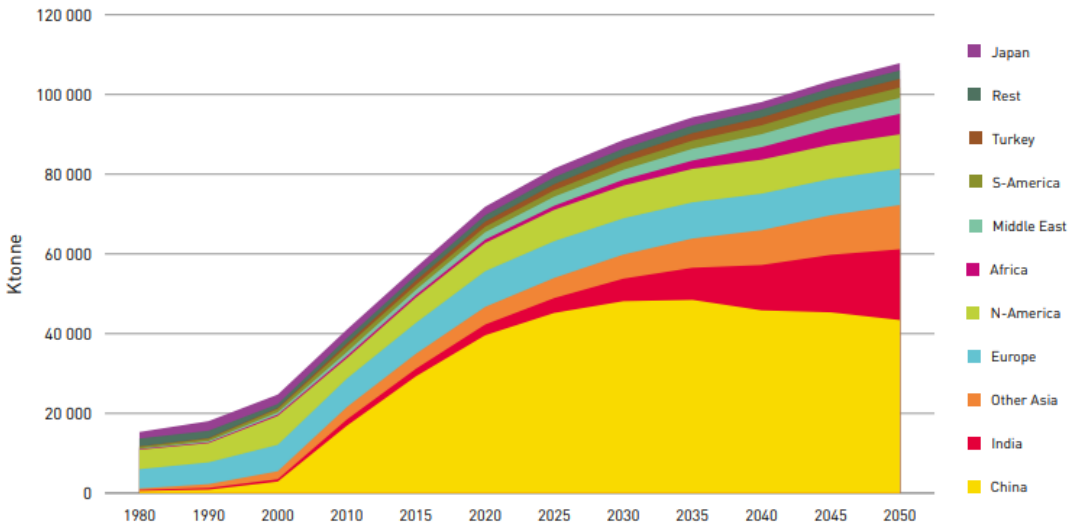

Figure 2.20: Global Demand for Primary Aluminium, EAA Projections [14]

2.3.8 Visualisation

The calculations of the model, made in a Microsoft Excel Workbook, are visualised in the form of a Sankey diagram in Python.

2.4 Results

2.4.1 MFA

Figure 2.21 shows the Sankey diagram for the calculated aluminium flows in 2030. The nodes in the diagram are ordered so that the flows can be followed in an intuitive way through the different life cycle phases of the aluminium. From left to right, the aluminium flows from recycled or primary sources in the resource phase through the manufacturing phase and use phase to the End-of-Life phase, where some of the aluminium returns to the resource phase in the form of recycled aluminium. The part of the diagram between the resource phase and the manufacturing phase gives detailed information about the flows of alloys to the different sectors. The Sankey diagrams for the years 1951, 1960, 1970, 1980, 1990, 2000, 2010, 2020, and 2040 can be found in Appendix B (Figure B.0.1 to Figure B.0.9).

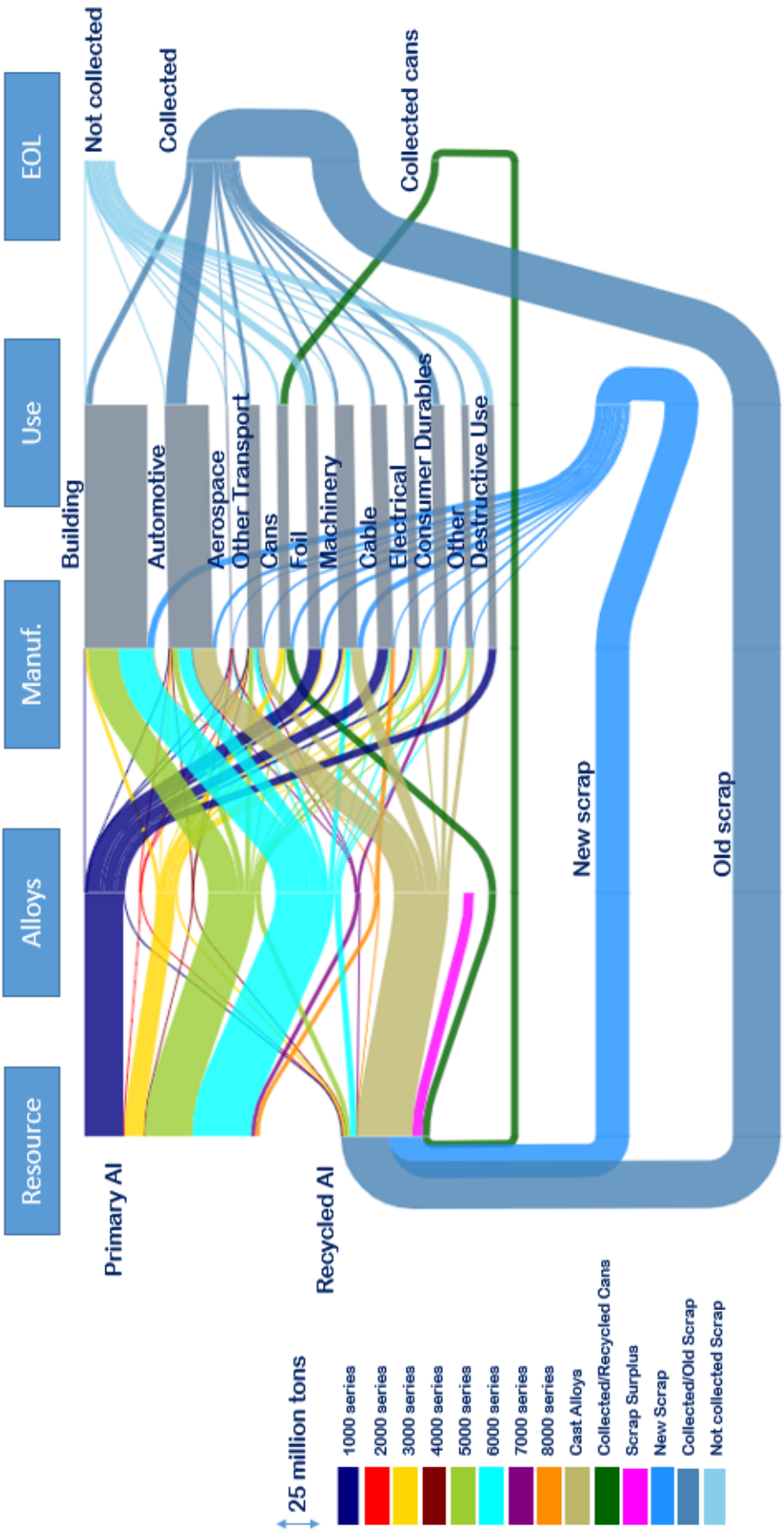

Figure 2.21: Sankey Diagram for 2030

In the model, the amount of recycled UBC flows directly to the node for cans in the manufacturing phase. This way of modelling the unique recycling method for aluminium beverage cans results in high values for the recycled content of newly manufactured beverage cans. For the year 2019, the model calculates a global average of 55% for the recycled content of newly fabricated beverage cans. If the recycling of aluminium cans would be modelled in the same way as the other collected old scrap, the calculated recycled content would only be around 11%.

Based on data from around the globe, 55% seems a much better estimate for the global average recycled content of beverage than 11%. In the United States, the American Aluminum Association reports an average recycled content of 73% for aluminium beverage cans, based on research in collaboration with the Can Manufacturers Institute (CMI) [80] [81] [82]. In Europe, the estimated recycled content of new beverage cans was around 47% in 2019 [83]. Due to large regional differences in the collection rates of aluminium beverage cans in EU and EFTA countries (from more than 98% in Germany, Norway, Finland and Belgium to less than 40% in Malta, Romania, Hungary and the Czech Republic), Europe does not succeed in attaining the same level of recycled content as the US [84]. Many developed and even developing countries succeed in achieving higher collection rates of aluminium UBC than Europe. The Japan Aluminium Can Recycling Association and the Japan Metal Bulletin both report Japanese collection rates of around 90% for aluminium UBC since 2005, compared to the record number of 74,5% in Europe in 2017 [84] [85] [86] [87]. The Brazilian Aluminum Association (ABAL), the Brazilian Association of Highly Recyclable Cans Manufacturers (ABRALATAS) and the Argentine Chamber of the Aluminum and Related Metals Industry (CAIAMA) have reported UBC collection rates of well over 90% for the past 15 years in Brazil and Argentina [86] [88]. Based on the different regional reports, the IAI puts the global average for the collection rate of aluminium UBC at 71%. For a collection rate of 71%, a recycled content of 55% seems a reasonable estimate, considering the fact that European beverage cans have a recycled content of 47% for a recycling rate of 74,5%. In any case, this way of modelling the flow of recycled UBC is much more accurate than when this flow would be added to the rest of the old scrap.

The high recycled content of aluminium beverage cans shows the large advantage of collecting UBC separately from other scrap. The next chapter examines techniques of sorting mixed collected scrap. However, other research has looked into the possibilities of collecting more aluminium scrap at the source of the waste, as is the case with UBC. Aluminium can already be collected very efficiently and in a profitable way from demolition sites in Europe [89]. Enhanced dismantling of End-of-Life Vehicles (ELV) can also contribute to separate more wrought aluminium alloys from the rest of the mixed metal scrap in an early stadium of the recycling process. However, the amount of aluminium that can be dismantled in a way that is technically end economically viable is currently limited in most car models [16]. Dismantling is also complicated by the growing trend to integrate more hybrid structures and use more multi-material designs in new car models [90] [91] [92] [93].

Another measure that would help to increase the maximum recycled content of wrought alloys and reduce the size of the scrap surplus is keeping the new scrap separated from the old scrap. Usually, new scrap has a far more homogeneous composition than old scrap, but since these two sorts of scrap are often collected in the same recycling facilities, a lot of potential gets lost. So far, the aluminium industry did not have many incentives to invest in methods to keep different alloys separated from each other. However, with the threat of a looming scrap surplus and under pressure to reduce its environmental impact, the aluminium industry is looking at a combination of tools to bolster its recycling capabilities.

2.4.2 Scrap surplus

The possible emergence of an aluminium scrap surplus has been mentioned already a couple of times in this thesis as one of the largest incentives of the aluminium industry to invest in methods that allow more wrought-to-wrought recycling. One of the advantages of this model is that it allows to estimate how imminent the scrap surplus is and how large it can become in the coming decades if no interventions are made to ramp up recycling capabilities. However, the calculation of the size of the global scrap surplus involves some serious uncertainties. Therefore, three graphs are used to present the size of the scrap surplus and its sensitivity to the most crucial parameters in the model.

In the developed model, the forecasted evolution in the demand for cast alloys in passenger cars relies on the projections of Modaresi et al., as explained in the *Materials* section [16]. In these projections, the share of cast alloys in the total demand for aluminium in the automotive sector plummets from more than 60% in 2010 to only 50% in 2040. However, other researchers have assumed different numbers for the demand for cast alloys, even for the period before 2015, when the sales of electric vehicles still constituted a negligible share of the total global car sales [20] [41]. Predictions for the future demand of cast alloys for cars and light trucks vary extremely, depending on the consulted source, due to the large uncertainty in the rate at which electric vehicles will increase their share in the car market in the coming decades.

To account for the uncertainty in the demand for cast alloys, the evolution of the scrap surplus is presented here for different scenarios. The projections of Modaresi are taken as a baseline scenario for the evolution of the share of cast alloys in the total demand for aluminium in the sector of autos and light trucks (see Figure 2.22). In addition, the size of the scrap surplus is calculated for three other scenarios. In a first alternative scenario, the share of cast alloys is decreased by 10 percentage points in comparison to the baseline scenario, for every year in the investigated time frame. Instead of falling to 50% in 2040, the share of cast alloys falls to 40% in this scenario. This scenario corresponds to a significantly faster penetration of electric vehicles in the car market. A second alternative scenario represents a situation where the share of cast alloys is 10 percentage points higher than in the baseline scenario. In 2040, the share of cast alloys reaches a minimum of 60% in this scenario. This situation corresponds to a slower penetration of electric vehicles. The third alternative scenario represents a situation where the share of cast alloys is even 20 percentage points higher than in the baseline scenario. In this scenario, cast alloys would still constitute 70% of the total aluminium use in global passenger cars. This is a very unrealistic scenario, since this would mean that the global use of cast alloys would still be at the same level as for European cars in 2010 [41]. Nevertheless, this scenario makes clear that even without the changes in demand in the automotive sector, a scrap surplus would probably still emerge eventually, which is interesting to consider.

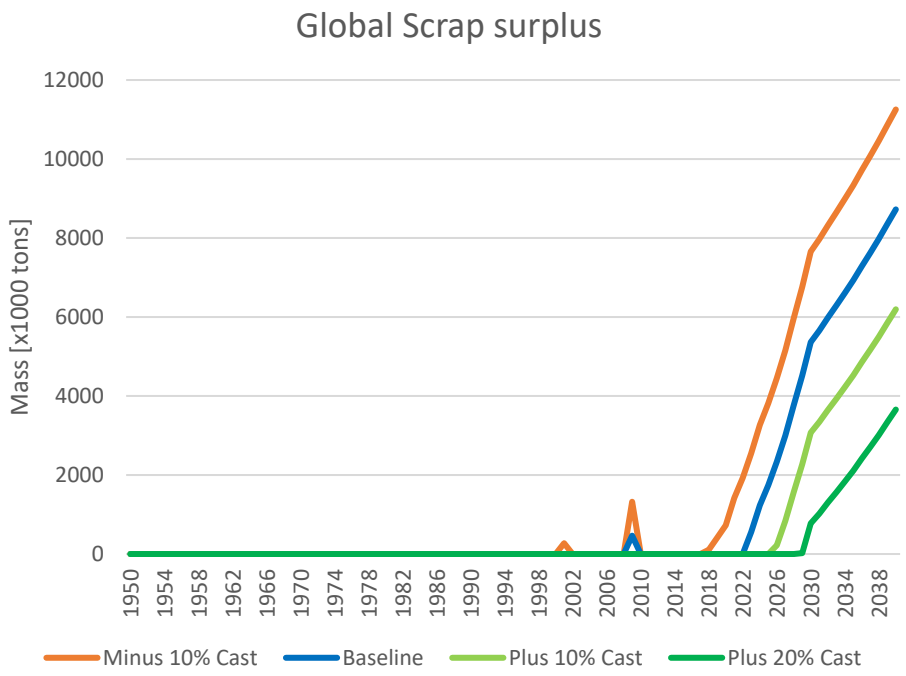

Figure 2.22: Sensitivity of the Global Scrap Surplus to the Use of Cast Alloys in Passenger Cars and Light Trucks

According to the calculations in the baseline scenario, a small scrap surplus first surfaced in 2009, the year that the global economy contracted by almost 2% [94]. In the year of the recession, the London Metal Exchange suffered significant financial losses when its stock of aluminium increased by 152% in one year to 2,34 million tons due to a massive collapse in demand for aluminium [95]. However, it is difficult to prove the contribution of the scrap surplus to this incident, since the largest part of these stocks was probably the simple result of the overproduction of primary aluminium, as the sudden collapse in demand took many aluminium producers by surprise. In all other years before 2023, the model reports no scrap surplus in the baseline scenario. Starting from 2023, a scrap surplus is consistently present until the end of the investigated time frame. The scrap surplus grows quickly to 5,4 million tons of aluminium in 2030 and then continues to grow on a slower pace to around 8,7 million tons in 2040.

Looking at the situation for the alternative scenarios makes clear that the transition towards electric vehicles will have a large influence on both the size of the scrap surplus and when it first emerges. In the first alternative scenario, that assumes an accelerated penetration of electric vehicles in the car market, a scrap surplus of 0,7 million tons is already predicted in 2020. The other scenarios assume that more time will pass before a scrap surplus occurs. Variations in the demand of cast alloys are so consequential because they can have a recycled content of almost 100%, compared to less than 10% for wrought alloys. Since there is such a large difference in the extent to which cast and wrought alloys can absorb the low-purity recycled aluminium, even limited deviations in the estimated shares can seriously impact the calculation. Deviations in the shares among the different wrought alloy series will be less consequential since the capacity of the various alloy series to absorb recycled aluminium differs not that much compared to the difference between the cast and the wrought alloys.

This does not mean, however, that the average recycled content of wrought alloys has little influence on the results of the calculations. In fact, errors in the estimates of the recycled content of the wrought alloy series could also seriously influence the results of the calculations. The calculated recycled

content for the different alloy series is 4% for the 1000 series, 4% for the 2000 series, 11% for the 3000 series, 4% for the 4000 series, 10% for the 5000 series, 10% for the 6000 series, 4% for the 7000 series and 4% for the 8000 series. As these numbers follow from a series of assumptions and simplifications, a high accuracy is not guaranteed. Especially if the average of these numbers would not be close to the real value, this error would significantly distort the calculated size of the scrap surplus.

Figure 2.23 shows again the calculated size of the scrap surplus in the baseline scenario. This time, two alternative scenarios demonstrate the influence of the recycled content of the wrought alloys on the results of the calculation. In the first alternative scenario, the recycled content of all wrought alloys is lowered by 3 percentage points. This reduction brings the values of the recycled content to 1% for the 1000, 2000, 4000, 7000 and 8000 series; to 7% for the 5000 and 6000 series; and to 8% for the 3000 series. The weighted average of the recycled content of all wrought alloys is around 5,5% in this scenario for the period between 2020 and 2040, compared to 8,5% in the baseline scenario. In the other alternative scenario, the recycled content of all the wrought alloy series is increased by 3 percentage points, bringing the weighted average to 11,5% for the period between 2020 and 2040.

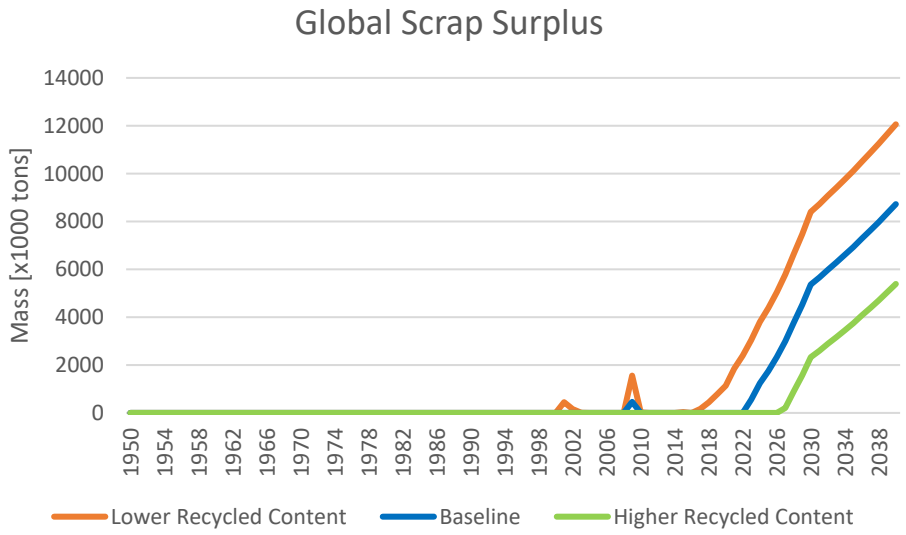

Figure 2.23: Sensitivity of the Global Scrap Surplus to the Recycled Content of Wrought Alloys

A comparison between the three scenarios shows that the recycled content of wrought alloys is also a very important parameter for the calculation of the scrap surplus. A deviation of 3 percentage points in the average recycled content has a similar effect as changing the share of cast alloys in the total use of aluminium in passenger cars by 10 percentage points. However, the errors in the estimated values for the recycled content of the wrought alloy series are probably not as large as 3 percentage points.

The LCI database Ecoinvent bases its calculations for the environmental impact of wrought alloys on the assumption that primary aluminium constitutes 90% of the total mass of wrought alloys and that the other 10% comes from new scrap [96]. This estimation does not consider the difference in tolerances for impurities between the different wrought alloy series. So, Ecoinvent sees 10% as a probable value for the average recycled content of wrought alloys, provided that only new scrap is used. In that light, 8,5% seems a reasonable value if the recycled aluminium contains a mix of old and new scrap.

Finally, Figure 2.24 shows how a combination of a deviation in the demand for cast alloys and a deviation in the recycled content of wrought alloys can influence the calculation of the size of the

scrap surplus. Apart from the baseline scenario, the figure shows a worst case and a best case scenario for the evolution of the scrap surplus. In the worst case scenario, the share of cast alloys in the total demand for aluminium in the sector “Auto & Light Truck” is 10 percentage points lower than in the baseline scenario and the recycled content of all wrought alloy series is 3 percentage points lower. In the best case scenario, the share of cast alloys in the total demand for aluminium in the sector “Auto & Light Truck” is 10 percentage points higher and the recycled content of all wrought alloy series is 3 percentage points higher.

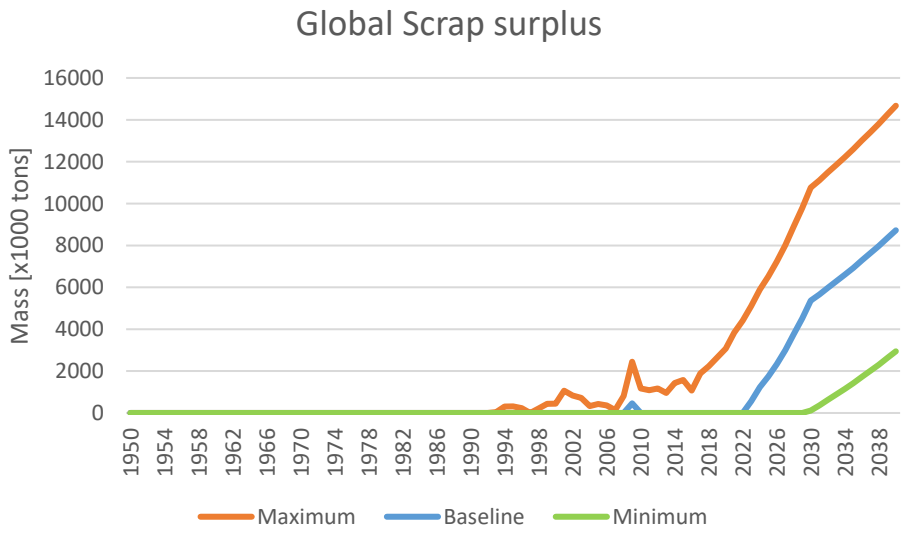

Figure 2.24: Range of Probable Values for the Size of the Scrap Surplus

Larger deviations from the baseline scenario are highly improbable, since in both the worst case and best case scenario, the values for the demand for cast alloys and the recycled content are on the extremes of what could be considered realistic. Therefore, the values for the size of the scrap surplus in the worst case and best case scenario delimit a range of probable values for the evolution of the scrap surplus in the coming decades. The values for the scrap surplus in the worst case scenario can be considered as a maximum of what can be expected, while the values in the best case scenario can be considered as a minimum.

2.4.3 Scrap Composition

In addition to calculating the size of the aluminium flows, this model allows to estimate the composition of most flows. As explained, it is possible to estimate the elemental composition of all scrap that is collected for recycling in a certain year. Figure 2.25 shows the elemental composition of all collected scrap in 2020. The amounts of recycled aluminum that can flow to the different alloy series in 2020 are calculated based on this composition.

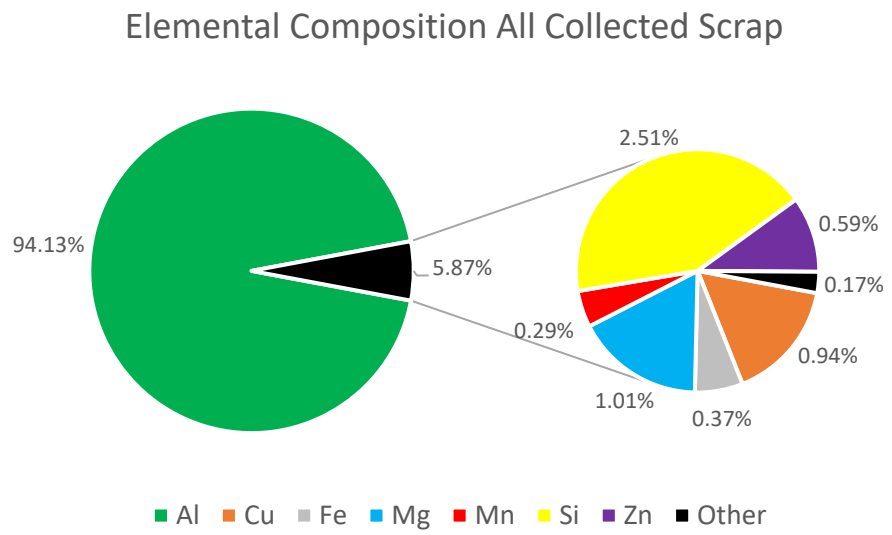

Figure 2.25: Elemental Composition All Collected Scrap

It is also possible to calculate the composition of scrap from a specific origin. Figure 2.26 shows the estimated composition of aluminium scrap collected from the "Auto & Light Truck" sector in 2020. If recycling companies know from which sectors their collected scrap originates, the results from this model allow them to make a first estimate of the elemental composition without doing any measurements. Even if the collected scrap originates from multiple sectors, it remains easy to estimate its composition, as long as the recycling companies know what the shares are of the different sectors in the total amount of collected scrap.

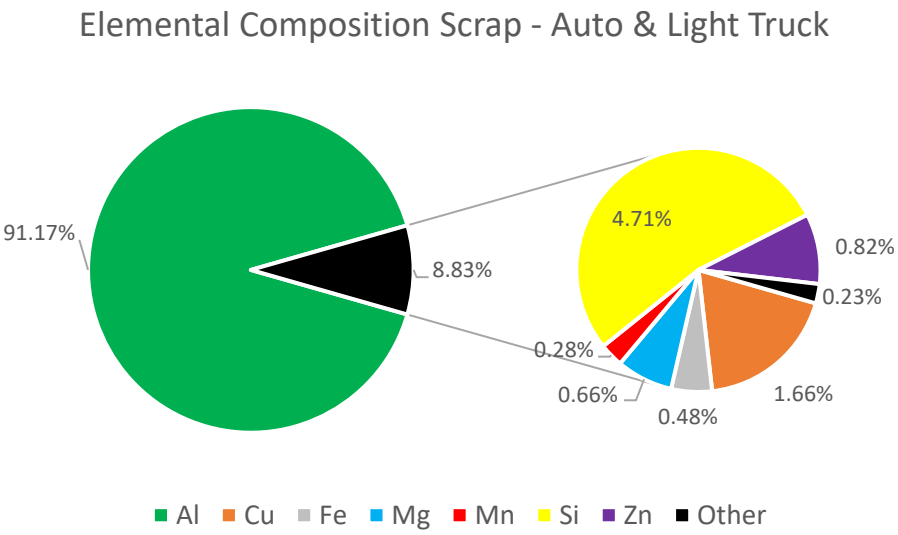

Figure 2.26: Elemental Composition Scrap – Auto & Light Truck

2.5 Discussion

The developed model offers a large number of useful insights in the global flows of aluminium. One of the most important conclusions is that there is a high probability that a significant scrap surplus will emerge in the coming decade. According to the calculations in the baseline scenario, a scrap surplus already emerges in 2023, grows to a size of 5,4 million tons by 2030 and reaches a size of 8,7 million tons by 2040. A scrap surplus of such magnitude is definitely problematic for the aluminium industry.

According to these calculations, the scrap surplus would constitute 11,4% of all collected aluminium scrap in 2030. This would mean that in 2030, only 88,6% of all collected and processed aluminium scrap could be used for the production of new wrought and cast alloys. By 2040, this share would rise from 11,4% to 15,8%. In such situation, the use of primary aluminium would continue to grow despite the abundant availability of aluminium scrap.

This prediction is relatively close to what other researchers predict. Hatayama et al. estimate the size of the scrap surplus at 6,1 million tons in 2030 [20]. Hatayama et al. do not base their calculations on the data of the IAI but use their own estimates for the lifetime of aluminium products and for the demand for aluminium in the different sectors [97]. Modaresi et al. forecast a scrap surplus of 4,2 million tons in 2030 that will grow to a size of 14 million tons by 2050 [16] [23]. However, they add that due to the uncertainty in their parameters, the actual size of the scrap surplus could lie anywhere between 3,3 and 18,3 million tons in 2050. For the calculation of the scrap surplus, Modaresi et al. also do not rely on the data of the IAI. Instead, they use data from the United Nations (UN), the International Energy Agency (IEA), the Organisation of European Aluminium Refiners and Remelters (OEA) and others to define relevant parameters such as global population growth, regional car ownership and the amounts of aluminium in passenger cars [98] [99] [100]. This thesis has therefore confirmed the conclusions of previous research in a unique way.

Based on the comparison of the developed model with the results of the other researchers, it seems likely that the actual size of the scrap surplus will be much closer to the calculated values in the baseline scenario than the values in the worst case or best case scenario in Figure 2.24. In 2030, the developed model predicts a scrap surplus of 5,4 million tons. This is 0,7 million tons less than what Hatayama predicts, and 1,2 million tons more than what Modaresi predicts. However, these differences are much smaller than the difference between the values in the worst and best case scenario in the model. In the worst case scenario, the scrap surplus is 5,3 million tons larger than in the baseline scenario. In the best case scenario, the scrap surplus is 5,3 million tons smaller, with a size of only 0,1 million tons. The fact that the baseline estimate in this model and the estimates of the other researchers lie in such a narrow range, suggests that the actual size of the scrap surplus will lie in the close vicinity of the baseline scenario, rather than on the extremes of the delimited range in Figure 2.24. In addition, under the conditions of the worst case scenario, a scrap surplus of 3,1 million tons would be present already in 2020. Since no noticeable scrap surplus has been reported in 2019, this seems somewhat unrealistic. However, if the demand for aluminium would plummet as sharply in 2020 as during the 2009 recession, a considerable scrap surplus might emerge already this year.

The uncertainty in the global economic growth adds to the level of complexity in these calculations. The large number of parameters on which these calculations depend make it extremely difficult to avoid large uncertainties in the estimates of future aluminium flows and to narrow the range of probable values. Even so, thanks to the studies about the aluminium scrap flows, it has become clear what the most crucial trends are that affect the evolution of the global aluminium flows. Furthermore, among the researchers who have investigated the evolution of the scrap surplus most thoroughly (Modaresi, Müller, Hatayama, Bertram, Rombach, Martchek and other authorities on the matter), there has grown a great consensus that the only way to mitigate the generation of unrecyclable scrap is alloy-based sorting of the collected aluminium scrap [16] [20] [23] [36].

2.6 Conclusion

The results of this chapter provide information on the size and composition of the aluminium flows that are most crucial for stakeholders in the recycling industry. The evolution of the size of the scrap surplus has been estimated, and the factors that have a major influence on this evolution have been

explained. The possible emergence of a scrap surplus is one of the largest challenges for the goals of the aluminium industry to increase its sustainability. Therefore, a proper understanding of the scrap surplus is crucial in order to find appropriate solutions for this problem.

Based on the results, recycling companies can also anticipate the composition of aluminium scrap that they collect from different sectors. Provided with this information, recycling companies can develop intelligent strategies to sort aluminium scrap, both at the source of the scrap and at the end of their sorting chain. By collecting and sorting aluminium scrap at the source, for example at demolition sites, recycling companies can avoid that the aluminium gets mixed with other materials. This way, a large number of sorting steps can be avoided, and the composition of the collected aluminium will be very homogeneous, as is the case for collected UBC. The calculations in the model show that the closed-loop recycling system for aluminium cans allows a significantly higher recycled content than what can be achieved from the recycling of mixed aluminium scrap. However, as this recycling strategy is not technically and economically feasible for all aluminium products, alloy based sorting must also happen "post-shredder", at the end of the sorting chain of aluminium recycling facilities, in order to sort the mixed aluminium scrap into different valuable subcategories of alloys.

The next chapter investigates how mixed aluminium scrap in a Belgian recycling facility can be optimally sorted with alloy based sorting methods to achieve a maximum financial return. This chapter has provided some crucial data for that purpose. Convincing recycling companies that alloy based sorting can be financially attractive is crucial for the rapid integration of enhanced sorting systems in existing recycling facilities. Only when alloy based sorting methods will be implemented on a large scale in Europe and the rest of the world, it will be possible to reduce the size of the scrap surplus or even eliminate it entirely. Therefore, alloy based sorting will be essential to achieve the environmental goals of the European aluminium industry.

3 Alloy Based Sorting

3.1 Introduction

The previous chapter has shown that soon, the current way of recycling might generate a considerable amount of unrecyclable aluminium scrap. If this situation would arise, the scrap would either have to be landfilled, sold at a much lower price to be used in low-value applications (as a substitute for iron or steel), or refined at a significant cost to upgrade the purity of the scrap. The extent to which companies would resort to the different options, depends on economic and legislative factors [101].

Neither of these options is attractive for the recycling companies or the environment. Therefore, many stakeholders in the aluminium industry have investigated methods to enable a higher share of recycled aluminium in the production mix of wrought alloys. As a result, a wide range of techniques has been developed, based on different physical principles, and with varying capabilities. Most research has focused on alloy based sorting techniques. These techniques allow recycling companies to sort out pieces of scrap that can be used for the production of certain wrought alloys. Simultaneously, some research has focused on chemical and metallurgical techniques to refine the aluminium scrap. These techniques are less interesting as a large scale solution for the recycling challenges since they are more energy intensive, more polluting, and more expensive than sorting, but they also allow recyclers to valorise low-purity scrap that would otherwise be difficult to sell [8].

Many sorting techniques have to some degree demonstrated success in sorting aluminium scrap into different groups of alloys. However, a great number of factors play a role in determining the economic and environmental value of a sorting technique [102]. For recycling companies, it is most important that the sorting process adds enough value to the scrap to justify its investment and operating costs. The reason why the developed enhanced sorting techniques are not yet integrated in most aluminium recycling facilities is that most of the developed sorting techniques struggle to attain sufficient added value under suboptimal circumstances.

One of the oldest techniques that has been tested for the separation of aluminium alloys is X-ray Transmission (XRT). XRT is best known for its application in airport luggage inspection, but it can also be used to identify metals, glass and plastics [103] [104]. XRT technology relies on differences in atomic densities between different materials [105]. The technique can identify target aluminium alloys by analysing the mass-absorption coefficient of the measured samples, which depends on their elemental composition [106]. However, since the ability of XRT to distinguish differences in composition is quite limited for aluminium alloys, the technique has been tested in combination with other techniques, such as XRF, eddy current separation and electromagnetic sensors, to improve its sorting accuracy [74] [107] [108].

Researchers of TU Delft have demonstrated that a combination of XRT and electromagnetic sensors can achieve reasonably good sorting results for a batch of mixed non-ferrous scrap. The electromagnetic sensors (EMS), that measure the interaction between the metal particles and the generated electromagnetic field, are particularly helpful for detecting stainless steel. However, the combination of the two techniques still fails to deliver very high sorting accuracies for aluminium alloys. The researchers used two measures for the sorting accuracy of the system: the grade and the recovery, also referred to as purity and yield. These are common concepts that are used to evaluate a wide variety of sorting processes [109] [110]. The grade of a sorting output is calculated by dividing the mass of desired material in the output by the total mass of the output. The recovery is a measure of how much of a certain material has ended up in the right output, for example how much of the wrought alloys in the mixed scrap ended up in the output stream of wrought alloys. In the experiment, the grade of the cast aluminium alloys was 81% at a recovery of 68%. The grade of the wrought

aluminium alloys was 70% at a recovery of 50%. The grades of stainless steel and magnesium were over 90% at recoveries over 85% [107]. This experiment shows that while the performance of XRT, even in combination with EMS, might overall be reasonably good for the sorting of mixed non-ferrous scrap, it is not particularly good at sorting wrought aluminium alloys from cast alloys.

Under ideal conditions, using flat and clean standard samples, better sorting results have been reported for a combination of XRT and eddy current separation [74]. It is, however, highly uncertain if these results can be reproduced under more realistic circumstances for post-consumer waste. Eddy current separation has also been tested on its own for the separation of different aluminium alloys. Hannula et al. have demonstrated the possibility to separate copper-rich aluminium samples from the rest of the aluminium scrap with a sequence of two eddy current separators, which enabled the production of two 2000 series wrought alloys from scrap, with only a small addition of primary aluminium [38]. Using eddy current separators to separate 2000 series alloys from other alloys can work to a certain extent since the electrical conductivity of copper is significantly higher than that of aluminium and the other alloying elements [8]. However, the differences in electrical conductivity among the other alloying elements are much smaller, which makes it almost impossible to apply this sorting technique for the production of other wrought alloy series.

Aluminium sorting also happens in some cases based on colour and shape. Automated colour sorters can separate magnesium alloys from aluminium alloys with an accuracy of more than 99% [111]. Wrought aluminium alloys can also be separated from each other to some extent. By etching the alloys with different chemicals in consecutive steps, mixed aluminium scrap can be divided into three clusters: a group of 2000, 3000 and 7000 series alloys; a group of 5000 and 6000 series alloys; and a rest group [112]. This is possible because the etching chemicals procure different colours on the surface of the aluminium scrap when they react with the present alloying elements. Separating the alloys in these clusters is to some extent useful, but the process is time consuming and the use of etching chemicals is costly and harmful for the environment. Furthermore, since the alloys cannot be sorted more specifically, this process is by itself not economically viable [113]. More advanced techniques with state-of-the art cameras are currently being developed to sort aluminium alloys, based on both their size and shape, in order to avoid the use of etching chemicals [106].

Aluminium sorting based on colour and shape also exists in a much less technological setting. Manual sorting in countries with a low labour cost can often successfully compete with automatic sorting methods in developed countries [106]. Chinese workers can reportedly achieve sorting accuracies of 99% while sorting non-ferrous automotive shreds, as such outperforming most automated processes that are designed to do similar tasks [114]. The high accuracy of experienced manual sorters explains why this way of sorting can stay competitive.

For the purpose of separating wrought alloys from cast alloys, a unique and accurate method has been developed by the U.S. Bureau of Mines. Heating aluminium above a temperature of 520-560°C makes cast alloys brittle while wrought alloys remain ductile. Hammering or crushing the heated aluminium reduces the pieces of cast alloys to dust, while the wrought alloys remain intact. This makes the alloys easy to separate based on size. This method, called the hot-crush technique or thermomechanical separation, allows to separate wrought alloys with a purity of 95% [113]. However, this energy intensive technique cannot be used for more specific sorting. Furthermore, reducing the size of the pieces complicates the logistics in the recycling process.

The most important recent advances in alloy based sorting have come from spectroscopic methods. X-ray fluorescence (XRF) sensors have been successfully integrated in some recycling facilities. XRF sensors emit a beam of X-rays towards the surface of the measured material, creating fluorescence

photons that can be detected by a photo cathode detector [106]. The energy of the photons is characteristic to the elements in the measured sample. That way, the detected photons indicate the composition of the measured material. At the moment, XRF is mainly used in metal recycling facilities to identify grades of stainless steel [115]. For identifying aluminium alloys, the technique is less suitable in on-line applications. XRF emissions from aluminium have a very low characteristic energy, which means that the generated photons are absorbed very quickly even in small amounts of air [8] [116]. A similar problem exists for other light elements such as silicon and magnesium. For the classification of aluminium alloys, XRF therefore relies on the detection of heavier elements. This identification method is accurate enough to recognise the alloy series of an aluminium scrap piece, but not the exact grade [28]. XRF also has the disadvantage that it penetrates the surface of the measured material only very shallowly. Therefore, the technique is very sensitive to surface contamination. Hence, the presence of contaminating elements on the surface of the measured piece can seriously distort the results of the XRF analysis.

Another spectroscopic characterisation method is Prompt Gamma Neutron Activation Analysis (PGNAA). PGNAA emits neutrons that collide with the nucleus of atoms in the measured material. Some of the neutrons are captured by the nuclei, thereby creating an unstable isotope. During this process, high-energy gamma radiation is released, that can be detected by a sensor. Comparable to the detection process of XRF, the energy intensity of the emitted gamma radiation is characteristic to the present elements in the measured material [106] [117]. The technique is mechanically simple and robust. Furthermore, since the effect of PGNAA penetrates deeper into the material, the measurement is independent of the state of the surface of the investigated piece. However, the technique is too slow to be implemented in sorting applications that require a high throughput.

Finally, the most promising spectroscopic characterisation method is Laser Induced Breakdown Spectroscopy (LIBS). A LIBS sensor is equipped with a laser that emits high-energy laser pulses at a typical wavelength of 1064 nm. The duration of the pulse is in the order of a few ns, while the pulse energy is in the order of 10 mJ [118]. The peak power of the laser pulses is therefore in the order of a few MW [26]. The energy of these laser pulses is high enough to ablate a very small amount of the material on the surface of the measured object, even if the object is a few decimetres away from the laser source. To ensure that the laser is focussed on the target when the pulse is emitted, the LIBS sensor can be controlled in different manners, for example with a distance sensor. The distance sensor triggers the emission of a laser pulse only when an object passes through the focus of the laser. Ablating the surface of a metal sample generates a hot plasma spark. Light from that spark can be detected by a light sensor and converted into an intensity spectrum by a spectrometer. From a spectrum, it is possible to deduce the chemical composition of the measured sample. Figure 3.1 shows a schematic overview of a typical LIBS setup, using a Nd: YAG laser and a Charge Coupled Device (CCD) spectrometer [26].

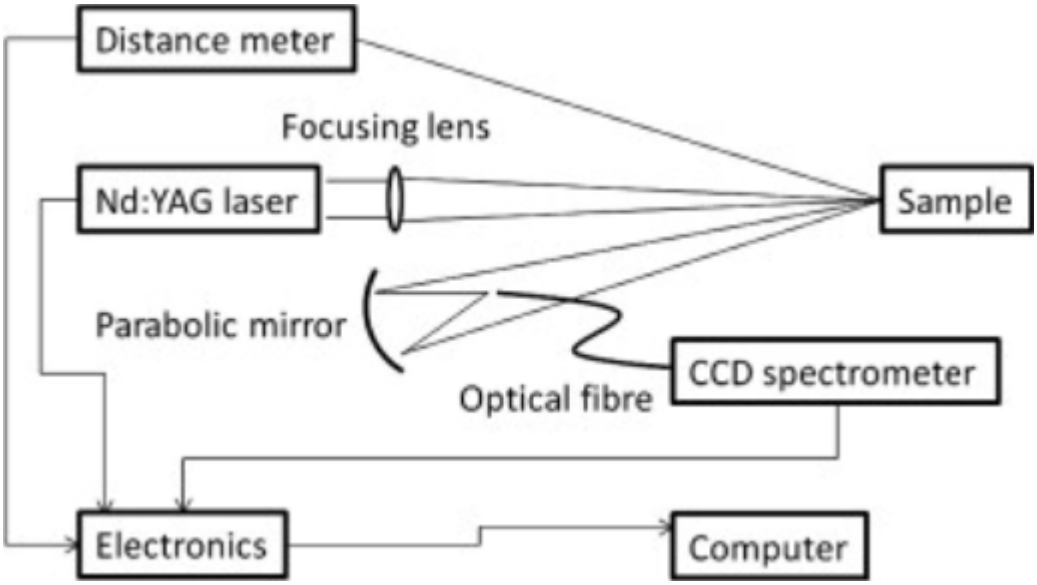

Figure 3.1: Schematic Overview of a Typical LIBS Setup [26]

LIBS has the major advantage that it can identify specific wrought and cast alloys [25]. Furthermore, it can process large volumes of scrap at high speeds [8] [116]. However, since the pulse laser can only penetrate metal to a depth of 30 ångström (3nm), the technique is very sensitive to surface contamination. Paints, lubricants, coatings, or other surface contaminants can be a major obstacle in acquiring good measurements. One solution that has been put forward for this problem is to separate the painted and coated samples with a colour sensor. These samples can then be cleaned by hot air in a fluidised-sand bed, producing cleaner, less oxidised scrap samples [113]. Alternatively, a second laser could be used to clean the sample prior to the measurement [26]. This could be a relatively cheap solution but aiming two lasers and a distance sensor at the exact same spot on a moving target is not evident, especially since the second laser has to be fired a fraction of a second later than the first one.

Hence, the design of a LIBS based sorting system comes with a number of challenges. However, the intrinsic potential of LIBS to quickly detect all alloying elements with good accuracy, makes it stand out among the multitude of techniques that have been developed in recent years. Overcoming the difficulties in designing a LIBS based sorting system will be essential to guarantee a quick adoption of the technology in existing recycling facilities. Eliminating the inaccuracies related to surface contamination is particularly important to increase the sorting accuracy of LIBS, and therefore to increase the added value of a LIBS system for recycling companies.

In this chapter, the aluminium scrap of one particular recycling facility is investigated. The goal is to investigate how alloy based sorting methods can maximise the value recovery of the mixed aluminium scrap, that is currently the end product of the recycling facility. To achieve that goal, a LIBS sensor and a handheld XRF sensor are used to identify the alloys in the aluminium scrap and to estimate the composition of all the scrap pieces. The combination of these methods is expected to lead to a reliable result that allows to determine an intelligent sorting strategy for the aluminium scrap stream.

3.2 Materials and Methods

3.2.1 Material Collection

The investigated aluminium scrap is collected at the Ropswalle site of the recycling company Galloo in Menen, Belgium. This site processes 150 000 tons of non-ferrous metals every year. The waste that arrives at the site is a highly mixed material stream from various origins. The aluminium that is included in this mix undergoes multiple sorting steps before it is completely separated from the other

collected materials. After size reduction of the input waste in a shredding process, Galloo first removes iron and fluff. Afterwards, a density separation process separates the plastics from the rest of the stream. After the density separation step, the material stream consists predominantly of metals. The common industry name for this shredded metal mix is Zorba. The Zorba fraction is sorted further by two additional density separation steps that remove magnesium, which is lighter than aluminium, and heavier metals, such as copper, zinc, and lead. The material that passes these steps goes through a sieve and an eddy current separation step. This way, rocks, cables, smaller aluminium pieces, and miscellaneous small objects are removed from the bulk of the stream. Finally, an optical separator and a magnet remove Printed Circuit Boards (PCB) and aluminium with a high iron content. The material that passes through all sorting steps is a mix that consists almost exclusively of aluminium alloys. The common industry name for this aluminium mix is Twitch (see Figure 3.2).

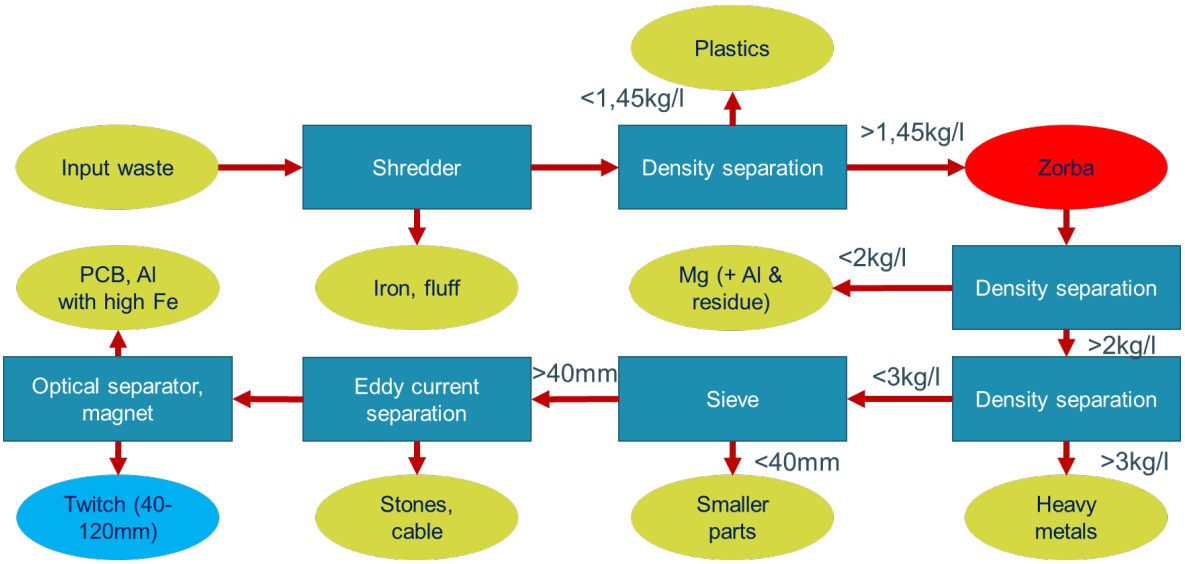

Figure 3.2: Simplified Overview of Galloo Sorting Chain

Of the 35 000 tons of aluminium scrap that enter the sorting system of Galloo at the Ropswalle site yearly, 20 000 tons end up in the Twitch (40-120 mm) fraction. The other 15 000 tons are mainly spread over three other fractions. Of the 15 000 tons of aluminium scrap that do not end up in the Twitch fraction, 10 500 tons go to the <40 mm fraction. Another significant part of the aluminium is separated together with magnesium in the second density separation step of the sorting process. Finally, some of the aluminium is separated from the Twitch fraction in the final step of the sorting process because it has a high iron concentration.

Based on their experience with the different fractions, experts from Galloo are convinced that the 40-120 mm Twitch fraction has a higher concentration of wrought alloys than the other aluminium fractions. Since the Twitch fraction is the largest aluminium fraction at Galloo and since it presumably has the largest concentration of wrought alloys, it is a logical choice to consider this fraction first for the application of alloy-based sorting methods. Therefore, 470 aluminium samples of the Twitch fraction are collected for composition analysis.

After collection, all samples of the Twitch fraction are labelled with a unique number. The weight of the individual samples is recorded, and two images (one of each side) of the samples are taken with a colour and 3D camera. These images can be used later to train deep learning models that can support the sorting system based on the appearance of the samples. As such, the gathered samples of the Twitch fraction can be the beginnings of a material library of non-ferrous scrap samples that can be used for different sorting tests and future studies.

3.2.2 LIBS Measurement

A first experiment with the collected samples is conducted at the research institute of Swerim AB in Stockholm. Swerim has constructed an experimental LIBS setup to study the characterisation and sorting capabilities of LIBS on different materials. Figure 3.3 shows a schematic top view of the LIBS sensor setup. In the setup, a nanosecond pulsed fibre laser emits a laser pulse with a wavelength of 1064 nm through a first lens, through a beam splitter, and through a second lens, onto the metal sample, at a repetition rate of 20 kHz. Light from the generated plasma spark travels back into the opposite direction until it is deflected by the beam splitter and caught by a CMOS detector (2048 pixels), that sends the light signal to the spectrometer. The spectrometer is a Czerny-Turner type CCD spectrometer from Ibsen with a spectral range of 174 – 430 nm, and a resolution of 0.15 nm FWHM (Full Width at Half Maximum). An aluminium housing protects the components and guarantees a fixed relative distance between them. The laser pulse leaves the housing by an aperture on the front of the sensor. Close to that aperture, a distance sensor is mounted that triggers the pulse laser when an object passes through the focus of the laser.

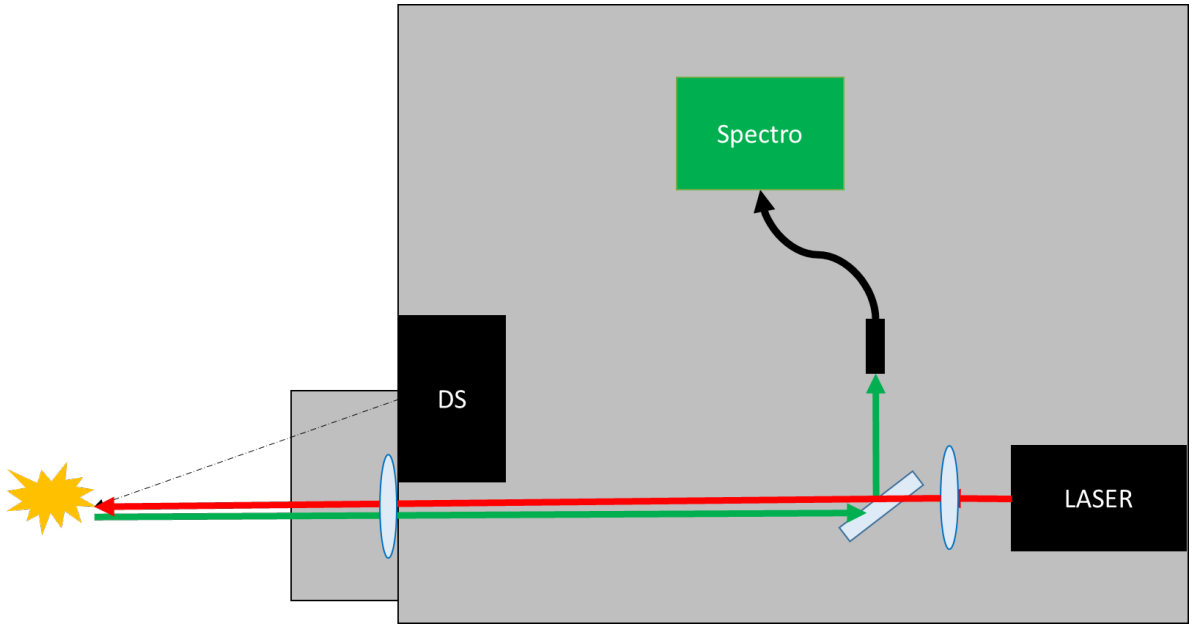

Figure 3.3: Schematic Top View of LIBS Sensor Developed by Swerim

The entire LIBS sensor is mounted by its housing a few decimetres above the conveyor belt, as shown in Figure 3.4. The samples on the conveyor belt are lined up on a grey strip in the middle of the belt to pass right under the sensor, in focus of the laser. The distance sensor and the optics can be adjusted to adapt the focal length of the laser. Every time the sensor is repositioned, these adjustments are necessary to guarantee that the focus of the laser is just above the conveyor belt, so that it can be triggered by passing scrap samples.

Figure 3.4: LIBS Setup at Swerim

In the experiment, all collected Twitch samples are passed multiple times in front of the LIBS sensor to generate a number of spectra for each individual sample. To get better measurement results, the samples are not put on the conveyor belt, but are held manually in front of the sensor. This approach ensures that the laser pulse generates a spark on a suitable part of the metal surface. Generating a spark on a painted or coated part of the surface results in very weak or completely distorted spectra. Therefore, the spark is preferably generated on a clean, flat area of the surface. Putting the samples on the running conveyor belt would yield many useless spectra for the elemental analysis, as suboptimal areas of the surface would be targeted by the laser.

The software of the spectrometer manufacturer allows to constantly monitor the measured spectra on a computer during the experiment. This way, it is possible to check that the spectrometer records spectra with a sufficient intensity for the composition analysis. For each sample, on average 40 spectra are taken, for some samples even more than 100, to guarantee at least one good spectrum for the analysis. The reason why it takes sometimes a great number of pulses to create a satisfying spectrum, is the contaminated state of the surface of some samples. Samples that are completely covered in paint have to be targeted by the laser over and over again until the laser pulses evaporate enough paint to penetrate the actual metal. This method is still faster than trying to remove the paint in another way, since the laser pulses remove the paint quite effectively and the time between two pulses can be less than one second.

All spectra are saved under the corresponding numbers on the labels, so it is clear which spectra belong to which sample. In addition, multiple spectra are collected for a set of 29 aluminium reference samples. Swerim has accurately determined the composition of the samples in this reference set in the past, with a combination of different measurement methods. These reference samples have a very flat and smooth surface, which makes it easier to perform such measurements. They are stored individually to prevent contamination with other materials. In this experiment, the reference samples are thoroughly cleaned with ethanol before and after the LIBS measurement in order to secure the reliability of the measured spectra and to preserve the quality of the reference samples.

Table C.0.1 in Appendix C shows the composition of the 29 aluminium reference samples, as recorded in the previous measurements by Swerim. The concentrations of silicon, iron, magnesium, copper,

zinc, manganese, and aluminium are determined individually. All other elements, that together accounted for 0,29% of the average weight of the samples, are not measured separately.

Figure 3.5, which is one of the recorded spectra for the 29th reference sample, illustrates well how a typical LIBS spectrum looks like for an aluminium sample. Intensity peaks in the spectrum are caused by the presence of different elements in the measured sample. The wavelengths at which the peaks occur, are linked to the elements that cause them. The American National Institute of Standards and Technology (NIST) holds extensive databases on which exact wavelengths correspond to which elements [119].

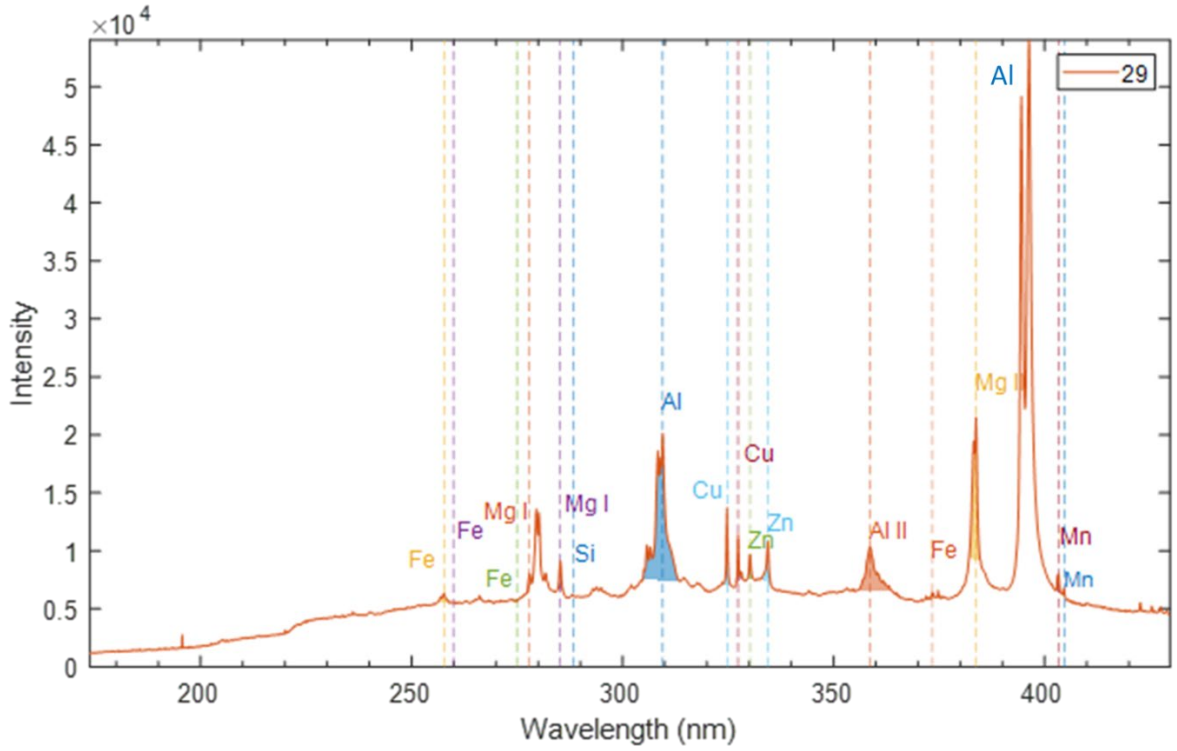

Figure 3.5: Typical Spectrum for Aluminium Samples

A single element can cause several peaks in the LIBS spectrum. Aluminium, for example, causes three intensity peaks in the range between 300 and 420 nm: one around 309 nm, one around 359 nm, and one around 396 nm [119]. Peaks can be caused both by neutral and ionised atoms. The level of ionisation of an atom is indicated in LIBS spectra by Roman numerals [120] [121]. Neutral atoms are indicated with the Roman numeral I (e.g. Al I), or simply without Roman numeral. Singly ionised atoms are indicated with the Roman numeral II (e.g. Al II). Higher levels of ionisation are indicated with higher Roman numerals.

In order to deduce the composition of the scrap samples from the recorded LIBS spectra, it is necessary to know the relationship between the intensity of the peaks in the recorded spectra and the concentrations of the corresponding elements in the samples. Such a relation can be established based on the known composition of the reference samples and their LIBS spectra. The common way in LIBS research to represent this relationship, is in the form of a calibration curve. Figure 3.6 shows a typical calibration curve, used in a LIBS application in the research field of marine biology [122]. In this example, the element of interest is magnesium, and calcium is the reference element for the measurement.

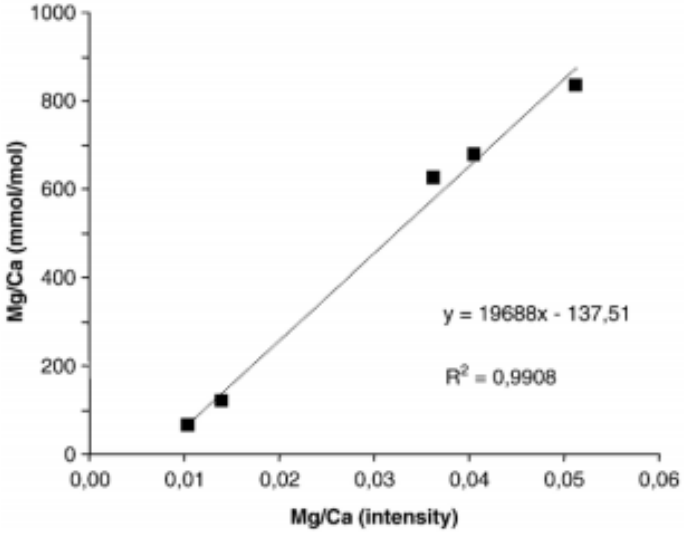

Figure 3.6: Typical LIBS Calibration Curve [122]

The x-axis of a calibration curve represents the intensity ratio between the peak of the element of interest and the peak of the reference element in the LIBS spectrum. The y-axis represents the ratio between the amount of substance, expressed in mol, of the element of interest and the amount of substance of the reference element in the sample material. Alternatively, the y-axis can represent the ratio between the masses of the two elements. This ratio should be known, as the calibration curve is based on reference samples with a known composition. All reference samples can be positioned on this graph, creating a collection of datapoints. Fitting a line or a curve to the datapoints by using, for example, a least-squares algorithm, allows to determine a mathematical relationship between the intensity ratios and the mass ratios of the two elements.

When later, more spectra are collected of materials with an unknown, but similar composition, these formulas can be used to calculate the mass ratio between the two elements on this curve, based on the intensities of the peaks in the spectra. Establishing these curves and these mathematical relationships for multiple elements, using the same reference element, allows to calculate the complete composition of the measured samples.

In this experiment, the aluminium peak at 309,51 nm is selected as the reference for the calibration. This means that the intensity of the peaks of the other elements are compared with the measured intensity of the aluminium peak at 309,51 nm to establish the calibration curves. An aluminium peak is selected as reference since the aluminium peaks have a high intensity in the spectra of all measured aluminium scrap samples. The peaks of the other elements vary significantly in intensity, since the concentration of the alloying elements in the scrap samples is also far from constant. Although there are variations in the concentration of aluminium as well among the collected samples, these differences are, relatively speaking, not as large as the variations in the concentrations of the alloying elements. Therefore, the intensity peaks of aluminium are more stable.

While there are three aluminium intensity peaks in the range between 300 nm and 420 nm, the aluminium intensity peak at 309,51 nm is by far the best candidate to serve as a reference. The two other aluminium peaks in this range are not as suitable. The intensity peak at 359 nm, caused by singly ionised aluminium atoms, is significantly weaker than the peak at 309,51 nm. The peak at 396 nm is caused by neutral atoms and is even stronger than the one at the reference wavelength. However, it is known that the peak at this wavelength is prone to self-absorption.

Self-absorption is a phenomenon whereby light, generated in the hottest region of the plasma, is absorbed by the plasma itself when it is moving away from the hot centre of the plasma through the colder outer regions [123]. Due to this effect, only a limited share of the generated light can reach the light detector on the LIBS sensor from the hottest regions of the plasma. When this phenomenon occurs, it is very easily recognisable in the spectra. The intensity at the centre of the peak is greatly reduced, due to the limited detection of the light from the hottest region of the plasma. The top of the peak is in fact inverted, thereby splitting the peak in what appear to be two smaller peaks close to each other (see Figure 3.7) [124] [125] [126]. This phenomenon is also visible in Figure 3.5, where the aluminium peak at 396 nm is inverted.

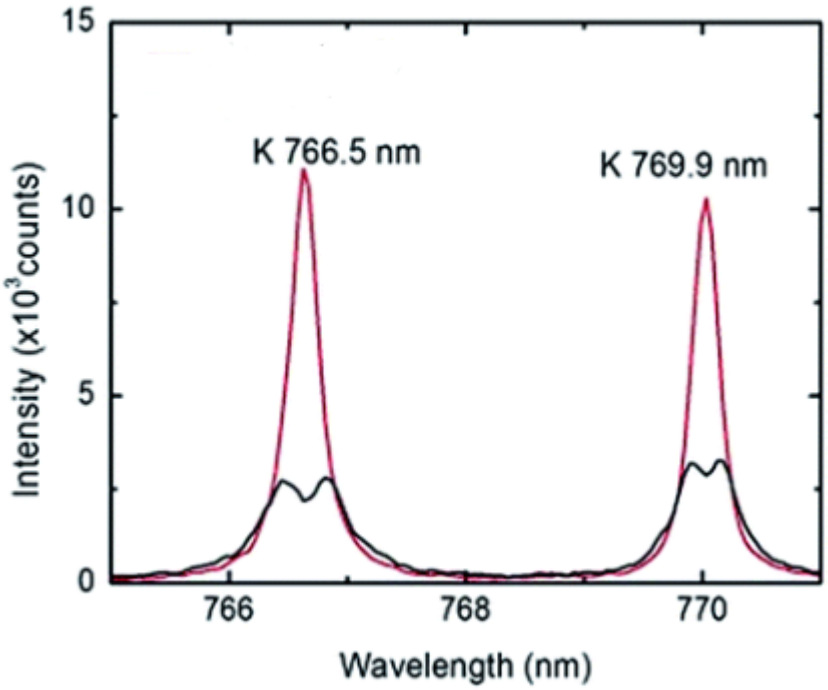

Figure 3.7 Effect of Self-Absorption on LIBS Spectra [125]

Using inverted intensity peaks as a reference for compositional analysis is only possible if the intensity values are corrected for this phenomenon. However, self-absorption correction is complicated. Therefore, selecting another intensity peak as a reference is more convenient, if this is possible within the range of properly measured wavelengths. In this experiment, the aluminium peak at 309,51 nm has a sufficient intensity, relative to the peaks of the other elements, and it has a suitable shape.

With the emission line of aluminium at 309,51 nm set as the reference line, the relation can be determined between the intensity of the peaks in the spectra of the 29 reference samples and their composition. Figure 3.8 shows the calibration curve for silicon. For silicon, the intensity peak at 288,23 nm is selected for the calibration. The x-axis represents the intensity ratio between the silicon peak at 288,23 nm and the aluminium peak at 309,51 nm, as measured with the LIBS sensor. To get one value per sample for the intensity ratio, from a large number of spectra per sample, an algorithm, developed by Swerim in previous research, is used. The algorithm first filters out the spectra that have no intensity peaks above 6000 counts. These spectra correspond to measurements that failed to ablate the actual metal, and instead ablated paint, a coating, or even nothing at all. After filtering out these spectra, an average value is taken for the silicon-aluminium intensity ratio. The y-axis represents the

ratio between the mass fractions of the two elements, according to the previous reference measurements. All 29 reference samples are as such positioned on the graph.

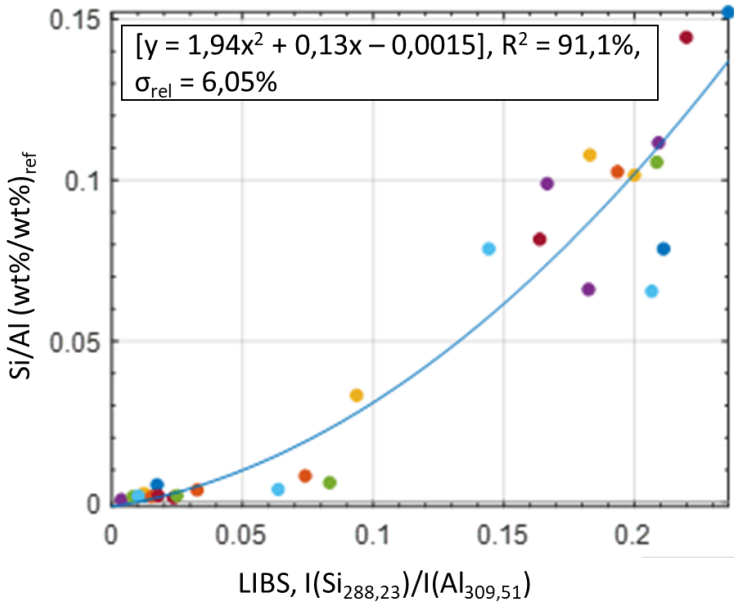

Figure 3.8: Calibration Curve for Silicon

With a least-squares based Matlab script, it is possible to fit a line or a curve to the datapoints. This curve is the actual calibration curve for silicon, for which the formula is noted in the top left corner of Figure 3.8. To quantify how good the calibration curve fits to the datapoints, the square of the correlation and the relative standard deviation are reported as well.

For the calibration curve of magnesium, the magnesium peak at 277,91 nm is selected. This peak, caused by neutral magnesium atoms, is not the strongest magnesium peak in the available range of wavelengths, but with the square of the correlation at 96,3%, the calibration curve for this peak has the best fit. Figure 3.9 shows that the datapoints indeed fit very well on the calculated curve.

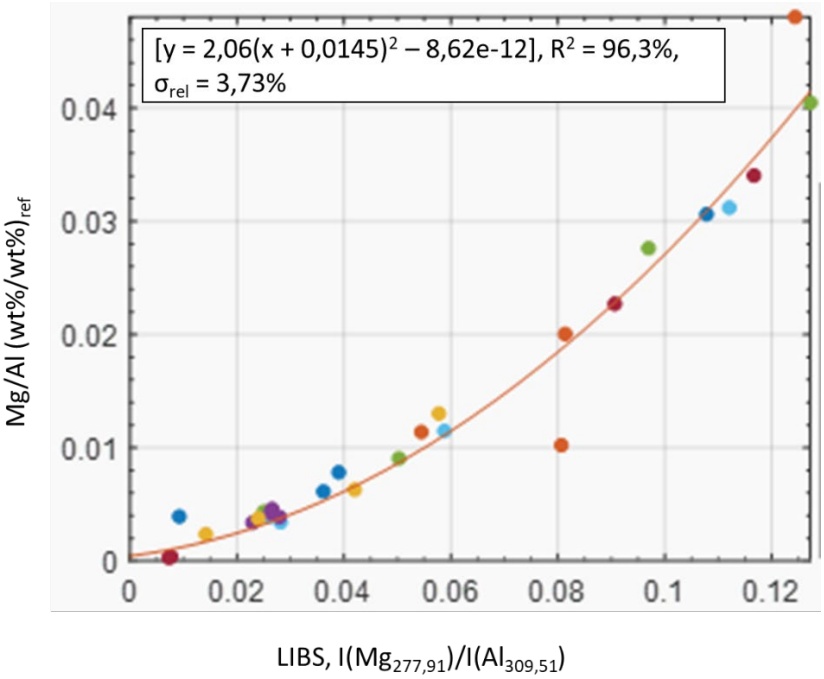

Figure 3.9: Calibration Curve for Magnesium

For zinc, the peak at 334,41 nm is selected for the calibration. This peak is by far the strongest of the three available peaks in the spectrum. The square of the correlation for this calibration curve is very high as well, at 98,4%. However, as can be seen in Figure 3.10, this high correlation is mainly due to the large number of reference samples that contain almost no zinc. There is a large gap between the highest and lowest concentrations of zinc in the set of reference samples. This will hurt the reliability of the composition analysis for scrap samples that have a zinc concentration in this middle region. However, no more reference samples are available at the moment than the 29 provided by Swerim.

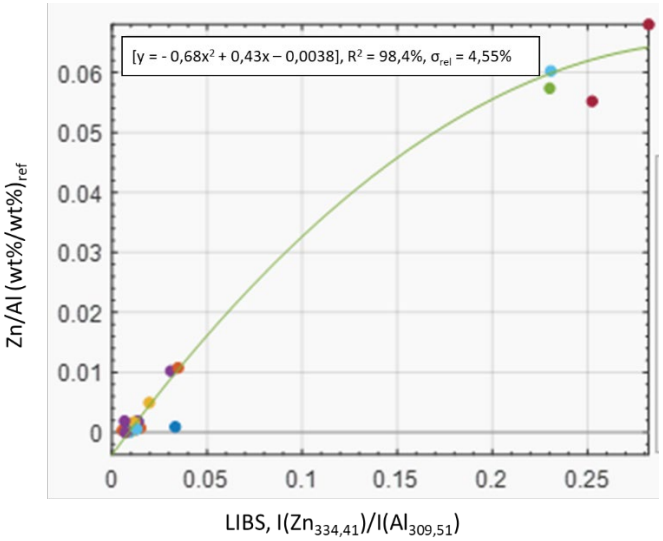

Figure 3.10: Calibration Curve for Zinc

For manganese, the concentrations in the reference samples are better spread, and cover the full range of manganese concentrations that occur in popular aluminium alloys, even those of the 3000 series that are highly alloyed with manganese. The strongest peak caused by neutral manganese

atoms in the available range of wavelengths is at 403,25 nm. The calibration curve for this manganese peak fits to the datapoints with a squared correlation of 94,6%, as can be seen in Figure 3.11.

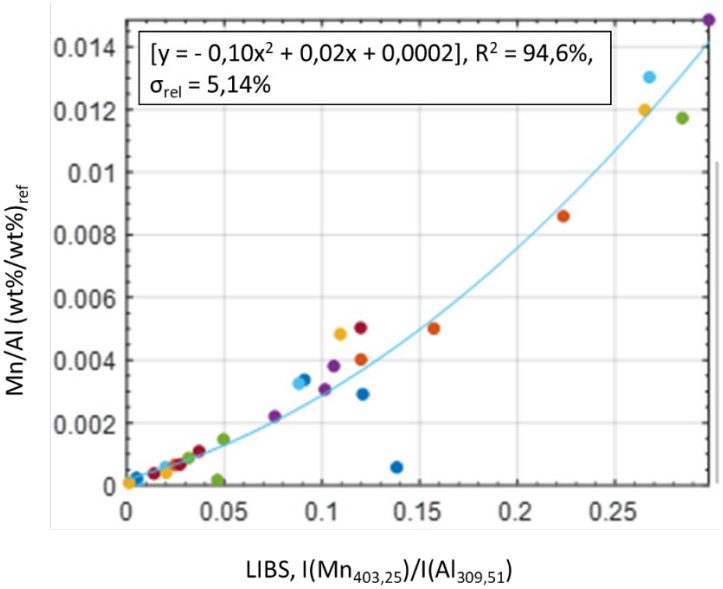

Figure 3.11: Calibration Curve for Manganese

The calibration curve for copper is based on the copper intensity peak at 324,73 nm, the strongest copper peak between 250 and 450 nm. The concentrations of the reference samples are distributed reasonably well, but the calibration curve does not fit to the datapoints as well as for the other elements. Multiple outliers, clearly visible in Figure 3.12, reduce the squared correlation to 73,8%, which is quite low for a calibration.

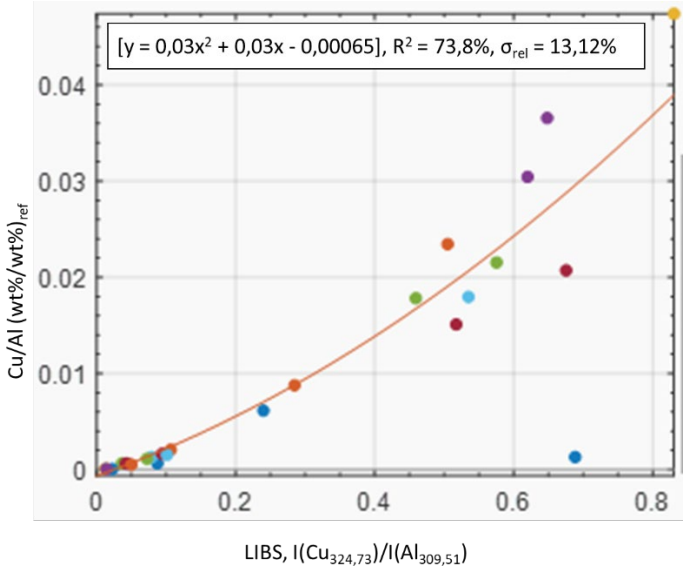

Figure 3.12: Calibration Curve for Copper

For iron, the situation is even worse. No clear correlation can be found between the intensity ratios and the mass ratios of iron, for any of the iron peaks in the spectrum. Therefore, the concentration of iron cannot be estimated separately with LIBS in this experiment.

With the formulas of the calibration curves, it is possible to calculate the mass ratio between silicon and aluminium, magnesium and aluminium, zinc and aluminium, manganese and aluminium, and copper and aluminium for each scrap sample, based on the measured spectra. In order to estimate the complete elemental composition of the scrap samples, the calibration curves of the different elements have to be combined. Formula 3.1 and Formula 3.2 show the general equations to calculate the concentration of the reference element (REF%) and the concentration of one of the other elements (ALLOY%) based on the mass ratios that are given by the calibration curves. There are as many known mass ratios as there are calibrated elements. In the calculations in this thesis, there are five calibrated elements (silicon, magnesium, manganese, copper, and zinc), and therefore five mass ratios in the denominator of Formula 3.1. Aluminium is the reference element. The value in the numerator of Formula 3.1 (TOT%) is equal to the sum of the concentrations of the reference element and the calibrated elements. In order to avoid that the number of variables exceeds the number of equations in the calculation of the composition, it is necessary to estimate this value. The sum of the concentrations of aluminium and the five most important alloying elements will be close to 100 wt% for most samples, since the concentration of iron and other tramp elements is usually limited to less than 1 wt%. Nevertheless, assigning a constant value to this variable always results in inaccuracies since the concentration of tramp elements varies for every sample. Therefore, it is useful to include as many elements as possible in the calibration. By calibrating also for iron, chromium, titanium, and other elements, the accuracy of these calculations could be increased drastically, while the uncertainty would be reduced to a minimum.

$$REF\% = \frac{TOT\%}{1 + \sum Mass\ Ratios} \tag{3.1}$$

$$ALLOY\% = TOT\% - REF\% * \left(1 - \frac{ALLOY\%}{REF\%} + \sum Mass\ Ratios\right) \tag{3.2}$$

For the calculations in this thesis, it is assumed that the concentrations of aluminium, silicon, magnesium, zinc, manganese, and copper add up to 100% of the mass of the scrap samples. Doing so, the presence of tramp elements is neglected completely. Since the tramp elements can constitute up to 1% of the mass of some samples, this simplification is not ideal. However, this approach is deemed more appropriate than assuming that the sum of the six most important elements adds up to, for example, 99,7 wt%. In this alternative approach, the concentration of tramp elements could be estimated more closely to true value. However, when assuming that the concentration of the tramp elements adds up to, in this example, 0,3 wt%, Formula 3.2 yields negative results for samples that have less than 0,3 wt% of tramp elements. To guarantee that there are never negative concentrations in the calculated results, the value for “TOT%” is kept at 100%. The drawback of this choice is that the calculated concentrations for aluminium and the calibrated alloying elements are slightly higher than the real values.

The formulas below show how this assumption leads to the exact formulas that are used to calculate the concentrations of aluminium, magnesium, manganese, copper, zinc, and silicon. First, the concentration of the reference element has to be calculated.

$$Al\% + Si\% + Mg\% + Zn\% + Mn\% + Cu\% = 100\% = 1 \tag{3.3}$$

$$\frac{Al\%}{Al\% + Si\% + Mg\% + Zn\% + Mn\% + Cu\%} = Al\% \tag{3.4}$$

$$\frac{1}{1 + \frac{Si\%}{Al\%} + \frac{Mg\%}{Al\%} + \frac{Zn\%}{Al\%} + \frac{Mn\%}{Al\%} + \frac{Cu\%}{Al\%}} = Al\% \tag{3.5}$$

Formula 3.5 shows how Formula 3.1 applies for this specific case. The value in the numerator is one, or 100%. In the denominator, there are five mass ratios, one for each calibrated element.

Once the concentration of the reference element is calculated, it is also possible to calculate the concentrations of the other elements. The simple derivation of the formula for the concentration of silicon, in function of the mass ratios of the other elements and the concentration of the reference element, is given below.

$$Al\% + Si\% + Mg\% + Zn\% + Mn\% + Cu\% = 100\% = 1 \tag{3.3}$$

$$1 - Al\% * \left(1 - \frac{Si\%}{Al\%} + \frac{Si\%}{Al\%} + \frac{Mg\%}{Al\%} + \frac{Zn\%}{Al\%} + \frac{Mn\%}{Al\%} + \frac{Cu\%}{Al\%}\right) = Si\% \tag{3.6}$$

Formula 3.6 is the applied version of the general formula, Formula 3.2. In this formula, it is necessary to know the concentration of the reference element. That is why the concentration of the reference element has to be calculated first. The fact that the calculation of each element depends so heavily on the value for the reference element also explains why it is so important to select a suitable reference peak in the spectra of the investigated samples.

With these formulas, the compositions of all collected Twitch samples are calculated. Unfortunately, due to the limited number of calibrated chemical elements, this experiment is only capable of producing rough estimates of the composition, considering only aluminium and the five most important alloying elements. Iron and other tramp elements could not be included in the LIBS composition analysis at this time.

3.2.3 XRF Measurement

In the second experiment, the composition of the Twitch samples is measured again, this time with a handheld XRF sensor. The used device is the *Thermo Scientific Niton XL2 Plus XRF Analyzer*. Table 3.1 shows the limits of detection of the device when aluminium is selected as the base material for the measurement [127]. The limit of detection is the lowest concentration of an element that can be measured by the XRF. More elements such as gold, silver, tungsten, and cadmium can be detected with the handheld XRF, but for these elements, the limit of detection is not specified by the manufacturer of the device.

Table 3.1: Limits of Detection of Handheld XRF

Element	LOD (wt%)	Element	LOD (wt%)	Element	LOD (wt%)	Element	LOD (wt%)
Bi	0,0020	Pd	0,0020	Ni	0,0080	V	0,0750
Pb	0,0020	Ru	0,0020	Co	0,0060	Ti	0,1600
W	0,0070	Nb	0,0040	Fe	0,0110	Si	0,0400
Sb	0,0040	Zn	0,0030	Mn	0,0150	Mg	0,3500
Sn	0,0025	Cu	0,0040	Cr	0,0330		

The elements that are marked in yellow in the table, are considered individually in the composition analysis. The rest of the elements are bundled under the name “Other”. The XRF calculates the concentration of aluminium by subtracting the measured concentrations of all other elements from 100%. The aluminium concentration is therefore not measured directly. XRF is also not particularly suitable to measure concentrations of light elements such as aluminium. The limits of detection of silicon and magnesium, other examples of light elements, illustrate this fact. The limit of detection of magnesium in particular is very high, compared to the other elements. From this table, it is clear that the XRF can in theory measure the concentrations of most elements quite accurately, but it will fail to detect low but non-negligible amounts of magnesium. That is why XRF devices in general count mostly on the accurate detection of the heavier elements to determine the grade of the aluminium alloys [113].

Prior to the XRF measurement, all samples have to be cleaned thoroughly to remove the contamination from a sufficiently large area of the surface. The LIBS experiment has confirmed the statements in literature that layers of paint and other contaminants are extremely detrimental for the measurement results. In this experiment, a part of the contaminated upper layer is scratched away with cutter knives. Subsequently, the sample is cleaned with ethanol to remove dust particles. This is a time consuming procedure, but under the circumstances, it is a more convenient solution than the alternative options.

A grinding wheel is tested as an alternative tool to clean the samples. This method immediately removes an upper layer of the material, exposing a large area of clean aluminium. However, the grinding wheel transfers material from the previously grinded samples to the next. In addition, the grinding wheel contaminates the samples with elements like vanadium, titanium, and niobium from previous grinding tasks. Other alternative strategies that are not tested yet are cleaning with a water jet or chemicals. To apply these strategies, the sample numbers would need to be engraved in the samples, since the current paper labels would not endure these procedures. Appropriate methods to clean aluminium with acids such as H_2SO_4, H_3PO_4, $H_2C_2O_4$, and HNO_3 are well documented in literature [128]. In future research, these methods should be investigated more thoroughly since they could speed up the cleaning process significantly. In addition, the use of chemicals probably reduces the amount of leftover surface contamination after cleaning in comparison with the results of manual workers with cutter knives.

After cleaning, the samples are placed directly under the eye of the XRF sensor for a measurement of 30 seconds. The software purchased along with the XRF automatically computes the composition of the measured samples, so in this experiment, there is no need to analyse the spectra. After measuring 275 samples, the calculated compositions are transferred to Microsoft Excel for a more thorough analysis.

3.2.4 Analysis Method

Based on the measured compositions, the Twitch samples are subdivided into categories. In a first step, they are subdivided based on the alloy series to which they belong. These alloy series are the standard series, defined by the American National Standards Institute (ANSI), that are also used in the previous chapter.

After consulting the R&D manager and the person responsible for selling the aluminium scrap at the Ropswalle site of Galloo, an additional category, called “High Purity Aluminium”, is defined. “High Purity Aluminium” is aluminium scrap for which the concentrations of both copper and zinc are below 0,02wt%, the concentration of manganese is below 0,1wt%, and the concentration of magnesium is below 1wt%. Galloo could sell aluminium scrap with such composition at a price of €1200 per ton in

the first months of 2020. For mixed aluminium scrap, the selling price was €900 per ton in the first months of 2020. Since the selling price for this type of aluminium scrap is so much higher than for mixed scrap, it is an interesting sorting target. Especially in the short run, the experts of Galloo see the greatest financial potential in sorting out aluminium scrap that meets these conditions.

Based on the defined categories, several sorting strategies are suggested. The benefits of each sorting strategy are explained.

3.3 Results and Discussion

3.3.1 Measurement Results

For 275 Twitch samples, the composition is measured with both the LIBS sensor and the XRF scanner. Figure 3.13 shows the average composition of all 275 samples, according to the XRF analysis and the LIBS analysis. The indicated concentrations on the figure are expressed in weight percentages. As can be seen, there are some considerable differences between the results of the two methods.

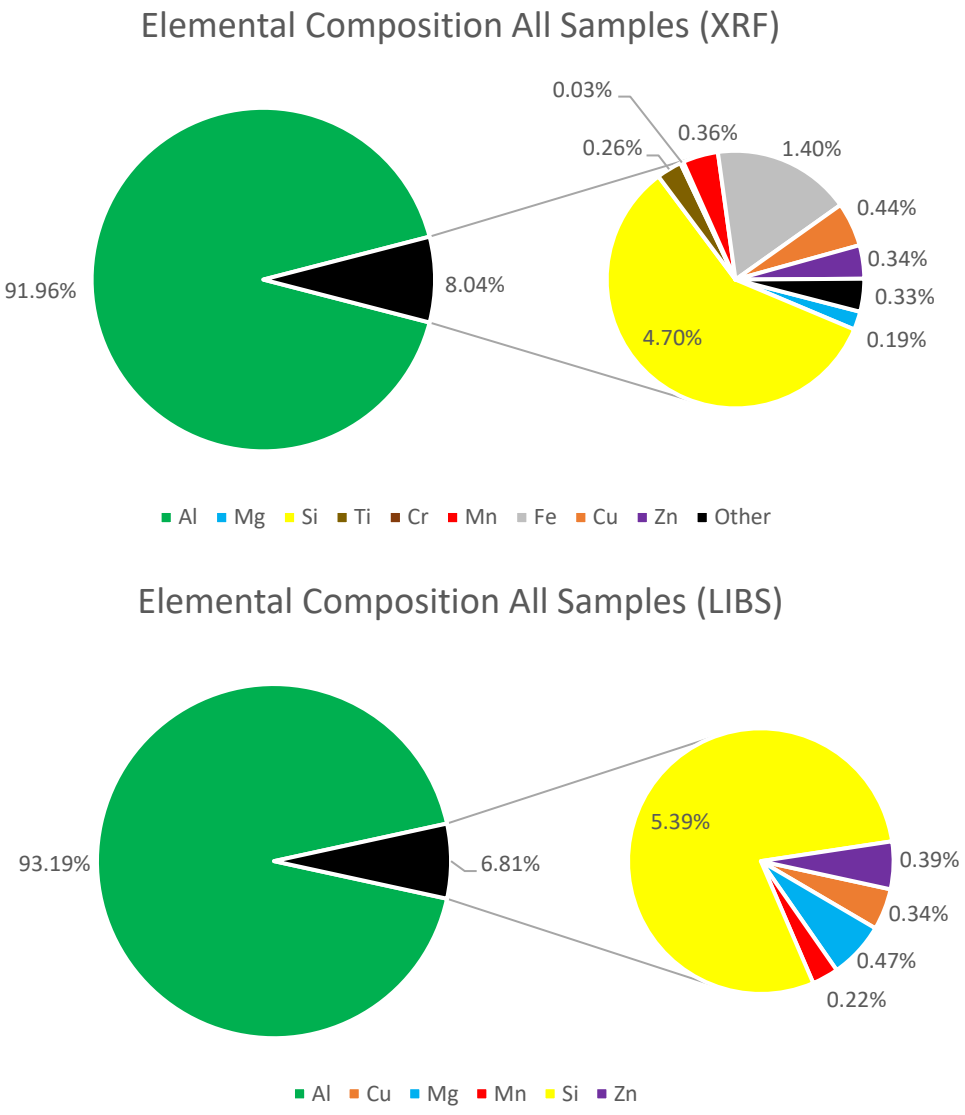

Figure 3.13: Elemental Composition All Samples According to XRF and LIBS

The XRF analysis indicates unusually high amounts of silicon, iron, chromium, titanium, cadmium, and lead in the composition of the measured samples. Titanium is sometimes used as an alloying element to increase the weldability of an aluminium alloy, but only in a concentration of up to 0,01wt% [129]. Cadmium is used in specific 2000 and 7000 series aerospace alloys to increase the strength and corrosion resistance. However, in other alloys, cadmium can decrease corrosion resistance. Furthermore, cadmium is highly toxic, posing significant health risks during melting and casting, as cadmium flumes can be released from the molten aluminium. Therefore, cadmium is not a common alloying element. Lead is not a common alloying element either. It is usually only present as a tramp element in aluminium alloys.

Therefore, the probability is high that these elements are detected due to leftover contaminants on the surface of the measured samples. A study of the American Environmental Protection Agency (EPA) shows that titanium dioxide, iron oxides, cadmium selenide and lead (chromate) are among the most popular components of paint in automobiles (see Table 3.2) [130]. The fact that unusually high concentrations of chromium are measured for some samples can be explained by the fact that the investigated Twitch samples have been stored together with scrap samples of the Zorba fraction, that have been collected for future work. Stainless steel, by far the most common metal in the Zorba fraction, contains high concentrations of chromium. It is probable that the Zorba samples have deposited both iron and chromium on the surface of the Twitch samples. Still, there appears to be yet another source of contaminants that has an even higher influence on the measurements. The unusually high concentrations of silicon and iron cannot be explained by the mentioned factors alone.

Table 3.2: Chemical Components in Automobile Paints [130]

Pigment Color	Chemical Components
White	Titanium dioxide, white lead, zinc oxide
Red	Iron oxides, calcium sulfate, cadmium selenide
Orange	Lead chromate-molybdate
Brown	Iron oxides
Yellow	Iron oxides, lead chromate, calcium sulfide
Green	Chromium oxide, copper, phosphotungstic acid, phosphomolybdic acid
Blue	Ferric ferrocyanide, copper
Purple	Manganese phosphate
Black	Black iron oxide
Metallic	Aluminum, bronze, copper, lead, nickel, stainless steel, silver, powdered zinc

A closer look at the sorting processes of Galloo reveals that a suspension of powdered ferrosilicon is used in the density separation steps. During density separation, materials that have a lower density than the medium in which they are immersed float, while heavier materials sink. Galloo has three different density separation processes. In each process, the density of the used medium is different. These differences in density are attained by adding ferrosilicon powder to the suspension. It appears that some of the ferrosilicon powder stays attached to the scrap pieces when they go through these sorting processes. Therefore, insufficient cleaning results in significantly higher measurements of silicon and iron. A similar issue is expected to occur at most recycling facilities, since the only common

alternatives for ferrosilicon powder in density separation processes are powders based on magnetite or arsenopyrite [131]. Magnetite and arsenopyrite are minerals. Magnetite is an iron oxide. Arsenopyrite is an iron arsenic sulphide. Using these mineral powders instead of ferrosilicon powder might mitigate the silicon contamination problem, but since these minerals contain iron, the problem of the iron contamination will most likely remain.

Another issue is that the LIBS analysis indicates considerably higher concentrations of magnesium than the XRF analysis. On average, the measured concentration of magnesium is almost 0,3wt% higher in the LIBS analysis than in the XRF analysis. The most important reason for this difference is that the limit of detection of the XRF scanner is 0,35wt% for magnesium. Therefore, the XRF scanner fails to detect the presence of magnesium in a large number of samples. As such, the indicated average magnesium concentration for the 275 samples is lower than the real concentration.

The differences between the LIBS analysis and the XRF analysis are smaller for copper, zinc, and manganese. It is expected that for these three elements, the relatively small differences between the two methods are mainly related to the limited quality of the LIBS calibration.

3.3.2 Subdivision According to Alloy Series

The 275 samples are divided in categories based on the alloy series they belong to. The allocation of the samples to the different categories relies only on the results of the XRF measurement since the results of the LIBS analysis are not accurate enough for this task. In a first step, the analysis software that is purchased along with the XRF can be used to determine the grade of most of the measured Twitch samples. The analysis software is able to determine the grade of 214 of the 275 samples. For the other 61 samples, the surface contamination makes it too challenging for the software to identify the grade. Figure 3.14 shows the result of allocating the first 214 samples to the defined categories with the help of the XRF software.

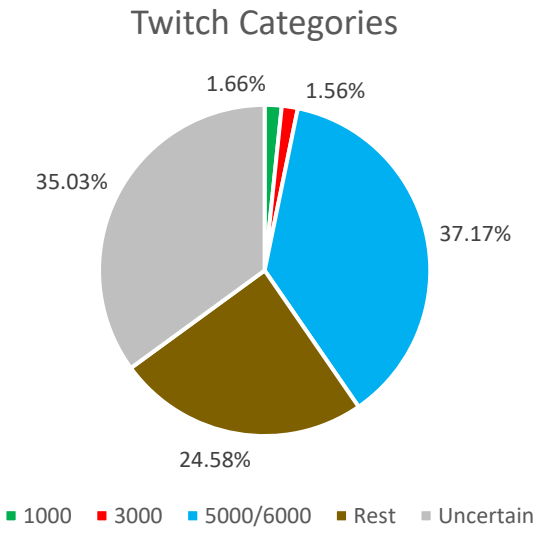

Figure 3.14: Allocation of the Samples to the Defined Categories Based on Automatic Identification XRF

Due to the limited accuracy of the XRF in measuring silicon and magnesium concentrations, it is not certain that the indicated grades are correct. For example, the distinction between the 6061 grade and the 6151 grade comes down to a difference of about 0,2wt% in the concentrations of magnesium

and silicon. However, literature suggests that XRF measurements can be trusted to indicate the alloy series of aluminium samples [28]. Still, to minimise the probability that samples get allocated to a wrong category, the 5000 series and 6000 series samples are bundled in one category. The distinction between 5000 series alloys and 6000 series alloys comes down to a small difference in the concentration of silicon. The concentrations of all other alloying elements are very similar in the 5000 and 6000 series. Since neither the XRF nor the LIBS measurement can be trusted completely to make the distinction between these two series based on the concentration of one element, it is considered a good choice with respect to the reliability of the allocation not to have two separate categories for the 5000 and 6000 series samples. The 2000, 4000, 7000, 8000 series samples and the cast alloy samples are bundled in one category as well. The reason to combine these series in one "Rest" category is that only a handful of samples are identified as alloys from the 2000/4000/7000/8000 series. The vast majority of the samples in this "Rest" category are cast alloys. Because these four wrought alloy series are so poorly represented in this set of samples, they do not have a separate category. Sorting these elements as a separate fraction would make little economic sense due to their limited presence in the collected scrap.

Since there are clear compositional differences between the four categories ("1000 series", "3000 series", "5000/6000 series", and "Rest"), it is expected that, with the help of the XRF analysis software, the 214 samples can be allocated to the right category. The other 61 samples, that account for 35% of the total mass of the 275 Twitch samples, have to be allocated to the defined categories without the help of the XRF analysis software.

In order to do so, compositional criteria are established for the defined categories. The remaining samples that, according to the XRF measurement, have an aluminium concentration higher than 95wt%, and have concentrations of magnesium, manganese, copper, and zinc that do not exceed 0,2wt%, are allocated to the "1000 series" category. Samples that have a manganese content higher than 0,95wt% and for which the sum of the concentrations of copper and zinc is lower than 0,3wt%, are allocated to the "3000 series" category. Samples that have an aluminium concentration higher than 92,5wt%, a magnesium concentration higher than 1wt% and copper and zinc concentrations lower than 0,1wt%, are allocated to the "5000/6000 series" category. Samples with either a zinc concentration above 5wt%, a silicon concentration above 10wt%, or an aluminium concentration below 92wt%, in combination with a manganese concentration below 0,9wt%, are assigned to the "Rest" category. With these criteria, another 38 samples can be allocated to the defined categories. After this step, 23 samples still remain unallocated, corresponding to 13% of the total mass of the 275 samples. This is illustrated in Figure 3.15.

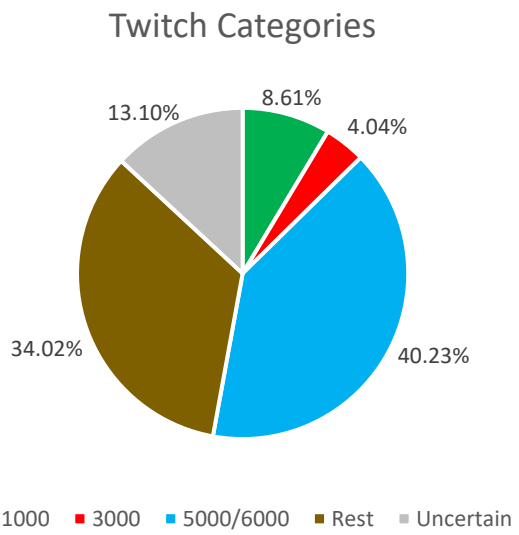

Figure 3.15: Allocation of the Samples to the Defined Categories Based on Automatic Identification XRF and Composition Criteria

The 23 samples that are left are the most difficult ones to allocate. The average concentration of titanium is over 1,5wt% in these samples, the average concentration of iron is over 2,9wt% and the average concentration of other tramp elements is over 0,7wt%. These are the samples with the most leftover surface contamination. The composition of each of these samples is studied individually to assess to which category they belong. 14 of the 23 samples are allocated to the “3000 series” category due to their high concentrations of aluminium and manganese. According to the results of the XRF measurement, these samples also contain elements that are not expected in a typical 3000 series alloy, but these are probably contaminants. The measured concentrations of manganese, an element for which the XRF measurement is usually quite accurate, are far too high for any alloy outside the 3000 series. Therefore, these samples can still be allocated to the “3000 series “ category with reasonable certainty. Three samples are allocated to the “5000/6000 series” category due to their high concentrations of magnesium. The last six samples are allocated to the “1000 series” category due to their very low concentrations of copper, zinc, and manganese. After this last step, all 275 scrap samples are allocated to one of the defined categories. The share of each category in the total mass of the collected scrap samples is visible in Figure 3.16.

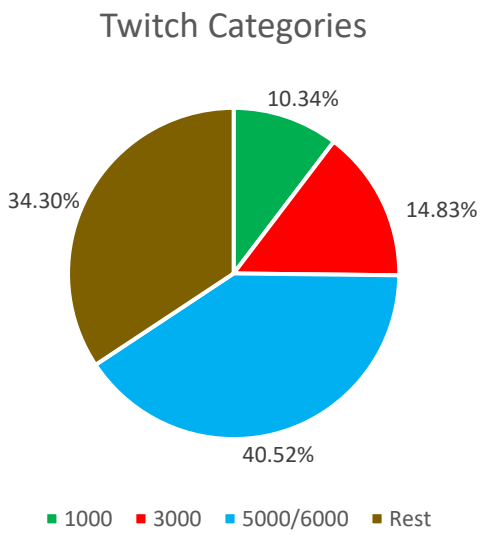

Figure 3.16: Complete Allocation of the Samples to the Defined Categories

3.3.3 High Purity Aluminium

Since Galloo has shown great interest in separating "High purity aluminium" from the rest of the mixed aluminium scrap, this category is in second instance added to the analysis. Of the collected 275 Twitch samples, 41 meet the conditions of this category. All these 41 samples either belong to the 1000, 5000, or 6000 series. Alloys of the other aluminium series typically do not meet the relatively severe restrictions on copper, zinc, and manganese. Figure 3.17 shows the shares of the different categories in the total mass of the 275 samples, when "High Purity Aluminium" is included as a category. The 41 samples in this category account for more than 10% of the total mass of the 275 samples.

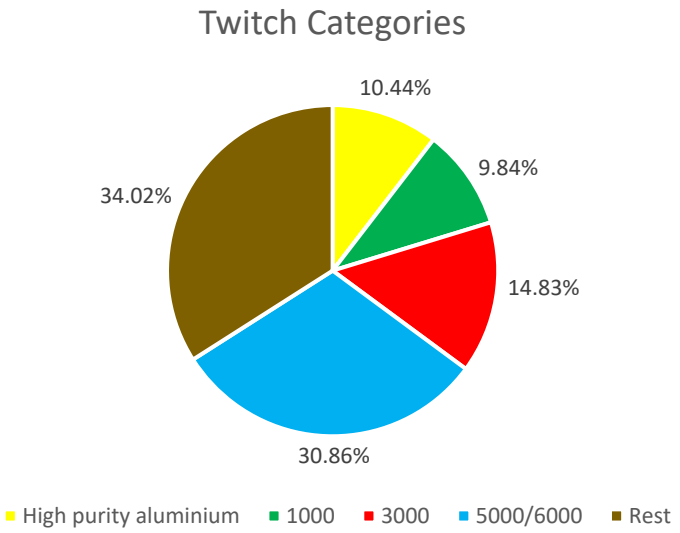

Figure 3.17: Complete Allocation of the Samples to the Defined Categories Including High Purity Aluminium

3.3.4 Comparison Between Measurements and Model

Before looking at the elemental composition of the defined categories, the results of the previous section are critically analysed. To verify that the proportions of the scrap categories are realistic for

what is typically collected at Galloo, they are compared with results from the developed global MFA model from the previous chapter. In Figure 3.18, the first pie chart shows the proportions of the different scrap categories, as calculated in the previous section. The second pie chart shows the alloy-level composition of all globally collected aluminium scrap in 2020, as calculated by the MFA model. The proportions of the different scrap categories are remarkably similar in the first two pie charts. Only the size of the "3000 series" category seems somewhat large in the first pie chart.

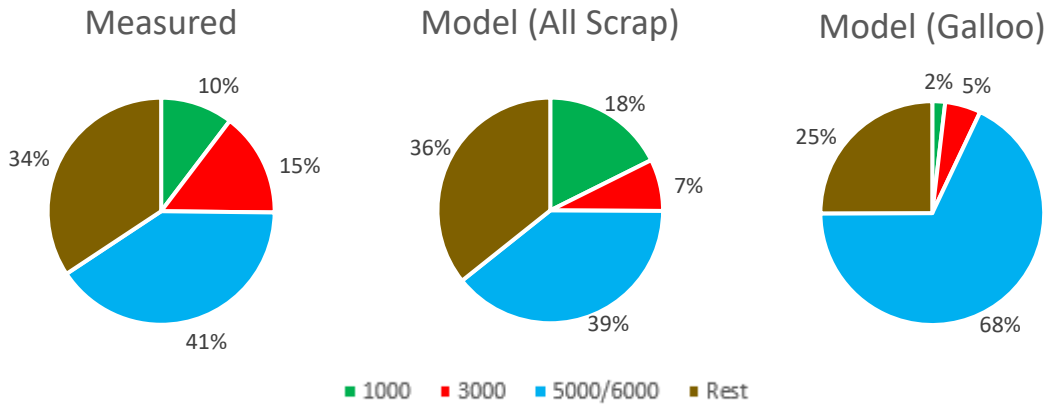

Figure 3.18: Alloy-Level Composition of Collected Scrap: A) Measured, B) Predicted for All Scrap, C) Predicted for Galloo

However, Galloo has indicated that the scrap that arrives at the Ropswalle site originates from a limited number of sectors. Based on conversations with Galloo employees, it is estimated that 60% of the incoming aluminium scrap at the Ropswalle site originates from the construction sector, 30% originates from the automobile sector, and 10% originates from consumer durables. These numbers are based on multi-year averages and show large variations in time. The third pie chart shows what the MFA model calculates for the alloy-level composition of the collected scrap at Galloo, based on the mentioned information about the origins of the scrap. Since the scrap in this case originates almost exclusively from buildings and ELV, the 5000 and 6000 series alloys take on a much larger share. As a result, there are significant differences between the proportions of the categories in the third pie chart and the proportions in the first two pie charts.

There are multiple plausible hypotheses that could explain these relatively large differences between the sizes of the categories in the charts. A first possibility is that a large number of samples is allocated to the wrong category due to inaccuracies in the XRF measurements. However, this is not very likely. To validate the results of the XRF measurement, they are compared with the results of the LIBS analysis. For all samples that are wrought alloys according to the XRF measurements, the LIBS analysis indicates an aluminium concentration above 94wt%. For 99% of the samples that are cast alloys according to the XRF measurements, the LIBS analysis indicates an aluminium concentration below 94wt%. As such, the LIBS analysis confirms the results of the XRF measurements. Furthermore, there is a distinct difference in the shape of cast alloy samples and wrought alloy samples. Most often, wrought alloy samples are extruded or rolled. Cast alloy samples are most often shaped by casting. While cleaning the samples prior to the measurement, it is often already clearly visible whether a sample is a wrought or a cast alloy. This clear difference also explains why workers in countries with low labour costs can separate wrought and cast alloys manually with extremely high accuracies. Since the XRF measurement, the LIBS analysis, and visual inspection come to the same conclusions about the division between wrought and cast alloys, it is unlikely that mistakes in the allocation of the measured samples are to blame for the differences between the measurements and the model.

Another theory is that there could be large compositional differences between the aluminium scrap that enters the sorting system of Galloo and the aluminium scrap that ends up in the Twitch fraction. Only 57% of the incoming aluminium scrap ends up in the Twitch fraction. Some of the aluminium pieces that do not go to the Twitch fraction are sorted out because they have a high iron concentration. Some are sorted out based on their size, and some are separated together with magnesium in one of the density separation steps. It is possible, and even likely, that the Twitch fraction is therefore not a perfect reflection of the entire amount of incoming scrap. Since the model predicts the composition of all the aluminium scrap that arrives at Galloo, this might explain some of the differences between the results of the model and the results of the measurements. However, cast alloys account for one third of the mass of the investigated samples, while the model predicts that less than 25% of the scrap consists of cast alloys. This difference cannot be explained by this theory since according to Galloo, the concentration of cast alloys is lower in the Twitch fraction than in the incoming scrap.

Therefore, the most likely reason for the differences between the measurements and the predictions of the model seems to be the uncertainty in the origins of the collected scrap samples. While, on average, Galloo receives most scrap from the construction sector, the high amount of cast alloys gives reason to believe that the collected samples originate mostly from ELV or other sectors. The fact that Galloo does not know the exact origins of the scrap samples that are collected for this thesis, makes it harder to compare the measurement results with data from the model. However, since the alloy-level composition of the measured samples is very similar to what the model predicts for mixed aluminium scrap of all sectors, it is expected that there are no large errors in the developed model. In the future, it will be worthwhile to compare the results of the model with the composition of scrap samples for which the origins are known. Only this way, it is really possible to validate the quality of the model and to improve it.

3.3.5 Composition Analysis of the Defined Categories

To be able to assess how interesting it would be to apply alloy-based sorting techniques on the mixed aluminium scrap in the Twitch fraction, the elemental compositions of the defined categories are analysed. Figure 3.19 shows the average composition of the “High purity aluminium” samples according to the XRF and LIBS measurement. According to the XRF measurement, the concentrations of manganese, copper, and zinc are almost negligible. Only considerable amounts of silicon, iron, and magnesium are measured in these samples.

The LIBS measurement indicates higher concentrations of copper, zinc, and manganese. The concentrations of copper and zinc are even so high, according to the LIBS measurement, that this fraction no longer meets the purity requirements to be sold at a higher price. However, due to the poor calibration for zinc and the moderate calibration for copper, the LIBS analysis is probably less reliable to assess the concentrations of these elements. Furthermore, the absence of iron and other tramp elements in the LIBS analysis distorts the entire calculation of the composition. Since the XRF is assumed to be more reliable for the detection of heavy elements such as copper and zinc, it is very likely that the threshold values for the high purity category will be achieved.

According to the XRF, the average concentration of magnesium in the “High purity aluminium” fraction is 0,07wt%. This is well below the XRF’s limit of detection for magnesium (0,35wt%). Therefore, the LIBS estimate of 0,58wt% might actually be closer to the truth. The concentration of silicon is also significantly lower in the LIBS measurement than in the XRF measurement, and as such, also more realistic. In conclusion, it is relatively certain that this fraction, that accounts for over 10% of the mass

of the 275 samples, meets the purity limits required to sell the scrap at a price of €1200 per ton, although the concentration of magnesium might be higher than indicated by the XRF.

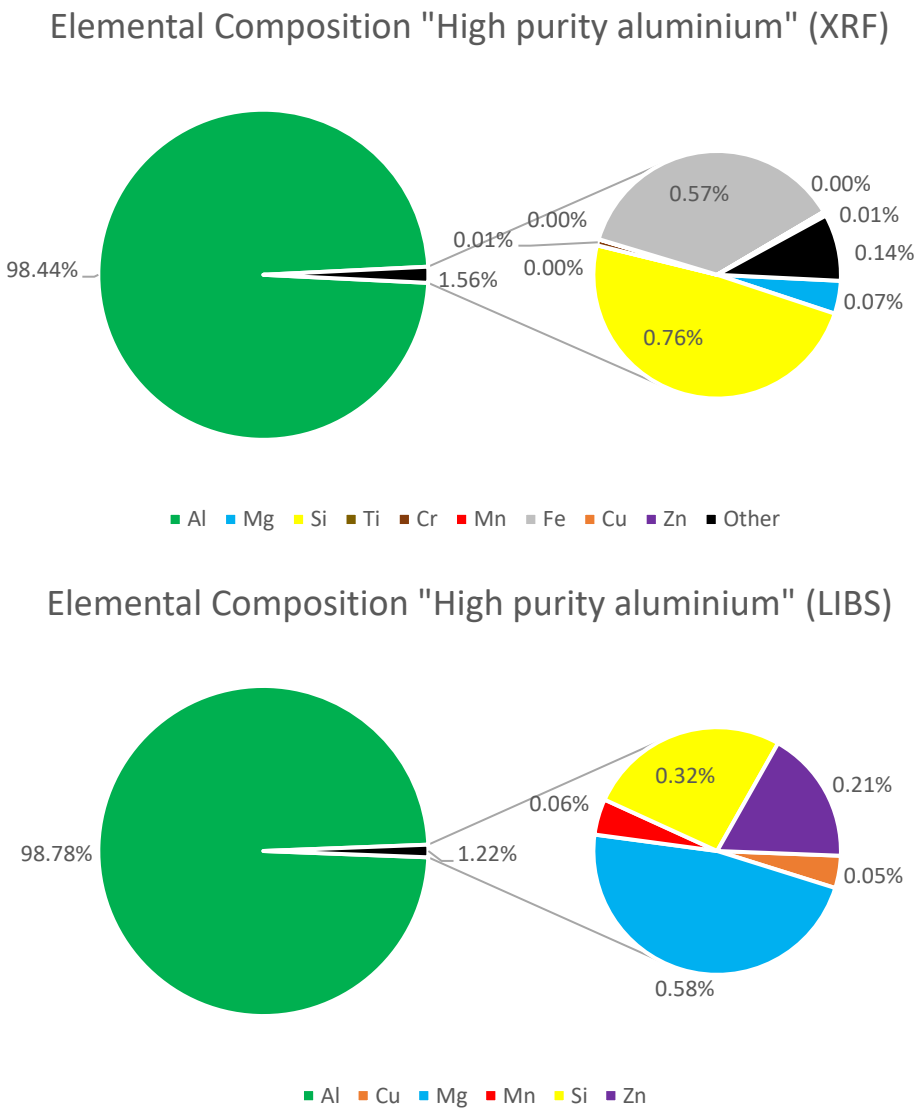

Figure 3.19: Elemental Composition "High purity aluminium" According to XRF and LIBS

The "1000 series" category accounts for another 10% of the mass of the 275 samples. The average composition of the samples in this category, according to the XRF and LIBS measurement, is shown in Figure 3.20. Although this fraction does not meet the purity criteria to be sold at €1200 per ton, it still has a suitable composition for the production of wrought alloys. Apart from silicon, iron, chromium, and titanium, the alloying and tramp elements only amount to 0,24wt% of this fraction, according to the XRF measurement. The copper and zinc concentrations are 0,04wt% and 0,06wt%, respectively.

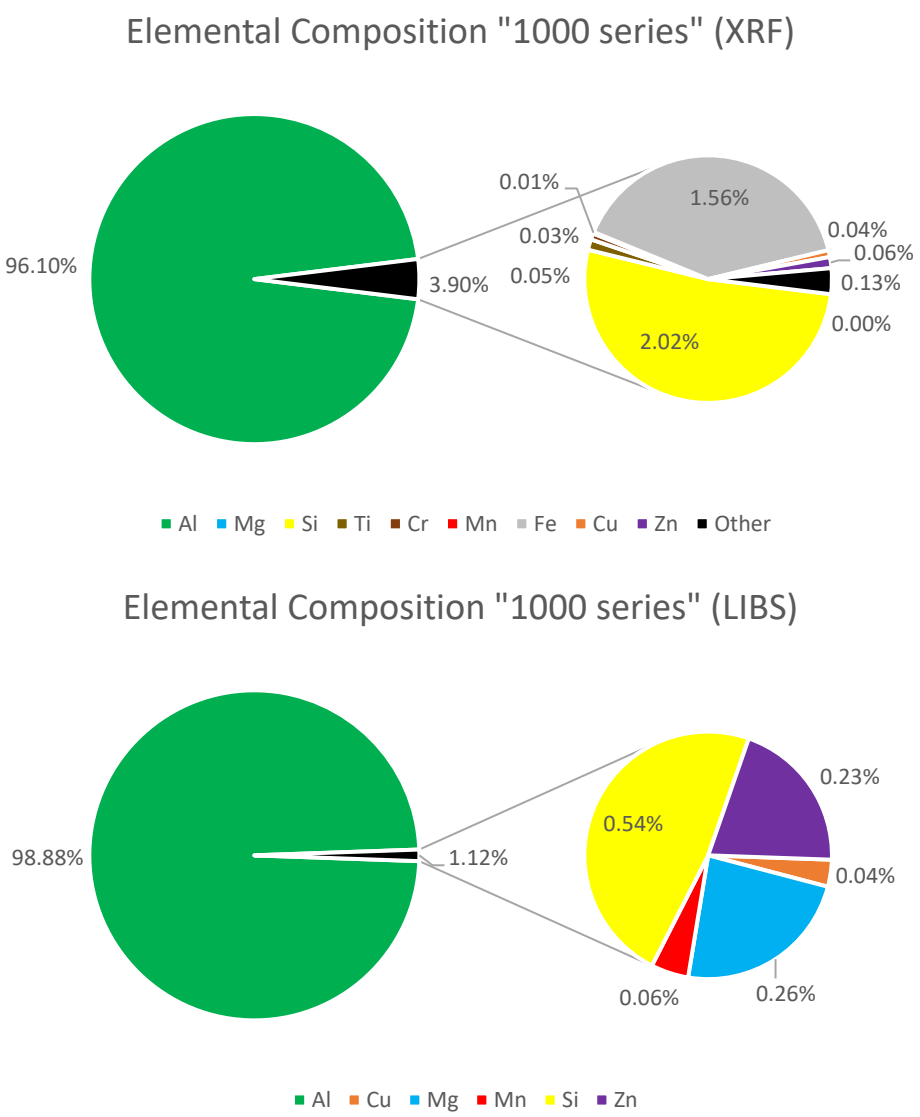

Figure 3.20: Elemental Composition "1000 series" According to XRF and LIBS

Sorting out this fraction might add considerable value to the Twitch fraction in the future. The concentrations of copper, zinc, and manganese in this fraction are still well below the tolerance limits of most wrought alloys, even if the manganese concentration is closer to 0,06wt%, as the LIBS measurement suggests. From a comparison between the results of the XRF and LIBS measurement, silicon and magnesium appear to be the largest obstacles in recycling this fraction. While the concentration of silicon in these samples is probably much closer to the LIBS value of 0,53wt% than to the 2,04wt% claimed by the XRF analysis, such concentration still exceeds the tolerance limits of all wrought alloys except the 4000 and 6000 series alloys. The concentration of magnesium in these samples is quite high as well. Although the XRF measurement indicates that the concentration of magnesium is 0,00wt%, it is likely that the LIBS analysis, claiming a magnesium concentration of 0,26wt%, gives a better indication of the real magnesium concentration. Since the limit of detection of the handheld XRF is 0,35wt% for magnesium, non-negligible amounts of magnesium go undetected with this device. As such, important information about this fraction would be lost if the LIBS measurement would not provide back up for the XRF measurement. A magnesium concentration of more than 0,20wt% exceeds the tolerance limits of all wrought alloys except the 5000 and 6000 series

alloys. Therefore, this element plays an important role in determining what the added value could be of separating this stream from the rest of the scrap.

Since the concentrations of all alloying elements in the “1000 series” fraction are below the tolerance limits of the most popular 6000 series alloys, it is theoretically possible to produce, for example, the 6061, 6063, and 6082 grades from this fraction without adding primary aluminium, provided that the iron concentration is considerably lower than indicated in the XRF measurement. Establishing the right compositions for these grades would only require the addition of the right alloying elements. Producing wrought alloys almost entirely from recycled aluminum does not exist yet as a common practice. This might change, however, when alloy based sorting methods succeed in separating large amounts of pure aluminium from the non-ferrous mixed scrap. Scrap samples in the “1000 series” category have a large intrinsic value due to their high purity but the price that recycling companies would get for this fraction, depends on the willingness of aluminium smelters to accept this material. The incentives have to be large enough for the smelters as well to adapt their current practices.

The composition of the “3000 series” samples is significantly less interesting for recycling. Figure 3.21 shows the average composition of this category according to the XRF and LIBS measurements. According to the XRF analysis, the concentrations of titanium, iron, and silicon are 1,36wt%, 2,66wt%, and 3,38wt%, respectively. These concentrations are clearly inflated by surface contaminants but even the samples that are automatically identified as 3000 series alloys by the XRF software, have an average silicon content of 0,65wt%. The concentrations of copper and zinc in these samples, both around 0,20wt%, are quite high as well according to the XRF analysis. Based on the results of the LIBS analysis, it is probable that the magnesium content of this fraction is also above 0,20wt%. It is therefore clear that besides manganese, the main alloying element of the 3000 series, there are high concentrations of the other alloying elements as well. This is not positive from a recycling perspective since in most wrought alloys, only one or two alloying elements are allowed to be prominently present. Especially when the concentrations of both manganese and iron are high, there is an increased risk that undesirable compounds will form during casting [129]. Furthermore, manganese is one of the least tolerable elements in most aluminium alloys outside the 3000 series [16]. If this fraction would be sorted out separately, it would only be useful for the production of new 3000 series alloys, and even then, the presence of the many alloying elements would impose limits on the use of this material. Therefore, the potential financial benefits of sorting out this fraction seem very limited, especially in the near future.

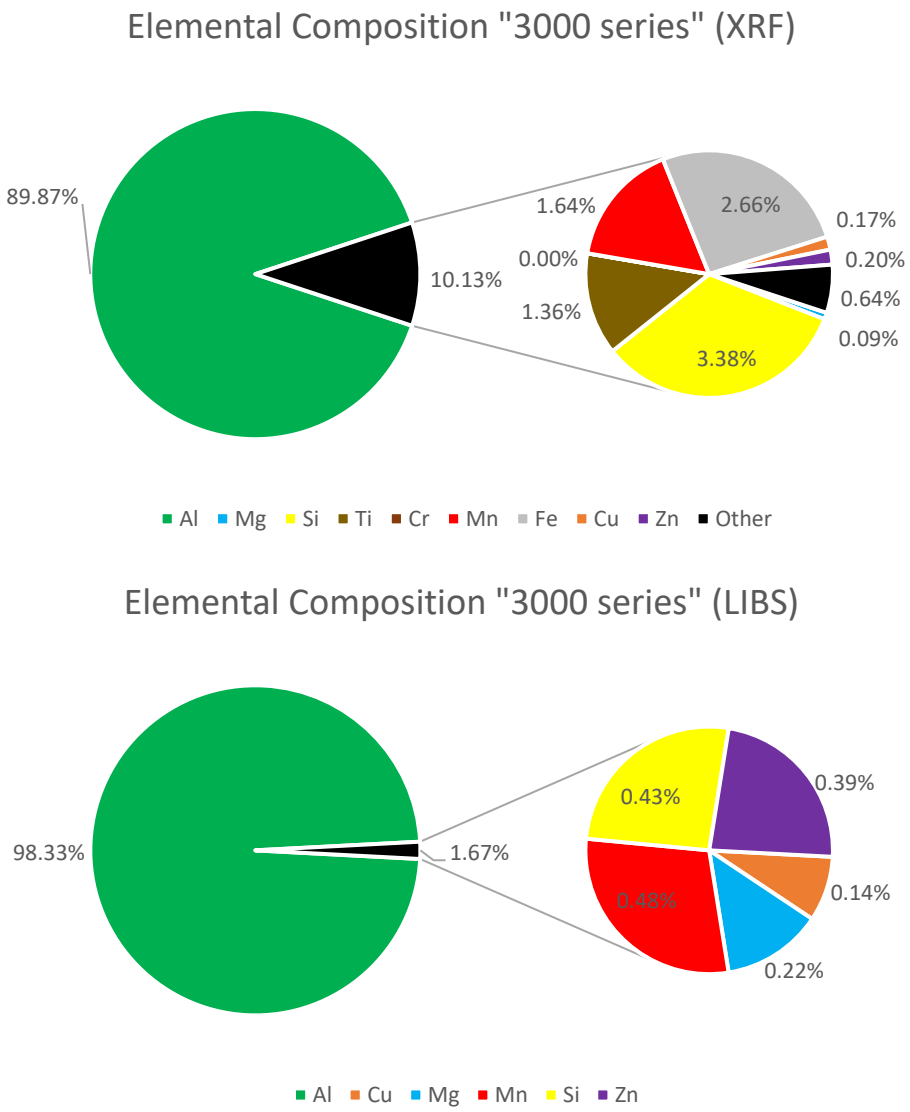

Figure 3.21: Elemental Composition "3000 series" According to XRF and LIBS

The composition of the "5000/6000 series" category, according to the XRF and LIBS measurements, is shown in Figure 3.22. The concentrations of copper and zinc in this fraction are low, at 0,05wt% each, according to the XRF measurement. The LIBS and XRF analyses both indicate that the manganese concentration is around 0,1wt%. The XRF measures quite high amounts of silicon, iron, and titanium but again, the true concentrations of these elements is probably only a fraction of what is indicated. The measured magnesium concentration is also high, even according to the XRF measurement. This makes sense since magnesium is the most important alloying element of the 5000 series and, after silicon, the second most important alloying element of the 6000 series.

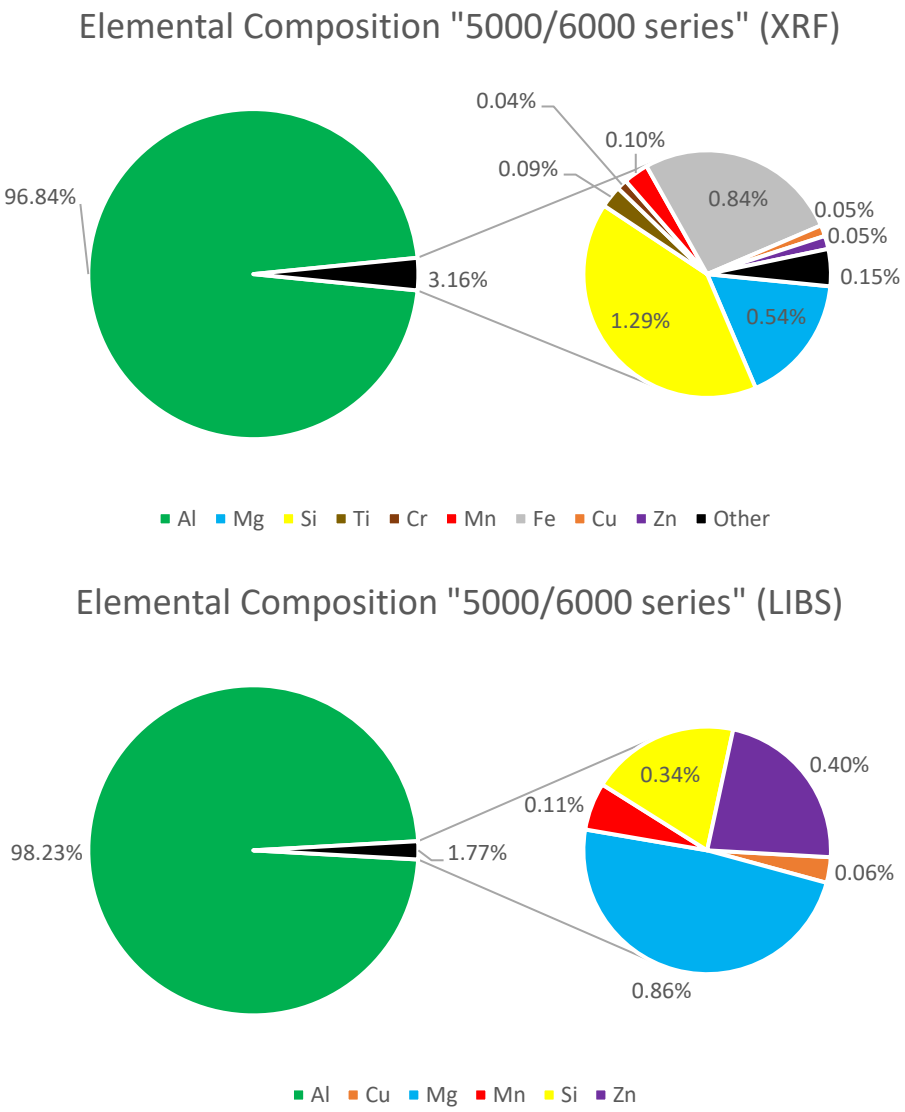

Figure 3.22: Elemental Composition "5000/6000 series" According to XRF and LIBS

Due to the high concentrations of silicon and magnesium, the composition of this fraction is not suitable for the production of most wrought alloys. However, provided that the real concentration of silicon, iron, and titanium is somewhat lower than what is indicated in the XRF measurement, this fraction could be suitable for the production of several popular 6000 series alloys. Table 3.3 shows the tolerance limits of the three most popular 6000 series alloys for the different alloying elements. Next to these numbers is a column with the measured concentrations of the alloying elements in the "5000/6000 series" category. Except for silicon and iron, the concentrations of all major alloying elements in this category are below the upper limits for the three most popular 6000 series alloys. If it can be proven that the real concentrations of silicon, iron, titanium, and other contaminating elements, are in fact much lower than what is indicated by the XRF measurement, this fraction could also become very valuable to separate from the rest of the mixed stream. Since this fraction has a large share (30%) in the total mass of the collected scrap, successfully separating it could yield major financial benefits. A similar scrap mix is not commonly sold today to smelters. However, since almost no dilution would be required to produce 6000 series alloys from aluminium scrap with this composition, it is probable that demand for this material will grow in the future.

Table 3.3: Tolerance Limits Popular 6000 Series Alloys

	6061	6063	6082	5000/6000
Cu	0.4	0.1	0.1	0.05
Fe	0.7	0.35	0.5	0.84
Mg	1.2	0.9	1.2	0.86 (LIBS)
Mn	0.15	0.1	1	0.1
Si	0.8	0.6	1.3	1.29
Zn	0.25	0.1	0.2	0.05
Other	0.15	0.15	0.15	0.28

The "Rest" category is the least pure (see Figure 3.23). Aluminium constitutes only 85% of the total mass of these samples while the silicon concentration is over 10wt%. However, Galloo confirms that the composition of this scrap is still acceptable to be sold for the production of cast alloys at a price of €900 per ton. So, picking out the purest scrap samples does not generate a worthless rest fraction. This is an extremely important assessment for the economic viability of alloy based sorting systems.

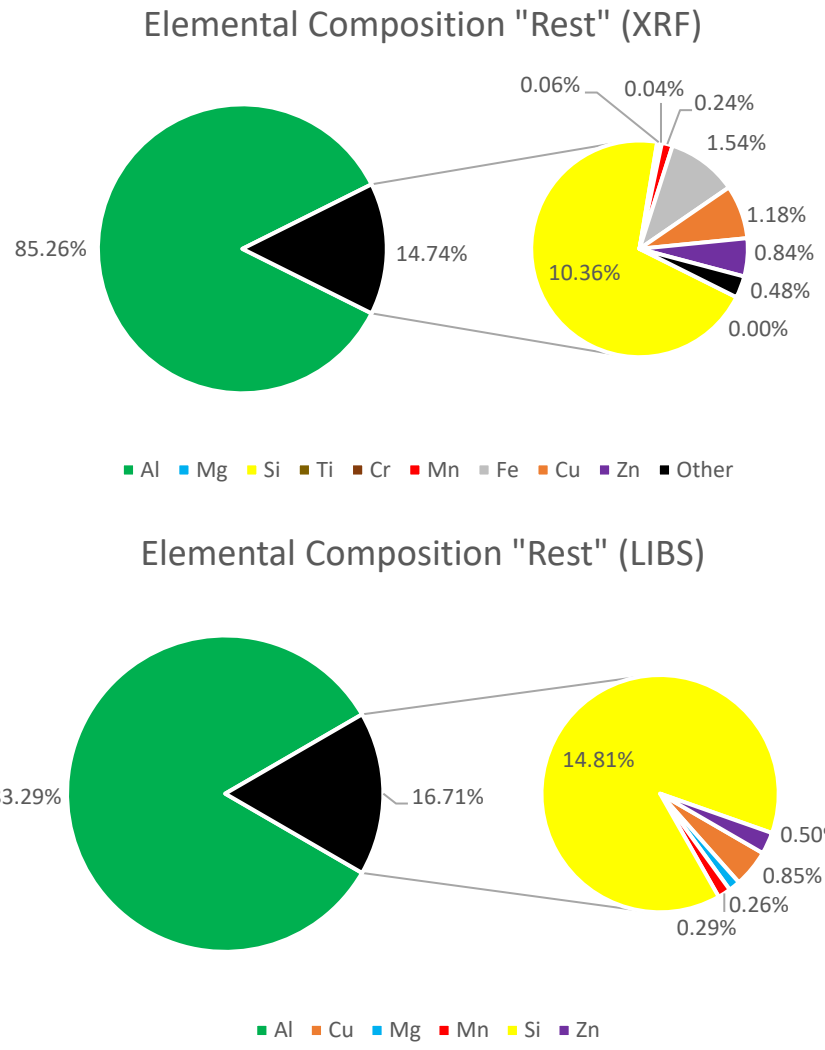

Figure 3.23: Elemental Composition "Rest" According to XRF and LIBS

3.3.6 Sorting Strategies

Based on the composition analysis of the different scrap categories, three sorting strategies seem reasonable. In a first strategy, only the “High purity aluminium” fraction is separated from the rest of the mixed aluminium scrap. Under market conditions similar to those in the early months of 2020, Galloo and other recyclers can immediately sell such fraction at a price of €1200 per ton, while selling the rest of the scrap at a price of €900 per ton. This strategy can be applied immediately once an alloy based sorting system is operational. Demand for “High purity aluminium” and mixed scrap already exist, so it would be easy for Galloo to sell these fractions. The disadvantage of this strategy is that only a limited fraction of the Twitch is valorised at a higher price. Figure 3.24 shows the compositions of the two output fractions of this sorting strategy, when applied to the 275 investigated Twitch samples, according to the XRF measurements.

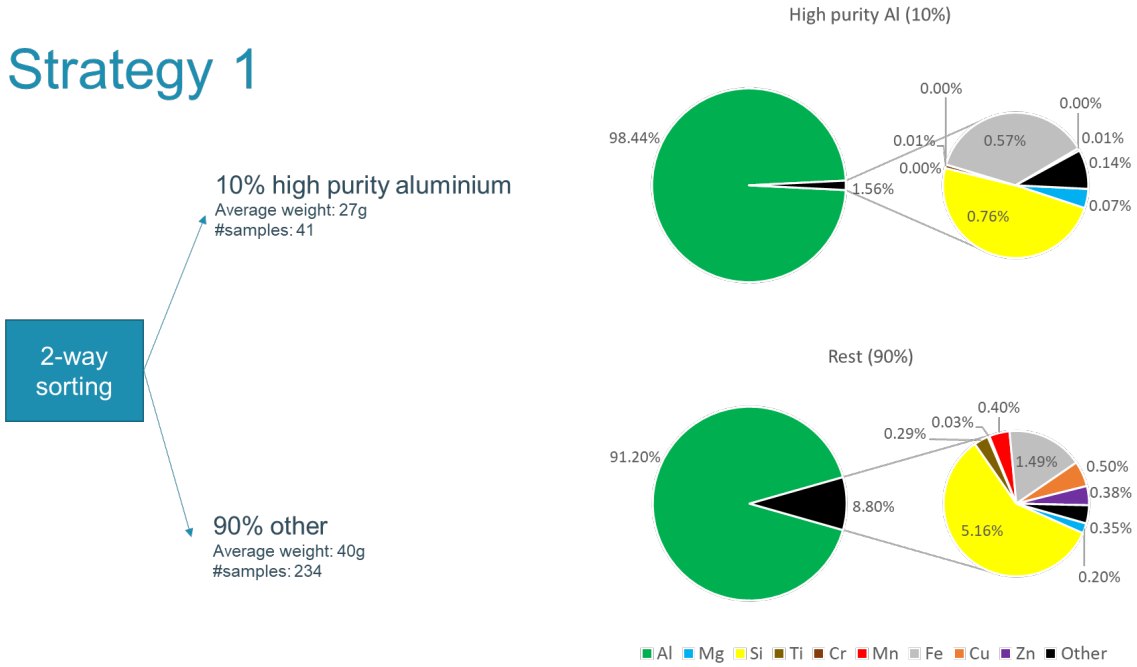

Figure 3.24: Sorting Strategy 1

In the second strategy, the “1000 series” samples separated from the mixed scrap as well, together with the “High purity aluminium” samples. Combining the “High purity aluminium” scrap and “1000 series” scrap gives a fraction that only slightly exceeds the purity limits to sell the scrap at a price of €1200 per ton. The copper concentration of such fraction would be around 0,02wt% and the zinc concentration would be around 0,03wt%. Since scrap can only be sold at a price of €1200 per ton if these concentrations are below 0,02wt%, recyclers should count on a lower price if they want to sell such fraction. The concentrations of manganese and magnesium would stay well below 0,1wt% and 1wt% respectively. While a combination of the two scrap fractions might not sell at an equally high price, the amount of separated scrap would double to 20wt% of the entire Twitch fraction. So, if recyclers can negotiate a price for this scrap that is closer to €1200 per ton than to €900 per ton, this second strategy would be more profitable than the first one. This strategy is illustrated in Figure 3.25.

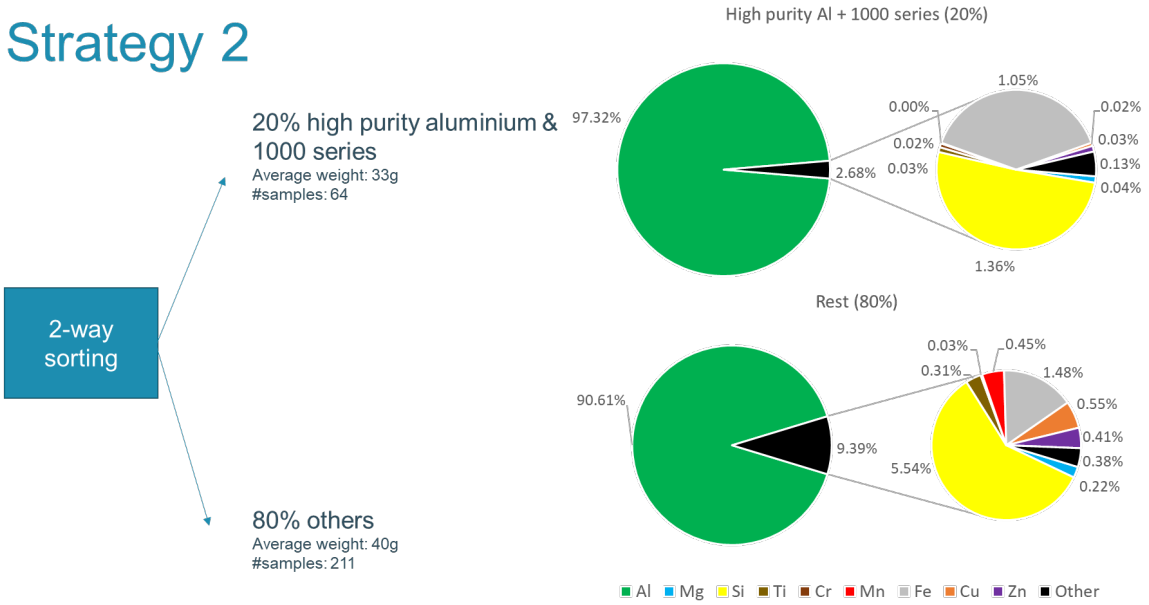

Figure 3.25: Sorting Strategy 2

The third strategy is to apply a three-way sorting system, illustrated in Figure 3.26. A three-way sorting system is more complex than a two-way sorting system. To divide the mixed scrap in three outputs, there are two options. The first one is to send the scrap twice through the sorting system, using different settings during the second run. This way, the mechanical design of the sorting system can be kept relatively simple. However, requiring two runs to sort the scrap significantly reduces the maximum throughput of the sorting system. The alternative option is to design a system that can sort the scrap in three outputs in one run. Having three outputs makes it more challenging to keep the sorting accuracies high. Therefore, adding a third output to the sorting system is only wise if it is worthwhile to separate another part of the scrap. In this strategy, the first output would be a combination of the “High purity aluminium” scrap and the “1000 series” scrap, the second output would be the “5000/6000 series” scrap, and the third output would be the rest of the mixed aluminium scrap. The additional design challenges that come with three-way sorting are justified by the fact that 50% of the scrap would be sorted out in this strategy to be sold at a higher price than the rest of the mixed scrap. This makes this third strategy the most promising one on the long term. However, negotiating a price for the “5000/6000 series” scrap might be even more complicated at first for the recyclers, as there are currently no smelters that pay a higher price for aluminium with such specific composition. This might change when smelters increase their efforts to use recycled aluminium in the production of wrought alloys.

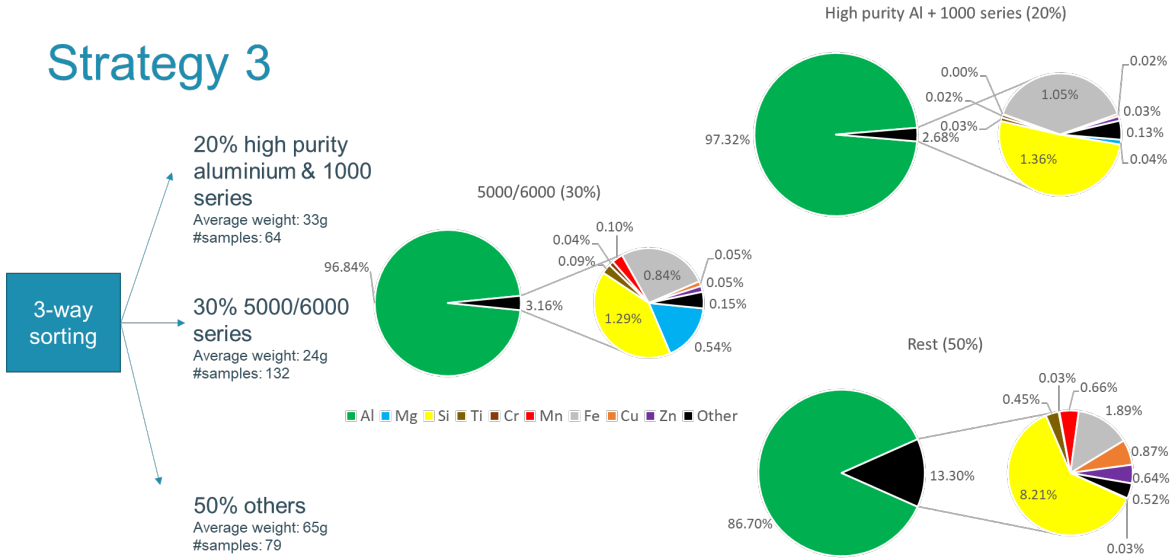

Figure 3.26: Sorting Strategy 3

To estimate what the future financial benefits could be of the different sorting strategies, engineers from the aluminium concern Norsk Hydro are consulted. Norsk Hydro purchases aluminium scrap from recycling companies such as Galloo to produce wrought and cast alloys. Since Norsk Hydro is committed to improving the sustainability of the European aluminium industry, some employees were prepared to support this research. The manager responsible for the purchase of the aluminium scrap that is used for the production of alloys at the Norwegian Holmestrand plant shared his insights on using recycled aluminium for the production of 1000 and 3000 series alloys. An engineer from the Hamburg plant of Norsk Hydro provided information on the use of recycled aluminium for the production of 5000 and 6000 series alloys. While the talks with these experts, and with Galloo, are still ongoing, and will continue after the due date of this thesis, some estimates can already be made about the added value of each sorting strategy based on the provided information.

Under market conditions similar to those in the first months of 2020, a mix of “High purity aluminium” and “1000 series” alloys could probably be sold to smelters at a price of approximately €1150 per ton. This is only slightly below the price of €1200 per ton that smelters are payed in the beginning of 2020 for “High purity aluminium”. Using slightly less pure aluminium requires only small adaptations to the processes of smelters. Therefore, the price difference is quite limited. Producing wrought alloys from “5000/6000 series” scrap would demand larger adaptations from the smelters and therefore the price for this category is somewhat lower. Still, it is estimated that in the near future, scrap with such composition could be sold for approximately €1100 per ton if the aluminium prices return to the levels of the first months of 2020. This is €200 per ton more than the price of mixed aluminium scrap. Table 3.4 shows the yearly total added value of the different sorting strategies, following from the mentioned price differences. The first sorting strategy could yield an added value of 600 000 euro per year for Galloo, the second strategy 1 million euro per year, and the third strategy 2,2 million euro per year. These numbers indicate that the financial benefits of alloy-based sorting could be large, especially when on top of the “high purity aluminium”, also other fractions of the mixed aluminium can be sold separately.

Table 3.4: Added Value Alloy-Based Sorting Strategies

	Str. 1	Str. 2	Str. 3
Price per ton "HPA"	€1200	€1200	€1200
Tons of "HPA"	2000	0	0
Price per ton "HPA + 1000"	€1150	€1150	€1150
Tons of "HPA + 1000"	0	4000	4000
Price per ton "5000/6000"	€1100	€1100	€1100
Tons of "5000/6000"	0	0	6000
Price per ton "Mixed Scrap"	€900	€900	€900
Tons of "Mixed Scrap"	18000	16000	10000
Total Value Twitch	€18,6M	€19M	€20,2M
Total Added Value Twitch	€0,6M	€1M	€2,2M

3.3.7 Effects of Sorting on the Scrap Surplus

The role of 6000 series alloys is crucial in all sorting strategies. In all fractions that could be interesting to separate from the rest of the mixed scrap, there is a relatively high concentration of magnesium. This is even the case for the “High purity aluminium” scrap. This makes the scrap most suitable for the production of 6000 series alloys since these have relatively high tolerances for both magnesium and silicon. High concentrations of magnesium are expected in all collected scrap worldwide, and especially at Galloo, since 5000 and 6000 series alloys are the most popular wrought alloys in the construction and automotive sector.

In particular the 6061, 6082, and 6111 grades can be produced from a typical mix of wrought alloys without requiring large amounts of primary aluminium [16] [111] [132]. To mitigate the growth of the scrap surplus, these 6000 series grades and other “recycle-friendly” wrought alloys should be produced to a larger extent from recycled aluminium. According to the developed MFA model, the current recycled content of the wrought alloy series is around 8,5%. By applying alloy-based sorting methods, this number can be drastically increased.

Figure 3.27 shows how the different sorting strategies can affect the size of the global scrap surplus. The sum of the stacked bars in the chart is equal to the total mass of all the collected scrap in 2030 (for the four bars on the left) and in 2040 (for the four bars on the right). The four bars on each side represent the discussed sorting strategies. The figure shows what would happen if globally, the sorting strategies would be applied in the same way as envisaged for Galloo. This means that the different sorting strategies would be applied to 57% of the collected aluminium scrap (the share of the Twitch fraction in the total amount of incoming aluminium scrap at the Ropswalle site of Galloo). For estimating the effect of the different sorting strategies, it is quite reasonable to extrapolate the results of the measurements, since Figure 3.18 has shown that, according to the developed model, the measured samples closely approximate the composition of all globally collected aluminium scrap.

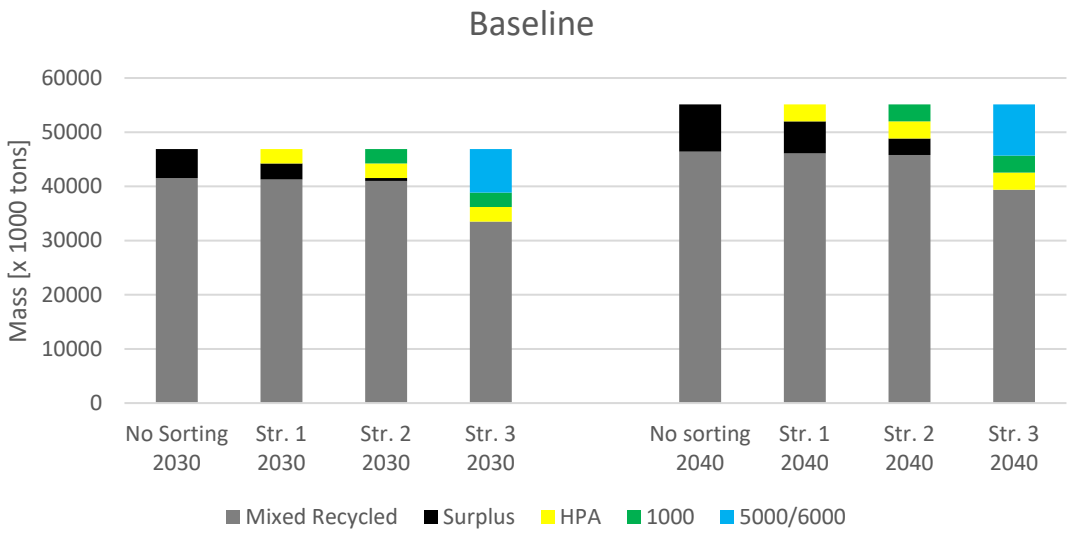

Figure 3.27: Effect of Sorting on the Size of the Scrap Surplus (Baseline Scenario)

In the baseline scenario of the developed model, it would take a three-way sorting approach to eliminate the entire scrap surplus. Applying the other strategies can have a significant impact on the size of the scrap surplus as well, but both in 2030 and 2040, a part of the scrap surplus would remain. Therefore, it is important to not only try to separate “High purity aluminium” (HPA), but other wrought alloys as well.

While calculating the effects of the sorting strategies on the size of the scrap surplus, it is considered that wrought-to-wrought recycling reduces the amount of scrap that can be recycled in the conventional way, by diluting it with primary aluminium, even when the scrap surplus is not entirely eliminated. This is because wrought-to-wrought recycling reduces the demand for conventionally produced wrought alloys. Since the recycled content of conventionally produced wrought alloys does not change in the different sorting strategies, the amount of mixed aluminium scrap that can be recycled declines together with the demand for conventionally produced wrought alloys. Therefore, the coloured bars in Figure 3.27 not only reduce the size of the black bar (the scrap surplus), but also the size of the grey bar, albeit to a lesser extent.

In each strategy, the majority of the collected aluminium scrap keeps being recycled in the conventional way, by diluting with primary aluminium, even though this amount is reduced when more alloys are sorted. As long as the scrap surplus is eliminated, this is not problematic, since recycled aluminium alone cannot meet the total global demand for aluminium. Primary aluminium has to be produced anyway to cover the difference between the total demand for aluminium and the amount of recyclable scrap.

In the best case scenario of the developed model, the first sorting strategy already suffices to eliminate the scrap surplus in 2030 entirely. In 2040, it would be necessary to sort the “1000 series” scrap as well, as can be seen in Figure 3.28.

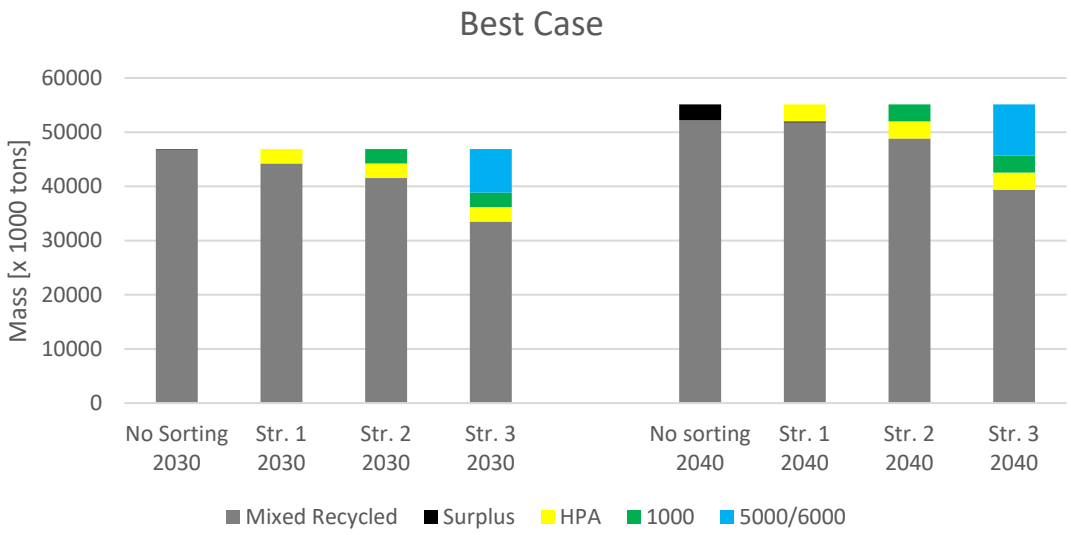

Figure 3.28: Effect of Sorting on the Size of the Scrap Surplus (Best Case Scenario)

In the worst case scenario of the developed model, the three-way sorting strategy is necessary to eliminate the scrap surplus in 2030 (see Figure 3.29). In 2040, a scrap surplus of 22 000 tons would still remain, even when the three-way sorting strategy is applied. On a total of 55 million tons of collected scrap, this is not a large number. However, every kilogram of primary aluminium that has to be produced extra is a burden for the environment.

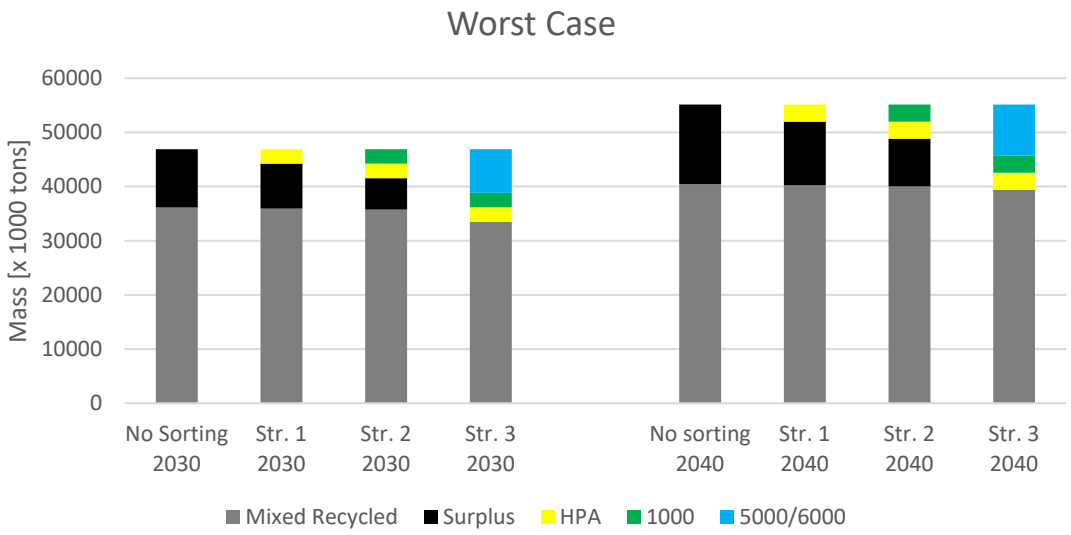

Figure 3.29: Effect of Sorting on the Size of the Scrap Surplus (Worst Case Scenario)

The three previous graphs show how effectively alloy-based sorting can reduce the size of the scrap surplus. The potential of alloy-based sorting can be increased even further, when it is applied to more aluminium scrap fractions. If Galloo would also apply alloy-based sorting on the <40 mm scrap fraction and the magnesium fraction, even more wrought aluminium alloys could be sold separately. When processing scrap from a different origin, it could also be useful to separate 3000 series alloys, or even

2000, 7000, and 8000 series alloys. Therefore, the limited number of strategies presented here are just an illustration of what could be achieved. In the grey bars of the three previous figures, there are still considerable amounts of wrought alloys left that could be separated as well.

While alloy-based sorting methods have a large potential to increase the recycled content in aluminium products, they would need to be implemented rather quickly to ensure that a scrap surplus does not emerge in the coming decade. The European Aluminium Association is optimistic in this sense and expects that the share of recycled aluminium in European end-use products will increase to 39% in 2025 and to 49% in 2050 [14]. The EAA clearly counts on a drastic increase in the recycled content of wrought alloys, as the role of cast alloys diminishes in the future of the aluminium industry. If Europe can achieve the recycling goals of the EAA, it will probably be able to avoid significant scrap surpluses on the continent. In parts of the world where the push for sustainability is less firm, it might take more time to increase the recycled content of wrought alloys if the financial incentives of sorting would remain moderate.

3.4 Conclusion

The results of the XRF and LIBS measurements allow a detailed composition analysis of the collected aluminium scrap samples. However, great care is necessary when interpreting the results of the measurements since the accuracy of both the XRF and LIBS measurements suffers from a couple of issues. For the XRF analysis, the largest issues are the presence of surface contamination and the low limits of the detection for light elements such as aluminium, magnesium, and silicon. For LIBS, the surface contamination is problematic as well. In addition, the quality of the LIBS calibration is not very high. It would be better to calibrate more chemical elements and use more reference samples. Especially for iron, the most common tramp element in aluminium alloys, an accurate calibration is needed to achieve an accurate composition analysis.

Despite these challenges, the measurements allow to assess which alloys are present in a set of scrap samples. Furthermore, the average elemental composition can be calculated for any selection of samples. Based on the composition of the samples, sorting strategies are developed for the Twitch fraction at the Ropswalle site. Separating “High purity aluminium”, “1000 series” alloys, and “5000/6000 series” alloys, seems to be the most promising strategy for Galloo. Globally, most collected aluminium scrap is also magnesium-rich, due to the presence of many 5000/6000 series extrusions from the construction and automotive sector. Therefore, it is expected that similar sorting strategies can be applied in many metal recycling plants worldwide.

Implementing alloy-based sorting techniques can result in an added value of a few hundred euro per ton for recyclers. In addition, it is a very effective way to reduce the size of the scrap surplus. This chapter has shown that the entire global scrap surplus can be eliminated when the right strategies are applied to sort the collected mixed aluminium scrap. Drastically increasing the recycled content of European end-use products, as the EAA ambitions, is therefore possible, if adequate alloy-based sorting systems are widely implemented in existing sorting facilities.

4 Conclusions

Changing the way that aluminium is recycled is beneficial for both economic and environmental reasons. The conventional way of recycling, or “downcycling”, by diluting secondary aluminium with primary aluminium, is coming under pressure due to changes in the global aluminium flows. More aluminium scrap is collected for recycling every year. Meanwhile, transitions in the automotive industry lead to a stagnating or decreasing demand for cast alloys, the most convenient destination for recycled aluminium. Mainly due to these two trends, an aluminium scrap surplus is expected to emerge in the next decade.

According to the MFA model that is developed in this thesis, a scrap surplus will emerge in 2023, grow to a size of 5,4 million tons by 2030 and reach a size of 8,7 million tons by 2040, unless additional measures are taken to enable more wrought-to-wrought recycling. An effective measure to reduce the size of the scrap surplus is to use alloy-based sorting techniques to separate certain wrought alloys from the collected aluminium scrap. At the Ropswalle site of Galloo, applying a three-way sorting strategy to sort the aluminium scrap in the Twitch fraction could allow to separate 10 000 tons of wrought alloys per year. This corresponds to 28,6% of the total 35 000 tons of aluminium scrap that arrive annually at the Ropswalle site. The alloys that would be separated in this strategy would be of the 1000, 5000, and 6000 series. On a global scale, separating such amount of wrought alloys from collected aluminium scrap could allow to eliminate the scrap surplus entirely. Even in the worst case scenario of the developed MFA model, such strategy would eliminate the scrap surplus entirely in 2030 and reduce it to a size of only a few thousand tons in 2040. As such, it is possible to avoid the production of millions of tons of primary aluminium.

The developed MFA model can assist recycling companies in selecting an optimal sorting strategy by estimating the composition of the collected aluminium scrap, based on its origins. Separating wrought alloys from mixed scrap yields a significant added value for recyclers. If the composition of the sorted scrap is suitable for the production of popular wrought alloys, its value can be a few hundred euro higher than that of mixed aluminium scrap. Therefore, selecting the right sorting strategy is crucial. Combining post-shredder sorting with the collection and dismantling of aluminium products at the source of the waste, can make it easier for recyclers to separate large amounts of wrought alloys. For aluminium products such as beverage cans, for which it is technically and economically feasible to collect them separately from other types of waste, closed-loop recycling models should therefore be encouraged.

Since the used LIBS sensor can measure scrap samples at high speeds, while placed several decimetres above the conveyor belt, it seems an appropriate method to be used in on-line sorting applications. In contrast to the XRF sensor, LIBS also has no intrinsic problems to detect light elements such as magnesium and silicon. However, there are still some challenges that need to be overcome in order to design an alloy-based sorting system that is capable of accurately separating the desired alloys. The results in this thesis show that an accurate calibration is necessary for a wide range of elements in order to achieve a satisfying reliability. Furthermore, it is important to find a way to mitigate the effect of surface contamination on the results of the measurements. Otherwise, substances such as ferrosilicon powder can severely compromise the sorting accuracy of the alloy-based sorting system.

5 Future Work

The results of this thesis can and will be used in the future development of a LIBS-based sorting system that can intelligently sort the aluminium scrap of the Twitch fraction at the Ropswalle site of Galloo. For the design of the system, the insights and conclusions of this thesis will be considered. More Twitch samples will be collected and measured with the handheld XRF sensor and the existing LIBS setup at Swerim in order to get an even better view on the composition of the scrap that arrives at Galloo. The conclusions of this thesis can significantly increase the efficiency of this task since the largest difficulties and ways for improving the measuring procedures have been identified.

To clean the collected samples, tests are planned with a waterjet and chemicals. This will speed up the cleaning process and will result in lower amounts of leftover surface contamination. For the LIBS calibration, more reference samples will be obtained. Furthermore, the algorithm to calculate the calibration curves will be significantly improved. Instead of using the maximum values of the intensity peaks, the area under the peaks will be used to establish the relation between the intensities and the mass ratios of the elements. It is expected that this will result in more accurate calibration curves.

A method will be sought to overcome the problem of surface contamination in the on-line sorting application of the LIBS sensor, so that the LIBS analysis can rely upon one or maybe a few spectra, instead of 40 or 100, as in this thesis. This is necessary to achieve a sufficiently high throughput for the sorting system.

In the future, it would also be worthwhile to investigate aluminium scrap from different origins. This thesis has concluded that the composition of the “3000 series” samples is less interesting for recycling. However, when harsher limits are applied to determine what samples are allocated to this category, the composition of this stream might become more valuable. If the silicon and magnesium concentrations in this fraction can be limited, this fraction could become suitable for the production of, for example, the 3004 and 3104 grades. Obtaining such fraction might be difficult from a batch of scrap that originates from the construction and automotive sector, but from scrap from different sources, this might be much more convenient.

The results of the MFA model and the composition analysis of the scrap samples can be used to investigate the environmental and economic benefits of sorting more precisely. In a Life Cycle Analysis (LCA), it is possible to look at the scrap surplus from an ecological perspective. Once it is more clear what smelters would be prepared to pay for the different types of scrap, it would be possible to compare the financial benefits of each suggested sorting strategy, by investigating the sorting system in a Life Cycle Costing (LCC) analysis.

Finally, it would be useful to update and finetune the developed MFA model to provide even more support for recyclers. The methods to calculate the aluminium flows and the ways to visualise them can also be adopted in future research, even for other metals.

Appendix

A. Composition Aluminium Alloys

Table A.0.1: Composition 1000 Series Alloys

	1050		1100		1200		1000	
	Min	Max	Min	Max	Min	Max	Tolerance	Average
Al	99.5	100	99	99.95	99	100		99.34
Cu	0	0.05	0.05	0.2	0	0.05	0.05	0.05
Fe	0	0.4	0	1	0	1	0.4	0.2
Mg	0	0.05	0	0.05	0	0.05	0.05	0.04
Mn	0	0.05	0	0.05	0	0.05	0.05	0.02
Si	0	0.25	0	1	0	1	0.25	0.2
Zn	0	0.05	0	0.1	0	0.1	0.05	0.05
Other	0	0.06	0	0.15	0	0.15	0.06	0.1

Table A.0.2: Composition 2000 Series Alloys

	2014		2024		2025		2000	
	Min	Max	Min	Max	Min	Max	Tolerance	Average
Al	90.4	95	90.7	94.7	90.9	95.2		93
Cu	3.9	5	3.8	4.9	3.9	5	4.9	4.5
Fe	0	0.7	0	0.5	0	1	0.5	0.2
Mg	0.2	0.8	1.2	1.8	0	0.05	0.05	1
Mn	0.4	1.2	0.3	0.9	0.4	1.2	0.9	0.5
Si	0.5	1.2	0	0.5	0	0.5	0.5	0.6
Zn	0	0.25	0	0.25	0	0.25	0.25	0.1
Other	0	0.15	0	0.15	0	0.15	0.15	0.1

Table A.0.3: Composition 3000 Series Alloys

	3004		3000	
	Min	Max	Tolerance	Average
Al	95.6	98.2		96.65
Cu	0	0.25	0.25	0.1
Fe	0	0.7	0.7	0.5
Mg	0.8	1.3	1.3	1.1
Mn	1	1.5	1.5	1.3
Si	0	0.3	0.3	0.15
Zn	0	0.25	0.25	0.1
Other	0	0.15	0.15	0.1

Table A.0.4: Composition 4000 Series Alloys

	4043		4000	
	Min	Max	Tolerance	Average
Al	92.3	95.5		94.29
Cu	0	0.3	0.3	0.1
Fe	0	0.8	0.8	0.2
Mg	0	0.05	0.05	0.03
Mn	0	0.05	0.05	0.03
Si	4.5	6	6	5.2
Zn	0	0.1	0.1	0.05
Other	0	0.15	0.15	0.1

Table A.0.5: Composition 5000 Series Alloys

	5005		5052		5083		5000	
	Min	Max	Min	Max	Min	Max	Tolerance	Average
Al	97	99.5	95.8	97.7	93.5	96		96.2
Cu	0	0.2	0	0.1	0	0.15	0.1	0.05
Fe	0	0.7	0	0.4	0	0.35	0.35	0.2
Mg	0.5	1.1	2.2	2.8	4	5	1.1	3
Mn	0	0.2	0	0.1	0	0.15	0.1	0.1
Si	0	0.3	0	0.25	0	0.4	0.25	0.25
Zn	0	0.25	0	0.1	0	0.25	0.1	0.1
Other	0	0.15	0	0.15	0	0.15	0.15	0.1

Table A.0.6: Composition 6000 Series Alloys

	6061		6063		6082		6000	
	Min	Max	Min	Max	Min	Max	Tolerance	Average
Al	95.9	98.6	97.5	99.4	95.2	98.3		97.2
Cu	0.15	0.4	0	0.1	0	0.1	0.1	0.2
Fe	0	0.7	0	0.35	0	0.5	0.35	0.3
Mg	0.8	1.2	0.45	0.9	0.6	1.2	0.9	1.1
Mn	0	0.15	0	0.1	0.4	1	0.1	0.3
Si	0.4	0.8	0.2	0.6	0.7	1.3	0.6	0.7
Zn	0	0.25	0	0.1	0	0.2	0.1	0.1
Other	0	0.15	0	0.15	0	0.15	0.15	0.1

Table A.0.7: Composition 7000 Series Alloys

	7050		7075		7475		7000	
	Min	Max	Min	Max	Min	Max	Tolerance	Average
Al	87.3	92.1	86.9	91.4	88.6	91.6		89.1
Cu	2	2.6	1.2	2	1.2	1.9	1.9	1.8
Fe	0	0.15	0	0.5	0	0.12	0.12	0.3
Mg	1.9	2.6	2.1	2.9	1.9	2.6	2.6	2.4
Mn	0	0.1	0	0.3	0	0.06	0.06	0.1
Si	0	0.12	0	0.4	0	0.1	0.1	0.1
Zn	5.7	6.7	5.1	6.1	5.1	6.2	6.1	6
Other	0	0.15	0	0.25	0	0.25	0.15	0.2

Table A.0.8: Composition 8000 Series Alloys

	8176		8000	
	Min	Max	Tolerance	Average
Al	98.5	100		98.9
Cu	0	0.05	0.05	0.05
Fe	0.4	1	1	0.7
Mg	0	0.05	0.05	0.05
Mn	0	0.05	0.05	0.05
Si	0.03	0.15	0.15	0.1
Zn	0	0.1	0.1	0.05
Other	0	0.15	0.15	0.1

Table A.0.9: Composition Cast Alloys

	319		356		380		Cast	
	Min	Max	Min	Max	Min	Max	Tolerance	Average
Al	85.8	91.5	90.1	93.3	79.6	89.5		87.7
Cu	3	4	0	0.25	3	4		2.5
Fe	0	1	0	0.6	0	2		0.6
Mg	0	0.1	0.2	0.45	0	0.1		0.3
Mn	0	0.5	0	0.35	0	0.5		0.3
Si	5.5	6.5	6.5	7.5	7.5	9.5		7.1
Zn	0	1	0	0.35	0	3		1.2
Other	0	0.5	0	0.15	0	0.5		0.3

B. Sankey Diagrams for Selected Years Between 1950 and 2040

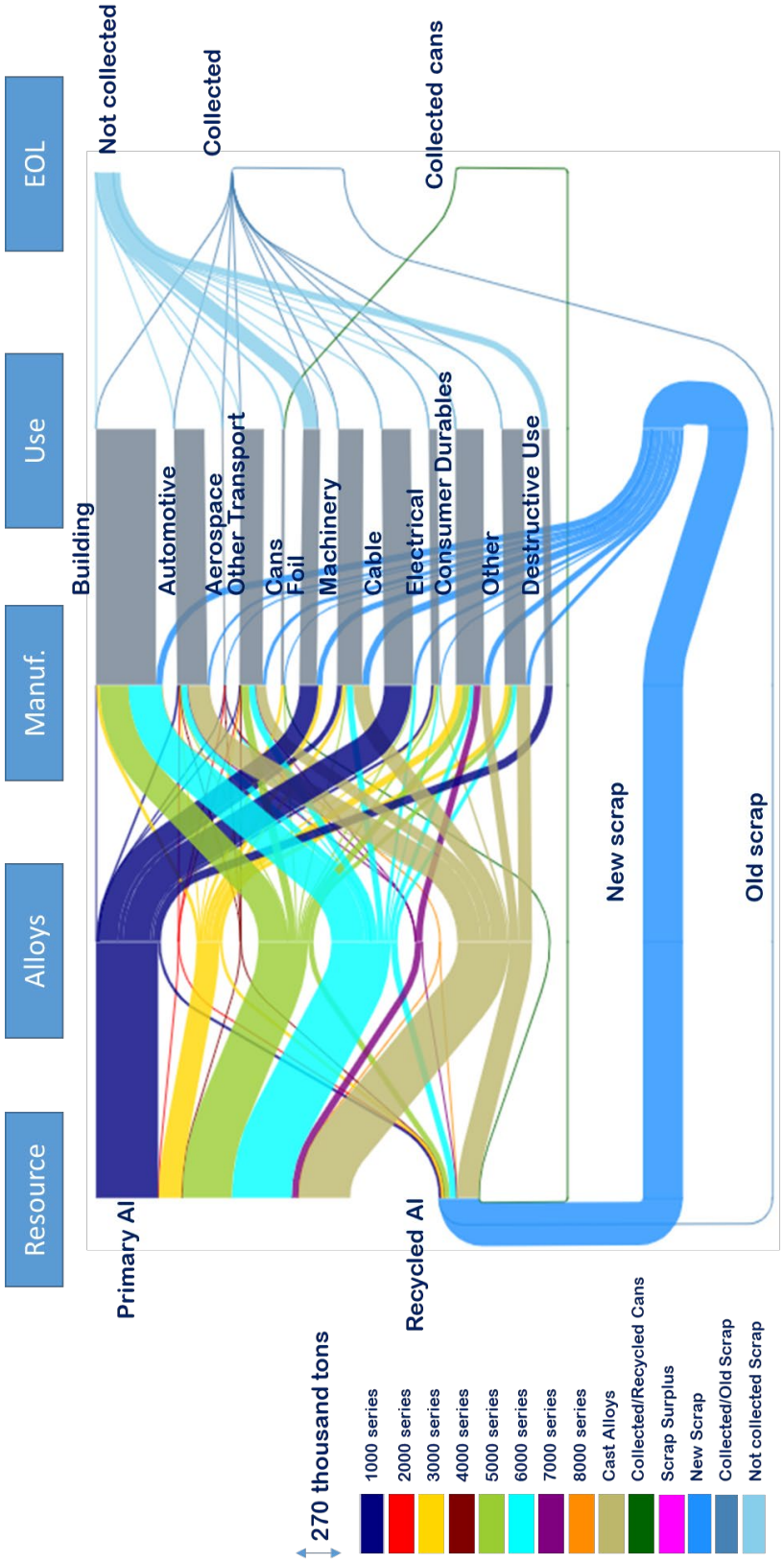

Figure B.0.1: Sankey Diagram for 1951

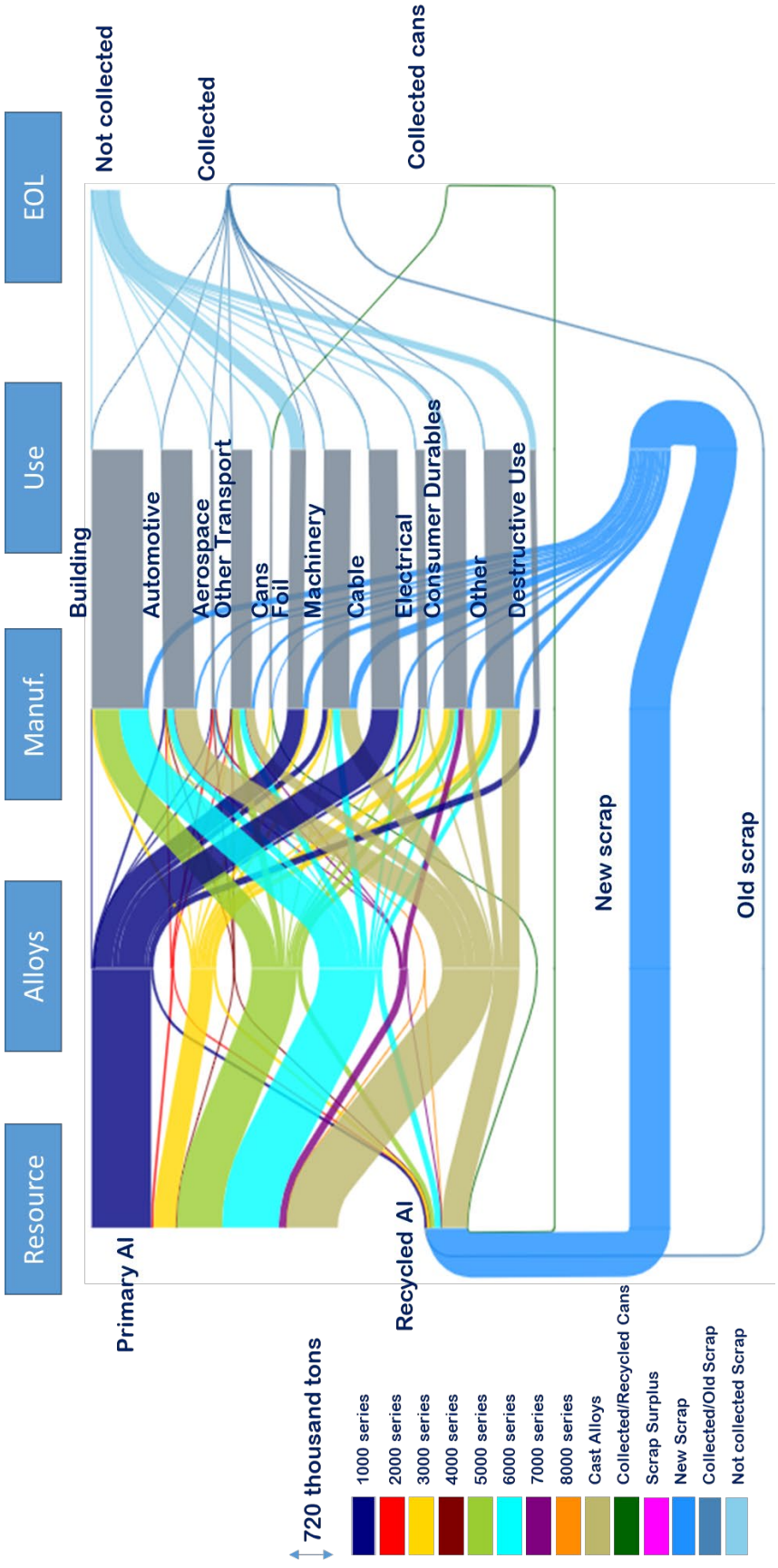

Figure B.0.2: Sankey Diagram for 1960

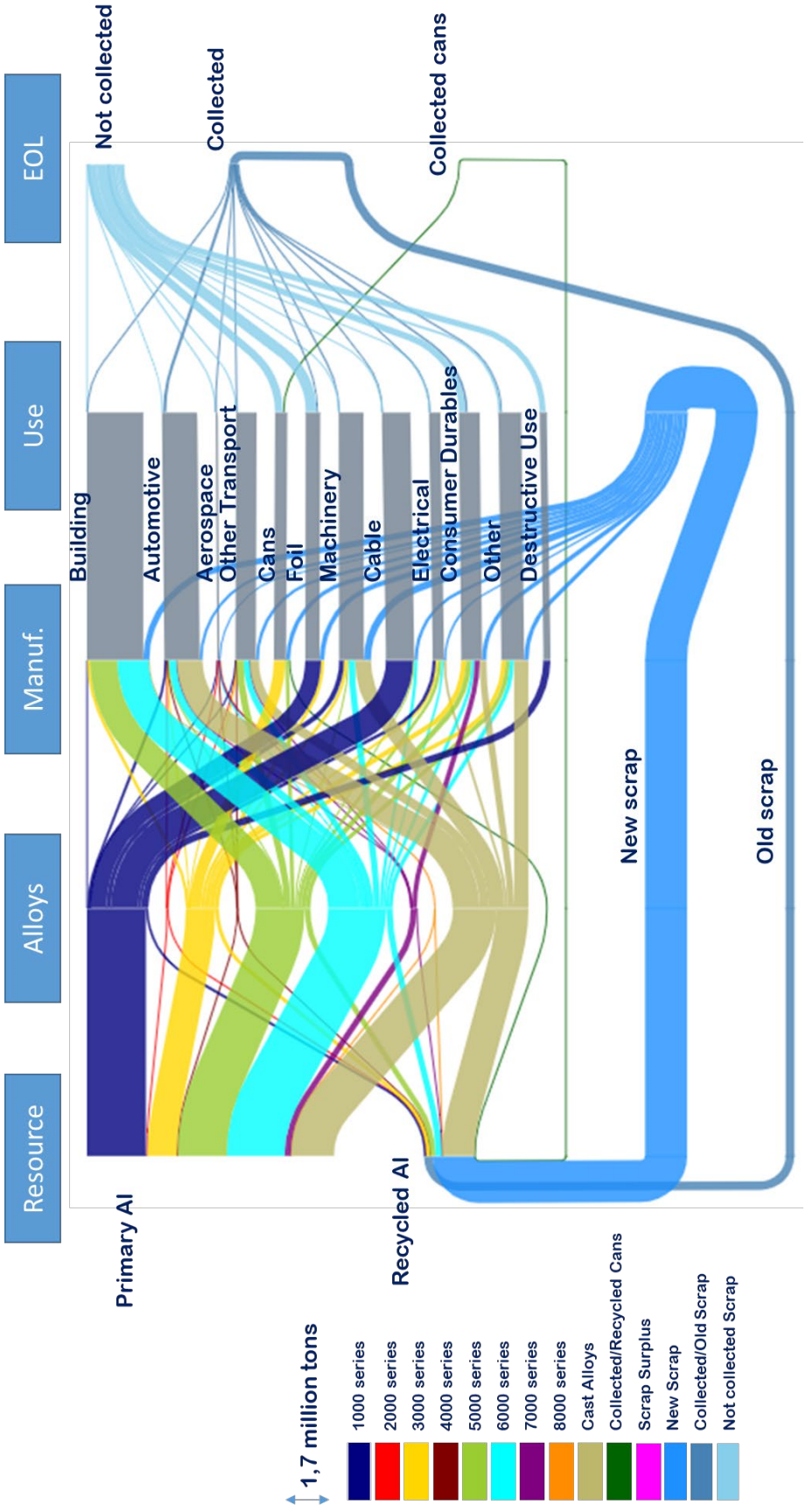

Figure B.0.3: Sankey Diagram for 1970

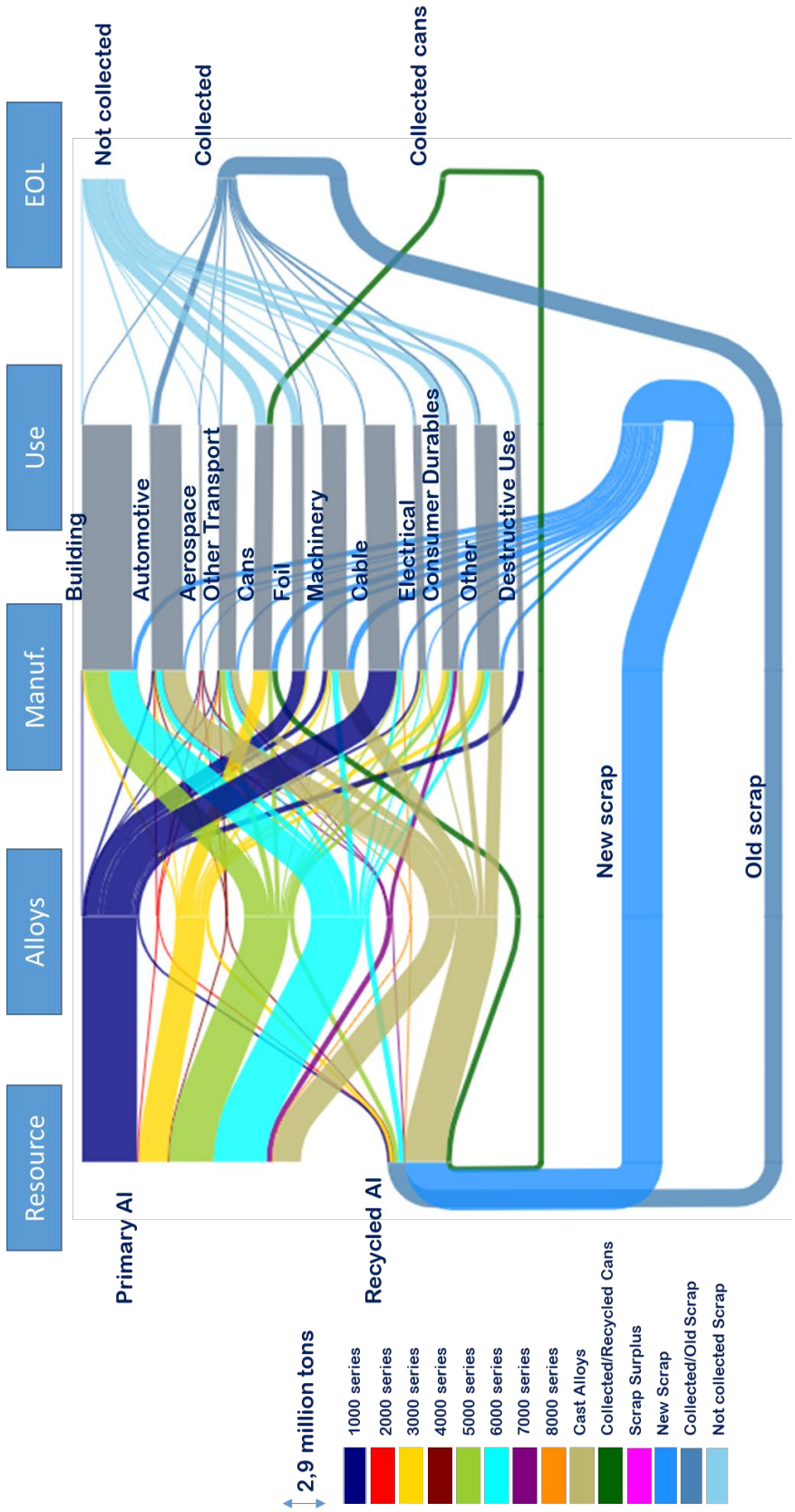

Figure B.0.4: Sankey Diagram for 1980

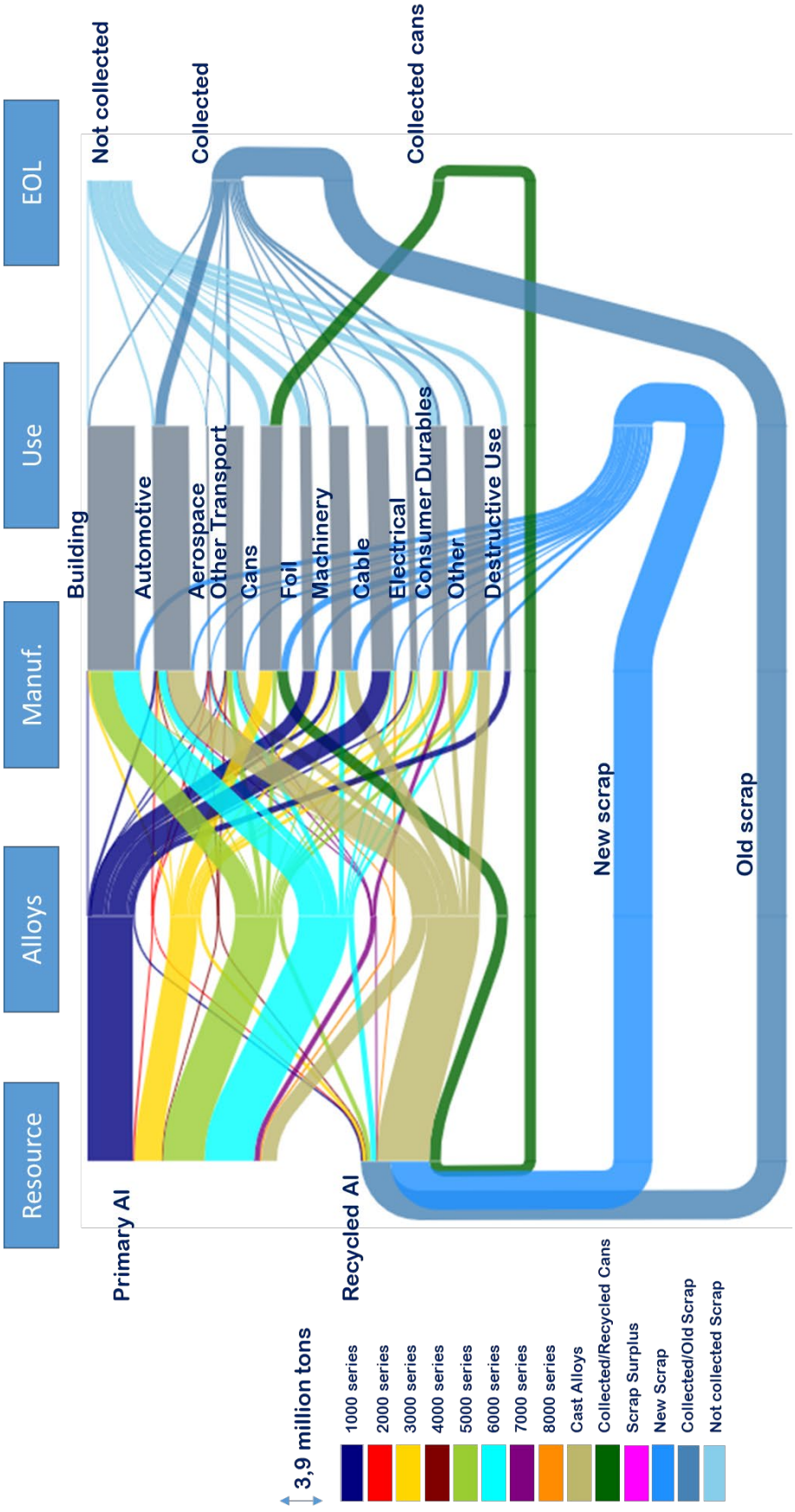

Figure B.0.5: Sankey Diagram for 1990

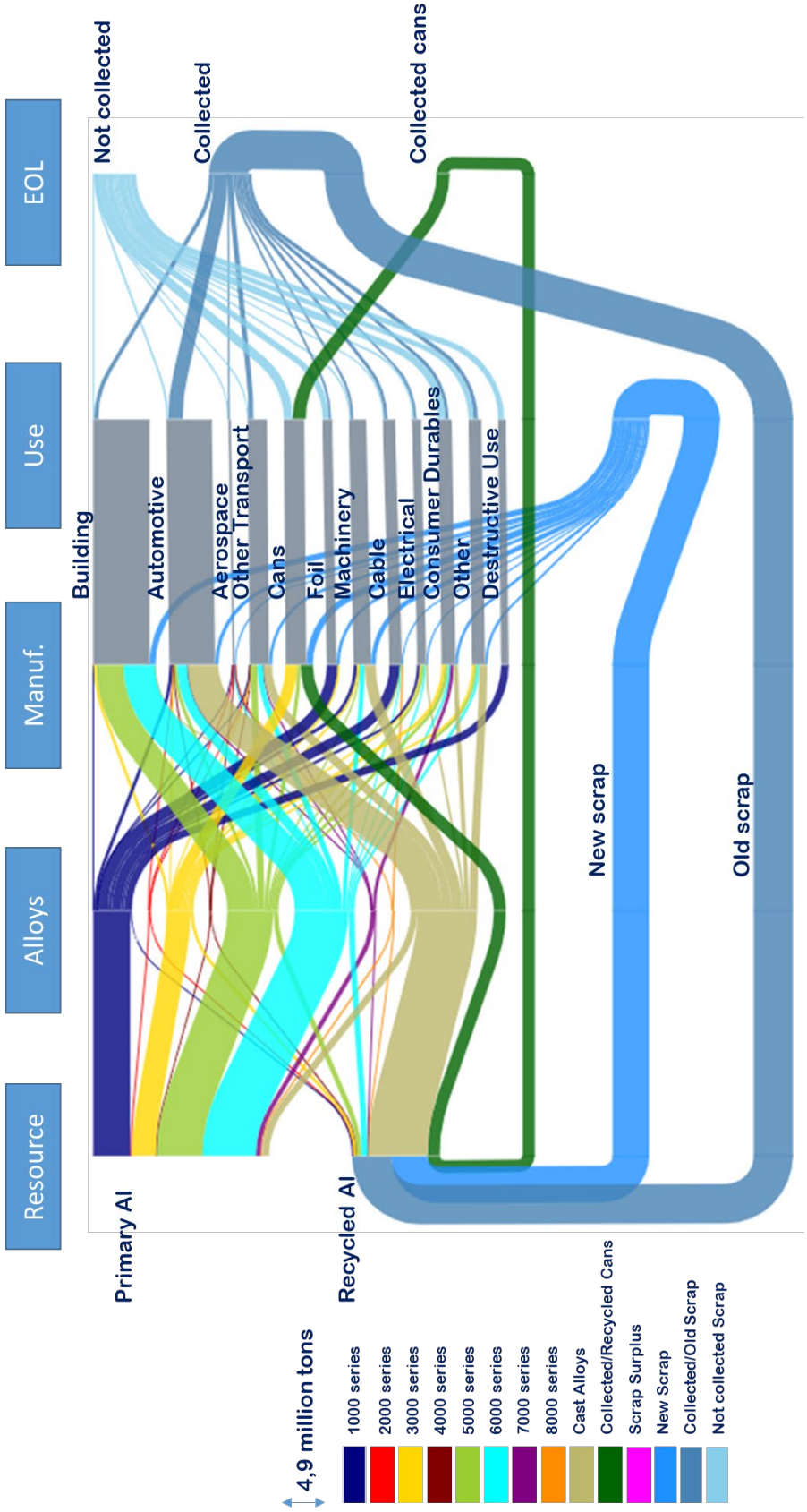

Figure B.0.6: Sankey Diagram for 2000

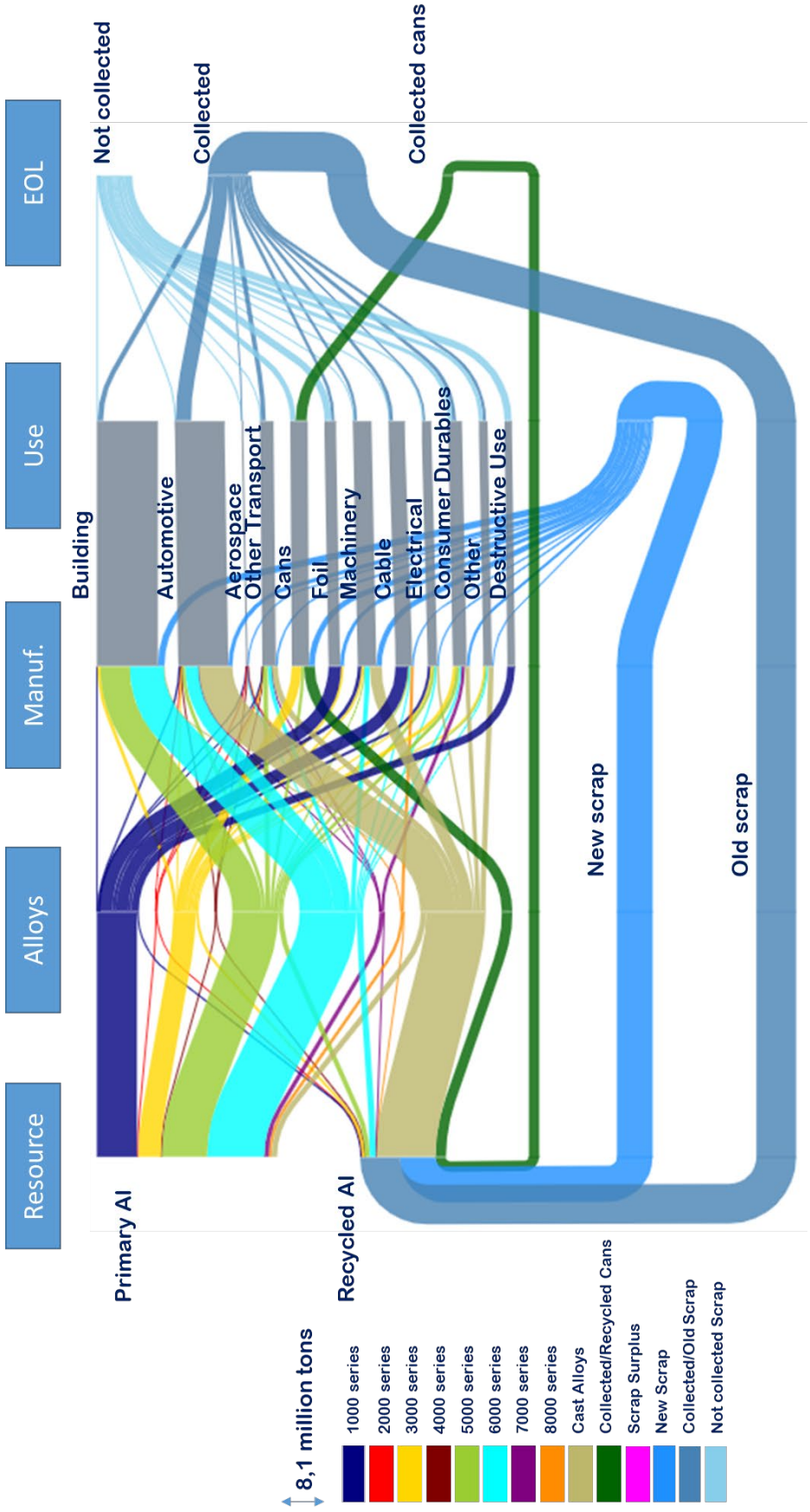

Figure B.0.7: Sankey Diagram for 2010

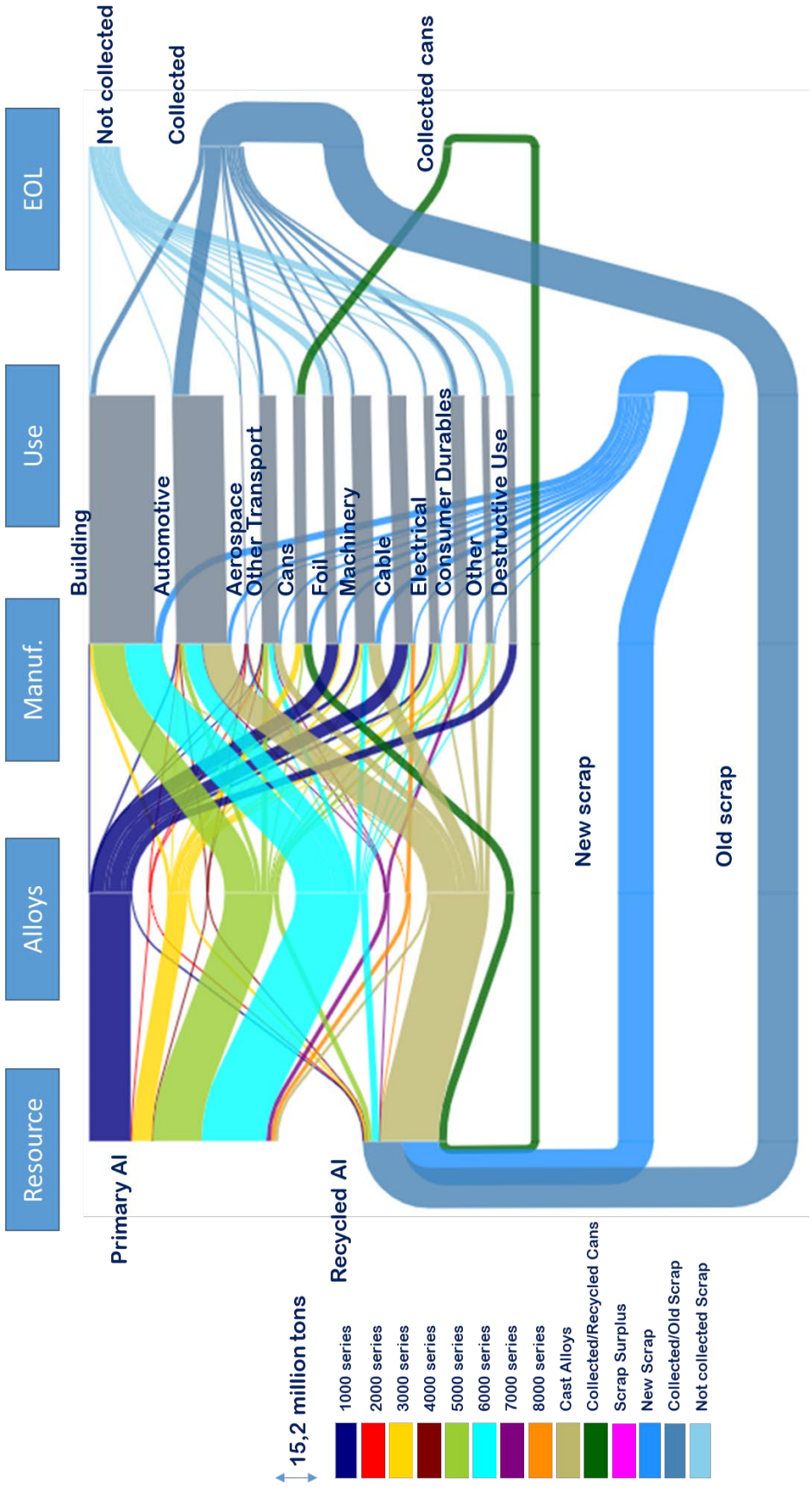

Figure B.0.8: Sankey Diagram for 2020

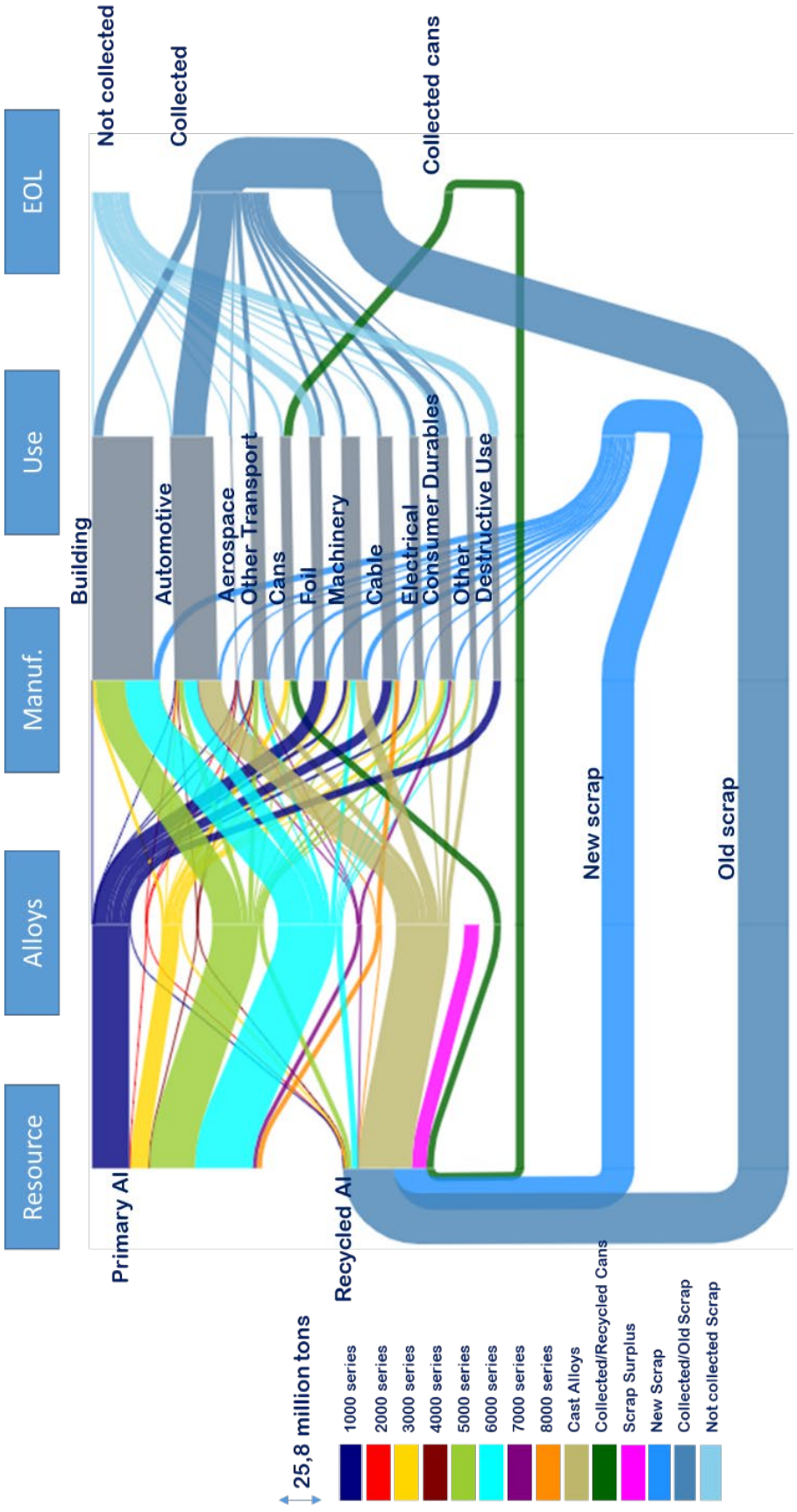

Figure B.0.9: Sankey Diagram for 2040

C. Composition Reference Samples

Table C.0.10 Composition Reference Samples (Concentrations in wt%)

Reference Name	Ref Number	Si	Fe	Mg	Cu	Zn	Mn	Al	Total
Alusuisse 10/525	1	0.185	0.228	2.94	0.0304	0.062	0.28	96	99.7254
Pech. 68453	2	0.36	0.6	1.1	0.07	0.2	0.83	96.5787	99.7387
SS 380 AG-24	3	9.14	1.01	0.2	0.42	3.6	0.41	84.777	99.557
BAM 306	4	8.565	0	0.293	0.887	2.636	0.33	86.565	99.276
O 3:3	5	9.5	0	0.391	0	0.058	0.016	90.021	99.986
NIST 1255a	6	7.22	0.14	0.36	0.084	0.12	0.053	91.809	99.786
4343-AA	7	7.46	0.53	0.036	0.14	0.15	0.1	91.414	99.83
Pech. 1012	8	12.9	0.12	0.52	0.155	0.52	0.286	84.7905	99.2915
Pech. 1010	9	8.75	0.46	1.71	0.029	2	0.056	85.31	98.315
Pech. 68454	10	0.26	0.42	1.26	0.02	0.004	1.16	96.8346	99.9586
Pech. 68451	11	0.07	0.1	0.41	0.18	0.06	1.45	97.6	99.87
Pech. 68452	12	0.16	0.31	0.88	0.1	0.11	1.14	97.15	99.85
J 2:3	13	6.12	0	0.32	0	0.0054	0.016	93.5352	99.9966
160-DO (PT)	14	12.53	0.31	0.025	0.05	0.056	0.033	86.818	99.822
HIT 6063	15	0.53	0.23	0.77	0.031	0.006	0.024	98.3881	99.9791
NBS 1241a	16	0.16	0.2	4.54	0.052	0.05	0.38	94.534	99.916
Pech. 1206	17	3	0.795	0.57	0.154	4.29	0.037	90.464	99.31
SAC 1306-30	18	9.46	1.19	0.39	0.16	3.1	0.26	84.807	99.367
Grängesal 6958-v-336	19	0.53	0.18	3.57	5.06	1.9	0.13	88.21	99.58
Grängesal 6958-v-337	20	0.35	0.27	2.78	5.37	1.6	0.29	89.05	99.71
Gränges al 6958-v-331	21	0.12	0.3	3.04	4.93	1.85	0.06	89.321	99.621
NIST 1255a	22	7.22	0.14	0.36	0.084	0.12	0.053	91.809	99.786
NBS 1258	23	0.78	0.079	0.98	1.03	0.84	0.48	95.8093	99.9983
J 3:3	24	9.19	0	0.339	0	0.0057	0.008	90.4538	99.9965
O 2:3	25	6.16	0	0.363	0	0.006	0.206	93.2574	99.9924
NIST 1259 (PT)	26	0.18	0.205	2.48	5.44	1.6	0.079	89.843	99.827
NBS 1240	28	0.18	0.5	1.11	0.052	0.15	1.26	96.721	99.973
Gränges al 6958-v-335	29	0.18	0.35	2.03	6.08	1.35	0.45	89.39	99.83
								Average	99.71033

Bibliography

[1] United Nations, Department of Economic and Social affairs, Population Division, 'World Population Prospects 2019: Highlights', 2019.

[2] United Nations, 'Paris Agreement', Dec. 2015.

[3] European Commission, 'The European Green Deal', Brussels, COMMUNICATION FROM THE COMMISSION TO THE EUROPEAN PARLIAMENT, THE EUROPEAN COUNCIL, THE COUNCIL, THE EUROPEAN ECONOMIC AND SOCIAL COMMITTEE AND THE COMMITTEE OF THE REGIONS, Dec. 2019.

[4] Jonathan M. Cullen and Julian M. Allwood, 'Mapping the global flow of aluminum: from liquid aluminum to end-use goods.', *Environmental science & technology*, vol. 47, no. 7, pp. 3057–3064, Apr. 2013.

[5] EAA, 'Aluminium in cars - Unlocking the light-weighting potential', Brussels, 2013.

[6] Kathrine Fog, 'Market Outlook', Norsk Hydro, Nov. 2019. [Online]. Available: https://www.hydro.com/Document/Index?name=Market%20outlook%20by%20Senior%20Vice%20President%20and%20Head%20of%20Corporate%20Strategy%20%26%20Analysis%20Kathrine%20Fog&id=7873.

[7] Granta Design Limited, *CES EduPack*. Cambridge, UK, 2009.

[8] Gabrielle Gaustad, Elsa Olivetti, and Randolph Kirchain, 'Improving aluminum recycling: A survey of sorting and impurity removal technologies', *Resources, Conservation and Recycling*, vol. 58, pp. 79–87, 2012.

[9] The Economist, 'The price of virtue', Jun. 07, 2007.

[10] Mark E. Schlesinger, *Aluminum Recycling*, 2nd ed. New York, 2014.

[11] The Aluminum Association, 'Bauxite'. https://www.aluminum.org/industries/production/bauxite (accessed Apr. 22, 2020).

[12] A. J. Gesing, M. A. Gesing, and T. Erdmann, 'Advanced Industrial Technologies for Aluminium Scrap Sorting', Oct. 12, 2010.

[13] International Aluminium Institute, 'World Aluminium — Publications', 2018. http://www.world-aluminium.org/publications/tagged/mass%20flow/ (accessed May 19, 2020).

[14] EAA, 'VISION 2050: European Aluminium's Contribution to the EU's Mid-Century Low-Carbon Roadmap', Brussels, 2019.

[15] Dimos Paraskevas, Karel Kellens, Wim Dewulf, and Joost R. Duflou, 'Environmental modelling of aluminium recycling: a Life Cycle Assessment tool for sustainable metal management', *Journal of Cleaner Production*, vol. 105, pp. 357–370, Oct. 2015.

[16] Roja Modaresi, Amund N. Løvik, and Daniel B. Müller, 'Component- and Alloy-Specific Modeling for Evaluating Aluminum Recycling Strategies for Vehicles', *JOM*, vol. 66, no. 11, pp. 2262–2271, Mar. 2014.

[17] Vi Kie Soo, Jef R. Peeters, Paul Compston, Matthew Doolan, and Joost R. Duflou, 'Economic and Environmental Evaluation of Aluminium Recycling based on a Belgian Case Study', *Procedia Manufacturing*, vol. 33, pp. 639–646, 2019.

[18] Colin A. McMillan, Michael R. Moore, Gregory A. Keoleian, and Jonathan W. Bulkley, 'Quantifying U.S. aluminum in-use stocks and their relationship witheconomic output', *Ecological Economics*, vol. 69, pp. 2606–2613, 2010.

[19] Qiang Yue, He-ming Wang, Zhong-wu Lu, and Sheng-ke Zhi, 'Analysis of anthropogenic aluminum cycle in China', *Transactions of Nonferrous Metals Society of China*, vol. 24, pp. 1134–1144, 2014.

[20] Hiroki Hatayama, Ichiro Daigo, Yasunari Matsuno, and Yoshihiro Adachi, 'Evolution of aluminum recycling initiated by the introduction of next-generation vehicles and scrap sorting technology', *Resources, Conservation and Recycling*, vol. 66, pp. 8–14, 2012.

[21] European Aluminium, 'Aluminium beverage can recycling at 74%!' Jun. 12, 2018, Accessed: Dec. 15, 2019. [Online]. Available: https://www.european-aluminium.eu/media/2275/european-aluminium-press-release-2015canrecyclingresult.pdf.

[22] BloombergNEF, 'Electric Vehicle Outlook 2019', 2019. [Online]. Available: https://about.bnef.com/electric-vehicle-outlook/#toc-viewreport.
[23] Roja Modaresi and Daniel B. Müller, 'The Role of Automobiles for the Future of Aluminum Recycling', vol. 46, pp. 8587–8594, 2012.
[24] Eva Sevigné-Itoiz, Carles M. Gasol, Joan Rierdevall, and Xavier Gabarrell, 'Environmental consequences of recycling aluminum old scrap in aglobal market', *Resources, Conservation and Recycling*, vol. 89, pp. 94–103, 2014.
[25] Jirang Cui and Hans J. Roven, 'Recycling of automotive aluminum', *Transactions of Nonferrous Metals Society of China*, vol. 20, pp. 2057–2063, 2010.
[26] J. Gurell, A. Bengtson, M. Falkenström, and B. A. M. Hansson, 'Laser induced breakdown spectroscopy for fast elemental analysis and sorting ofmetallic scrap pieces using certified reference materials', *Spectrochimica Acta Part B*, vol. 74–75, pp. 46–50, 2012.
[27] Patrick Werheit, Cord Fricke-Begemann, Mark Gesing, and Reinhard Noll, 'Fast single piece identification with a 3D scanning LIBS for aluminium cast and wrought alloys recycling', *Journal of Analytical Atomic Spectroscopy*, vol. 26, no. 11, pp. 2166–2174, Jul. 2011.
[28] B. Campanella *et al.*, 'Classification of wrought aluminum alloys by Artificial Neural Networks evaluation of Laser Induced Breakdown Spectroscopy spectra from aluminum scrap samples', *Spectrochimica Acta Part B: Atomic Spectroscopy*, vol. 134, pp. 52–57, Jun. 2017.
[29] International Aluminium Institute, 'Aluminium in Transport – Recyclable'. http://transport.world-aluminium.org/benefits/recyclable/ (accessed Apr. 23, 2020).
[30] M. Bertram, K.J. Martchek, and G. Rombach, 'Material Flow Analysis in the Aluminium Industry', *Journal of Industrial Ecology*, vol. 13, pp. 650–654, 2009.
[31] P. R. Bruggink and K.J. Martchek, 'Worldwide recycled aluminum supply and environmental impact model', *Light Metals 2004*, 2004.
[32] EAA/OEA (European Aluminium Association), 'Aluminium recycling: The road to high quality products', Brussels, 2008.
[33] International Aluminium Institute, 'Life cycle assessment: Inventory data for the primary aluminium industry', London, 2007.
[34] International Aluminium Institute, 'Sustainability update 2008', London, 2008.
[35] International Aluminium Institute, 'Fourth sustainable bauxite mining report', London, 2009.
[36] M. Bertram *et al.*, 'A regionally-linked, dynamic material flow modelling tool for rolled, extruded and cast aluminium products', *Resources, Conservation and Recycling*, vol. 125, pp. 48–69, 2017.
[37] NTNU, International Aluminium Institute, TruthStudio, and Jason Davies, 'World Aluminium — Mass Flow Statistics'. http://www.world-aluminium.org/statistics/massflow/ (accessed Apr. 06, 2020).
[38] J. Hannula, J. R. A. Godinho, A. Abadías Llamas, S. Luukkanen, and M. A. Reuter, 'Simulation-Based Exergy and LCA Analysis of Aluminum Recycling: Linking Predictive Physical Separation and Re-melting Process Models with Specific Alloy Production', *Journal of Sustainable Metallurgy*, vol. 6, pp. 174–189, Feb. 2020.
[39] F. Passarini, L. Ciacci, P. Nuss, and S. Manfredi, 'Material Flow Analysis of Aluminium, Copper, and Iron in the EU-28', Luxembourg, 2018.
[40] Wei-Qiang Chen and T. E. Graedel, 'Dynamic analysis of aluminum stocks and flows in the United States: 1900-2009', *Ecological Economics*, vol. 81, pp. 92–102, 2012.
[41] Hanno Buchner, David Laner, Helmut Rechberger, and Johann Fellner, 'Potential recycling constraints due to future supply and demand of wrought and cast Al scrap - A closed system perspective on Austria', *Resources, Conservation and Recycling*, vol. 122, pp. 135–142, Jul. 2017.
[42] G. Liu and Daniel B. Müller, 'Mapping the Global Journey of Anthropogenic Aluminium: A Trade-Linked Multilevel Material Flow Analysis', *Environmental science & technology*, vol. 47, pp. 11873–11881, 2013.

[43] Subodh K. Das, John A. S. Green, J. Gilbert Kaufman, Daryoush Emadi, and M. Mahfoud, 'Aluminum Recycling - An integrated, Industrywide Approach', *JOM*, vol. 62, no. 2, pp. 23–26, Feb. 2016.
[44] Julian M. Allwood and Jonathan M. Cullen, *Sustainable Materials with both eyes open*. Cambridge, 2012.
[45] Eugene A. Avallone, Theodore Baumeister III, and Ali M. Sadegh, *Marks' standard handbook for mechanical engineers*, 11th ed. McGraw-Hill Education, 2006.
[46] Hiroki Hatayama, Hiroyuki Yamada, Ichiro Daigo, Yasunari Matsuno, and Yoshihiro Adachi, 'Dynamic Substance Flow Analysis of Aluminum and Its Alloying Elements', *Materials Transactions*, vol. 48, pp. 2518–2524, 2007.
[47] Ducker Worldwide, 'Update on North American Light Vehicle Aluminum Content Compared to the Other Countries and Regions of the World', Troy, Michigan, USA, 2008.
[48] Ducker Worldwide, 'Aluminum in 2012 North American Light Vehicles', Troy, Michigan, USA, 2011.
[49] Ducker Worldwide, 'EAA Aluminium Penetration in Cars 2012', Troy, Michigan, USA, 2012.
[50] Ducker Worldwide, 'Aluminum Content in North American Light Vehicles 2016 to 2028', Troy, Michigan, USA, Summary report, Jul. 2017. Accessed: Apr. 07, 2020. [Online]. Available: http://www.drivealuminum.org/wp-content/uploads/2017/10/Ducker-Public_FINAL.pdf.
[51] N. Eswara Prasad and R. J. H. Wanhill, *Aerospace Materials and Material Technologies: Volume 1: Aerospace Materials*. 2017.
[52] Juraj Belan, Alan Vaško, and Lenka Kuchariková, 'A brief overview and metallography for commonly used materials in aero jet engine construction', *Production Engineering Archives*, vol. 17, pp. 8–13, 2017.
[53] F. C. Campbell, *Manufacturing Technology for Aerospace Structural Materials*, 1st ed. 2006.
[54] Goran Djukanovic, 'Aluminium alloys in shipbuilding - a fast growing trend', Jun. 13, 2016.
[55] Goran Djukanovic, 'Aluminium use in the production of trains steams ahead', Apr. 27, 2017.
[56] R. Padmanabhan, M.C. Oliveira, and L.F. Menezes, *Tailor Welded Blanks for Advanced Manufacturing*. Elsevier, 2011.
[57] Kenichi Nakajima, Osamu Takeda, Takahiro Miki, Kazuyo Matsubae, Shinichiro Nakamura, and Tetsuya Nagasaka, 'Thermodynamic Analysis of Contamination by Alloying Elements in Aluminum Recycling', vol. 44, pp. 5594–5600, 2010.
[58] European Aluminium Association, 'The Aluminium Automotive Manual'. 2015.
[59] 'Products | Southwire Overhead Transmission'. https://overheadtransmission.southwire.com/products/ (accessed Apr. 09, 2020).
[60] 'Aluminium alloys - Lamifil'. https://lamifil.be/products/aluminium-alloys/ (accessed Apr. 09, 2020).
[61] Lamifil, 'Specialty wires'. [Online]. Available: https://lamifil.be/wp-content/uploads/2016/04/04-10-2019-specialities-brochure-lr.pdf.
[62] G. Chen, X. Wang, J. Wang, J. Liu, T. Zhang, and W. Tang, 'Damage investigation of the aged aluminium cable steel reinforced (ACSR) conductors in a high-voltage transmission line', *Engineering Failure Analysis*, vol. 19, pp. 13–21, Jan. 2012.
[63] The Aluminum Association, *Aluminum Electrical Conductor Handbook*, 3rd ed. Washington, DC, 1989.
[64] Christel Hunter, 'Aluminum Building Wire Installation and Terminations', *IAEI NEWS*, p. 8, Jan. 2006.
[65] Yongxian Zhu and Daniel R. Cooper, 'An Optimal Reverse Material Supply Chain for U.S. Aluminum Scrap', *Procedia CIRP*, vol. 80, pp. 677–682, 2019.
[66] George W. Auxier, 'Aluminum and Magnesium: History of the Aluminum and Magnesium Division of the National Production Authority'. Jun. 15, 1953.
[67] Mario Schmidt, 'The Sankey Diagram in Energy and Material Flow Management', *Journal of Industrial Ecology*, vol. 12, 82-94.

[68] Mario Schmidt, 'The Sankey Diagram in Energy and Material Flow Management', *Journal of Industrial Ecology*, vol. 12, pp. 173–185.
[69] Jonathan M. Cullen, Julian M. Allwood, and Margarita D. Bambach, 'Mapping the Global Flow of Steel: From Steelmaking to End-Use Goods', *Environmental science & technology*, vol. 46, pp. 13048–13055, 2012.
[70] Ana Gonzalez Hernandez, Richard Lupton, Chris Williams, and Jonathan M. Cullen, 'From control data to real-time resource maps in a steel-making plant', *Energy Procedia*, vol. 142, pp. 2377–2383, Dec. 2017.
[71] Ana Gonzalez Hernandez, Richard Lupton, Chris Williams, and Jonathan M. Cullen, 'Control data, Sankey diagrams, and exergy: Assessing the resource efficiency of industrial plants', *Applied Energy*, vol. 218, pp. 232–245, May 2018.
[72] Richard Lupton and Jonathan M. Cullen, 'Hybrid Sankey diagrams: Visual analysis of multidimensional data for understanding resource use', *Resources, Conservation and Recycling*, vol. 124, pp. 141–151, Sep. 2017.
[73] Yongxian Zhu, Kyle Syndergaard, and Daniel R. Cooper, 'Mapping the Annual Flow of Steel in the United States', *Environmental science & technology*, vol. 53, pp. 11260–11268, 2019.
[74] T. Takezawa, M. Uemoto, and K. Itoh, 'Combination of X-ray transmission and eddy-current testing for the closed-loop recycling of aluminium alloys', *Journal of Material Cycles and Waste Management*, vol. 17, pp. 84–90, 2015.
[75] MakeItFrom, 'Aluminum Alloys'. https://www.makeitfrom.com/material-group/Aluminum-Alloy (accessed Apr. 30, 2020).
[76] Aircraft Materials, 'Alloy 4043/ Aluminium Welding Alloy 4043'. https://www.aircraftmaterials.com/data/weld/4043.html (accessed Apr. 29, 2020).
[77] Matweb, 'Aluminum 4043-H18'. http://www.matweb.com/search/datasheet_print.aspx?matguid=2541bb0127b34c7294612c77393ead8c (accessed Apr. 29, 2020).
[78] AZO Materials, 'Aluminium Alloys - Aluminium 5083 Properties, Fabrication and Applications'. https://www.azom.com/article.aspx?ArticleID=2804 (accessed Apr. 29, 2020).
[79] AZO Materials, 'Aluminum 8176 Alloy (UNS A98176)'. https://www.azom.com/article.aspx?ArticleID=8788 (accessed Apr. 29, 2020).
[80] The Aluminum Association, 'The Aluminum Can Advantage'. https://www.aluminum.org/aluminum-can-advantage (accessed Apr. 16, 2020).
[81] The Aluminum Association, 'The Aluminum Can Advantage, Key Sustainability Performance Indicators, September 2019', Sep. 2019.
[82] Aluminium Insider, 'Aluminium Can Recycled Content Rises To 73 Percent: Report'. https://aluminiuminsider.com/aluminium-can-recycled-content-rises-to-73-percent-report/ (accessed Apr. 16, 2020).
[83] Abigail Spink, 'Don't bottle it: why aluminium cans may be the answer to the world's plastic problem', *Geograpchical*, Dec. 18, 2019.
[84] Metal Packaging Europe, 'Aluminium beverage can recycling in Europe hits record 74.5% in 2017'. https://www.metalpackagingeurope.org/article/aluminium-beverage-can-recycling-europe-hits-record-745-2017 (accessed Apr. 16, 2020).
[85] International Aluminium Institute, 'Aluminium Recycling – Japan'. http://recycling.world-aluminium.org/regional-reports/japan/ (accessed Apr. 16, 2020).
[86] Associação Brasileira do Alumínio (ABAL), 'Aluminum cans recycling hits new record and Brazil remains as the world leader'. http://abal.org.br/en/noticia/aluminum-cans-recycling-hits-new-record-and-brazil-remains-as-the-world-leader/ (accessed Apr. 16, 2020).
[87] Japan Metal Bulletin, 'Japanese Aluminium Can Recycling Rate Keeps 90% for 3 Years'. http://www.japanmetalbulletin.com/?p=20993 (accessed Apr. 16, 2020).
[88] International Aluminium Institute, 'Aluminium Recycling – Brazil'. http://recycling.world-aluminium.org/regional-reports/brazil/ (accessed Apr. 16, 2020).

[89] EAA, ‘Collection of Aluminium from Buildings in Europe’, Brussels, 2004.
[90] Vi Kie Soo, Jef R. Peeters, Dimos Paraskevas, Paul Compston, Matthew Doolan, and Joost R. Duflou, ‘Sustainable aluminium recycling of end-of-life products: A joining techniques perspective’, *Journal of Cleaner Production*, vol. 178, pp. 119–132, 2018.
[91] Vi Kie Soo, Paul Compston, and Matthew Doolan, ‘The influence of joint technologies on ELV recyclability’, *Waste Management*, vol. 68, pp. 421–433, 2017.
[92] Vi Kie Soo, Jef R. Peeters, Paul Compston, Matthew Doolan, and Joost R. Duflou, ‘Comparative Study of End-of-Life Vehicle Recycling in Australia and Belgium’, *Procedia CIRP*, vol. 61, pp. 269–274, 2017.
[93] Vi Kie Soo, Paul Compston, and Matthew Doolan, ‘Interaction between New Car Design and Recycling Impact on Life Cycle Assessment’, *Procedia CIRP*, vol. 29, pp. 426–431, 2015.
[94] The World Bank, ‘GDP growth (annual %) | Data’. https://data.worldbank.org/indicator/ny.gdp.mktp.kd.zg (accessed Apr. 17, 2020).
[95] Ken Salazar and Marcia K. McNutt, *Minerals Yearbook*, vol. 1. Reston, Virginia, USA: US Department of the Interior, 2010.
[96] M. Classen *et al.*, ‘Life Cycle Inventories of Metals’, Swiss Center for Life Cycle Inventories, Dübendorf, Final report ecoinvent data v2.1 10, 2009. [Online]. Available: www.ecoinvent.ch.
[97] Hiroki Hatayama, Ichiro Daigo, Yasunari Matsuno, and Yoshihiro Adachi, ‘Assessment of Recycling Potential of Aluminium in Japan, the United States, Europe and China’, *Journal Of The Japan Institute Of Metals*, vol. 72, no. 10, pp. 812–818, 2008.
[98] Department of Economic and Social Affairs, ‘World Population in 2300’, United Nations, New York, 2003.
[99] IEA, ‘Scenarios and Strategies to 2050’, *Energy Technology Perspectives 2010*, 2009.
[100] G. Kirchner, ‘The Future of Aluminium Recycling in Europe’, OEA, 2009.
[101] A. J. Gesing, ‘Assuring the Continued Recycling of Light Metals in End-of-Life Vehicles: A Global Perspective’, *Journal of Materials*, vol. 56, no. 8, pp. 18–27, 2004.
[102] Gabrielle Gaustad, Elsa Olivetti, and Randolph Kirchain, ‘Economic and environmental evaluation of various aluminium scrap upgrading options using chance constrained optimization modeling’, presented at the Global symposium on recycling, waste treatment, and clean technology (REWAS), Cancun, Mexico, 2008.
[103] Deepak Malhorta, Patrick R. Taylor, Erik Spiller, and Marc LeVier, *Recent Advances in Mineral Processing Plant Design*. Littleton, Colorado, USA: Society for Mining, Metallurgy & Exploration, 2009.
[104] D. Sauter and D. Theilliol, *Automation in Mining, Mineral and Metal Processing 2004*. Nancy, France: Elsevier, 2004.
[105] Barry A. Wills and James A. Finch, *Wills’ Mineral Processing Technology*, 8th ed. Elsevier, 2016.
[106] Stefano Capuzzi and Giulio Timelli, ‘Preparation and Melting of Scrap in Aluminium Recycling: A Review’, *Metals*, vol. 8, 2018.
[107] M.B. Mesina, T.P.R. de Jong, and W.L. Dalmijn, ‘Automatic sorting of scrap metals with a combined electromagnetic and dual energy X-ray transmission sensor’, *International Journal of Mineral Processing*, vol. 82, pp. 222–232, 2007.
[108] K. Tsuchiya *et al.*, ‘Establishment of aluminium “Sash to Sash” Recycling by using XRT and XRF Sorters’, presented at the 11th International Conference on Mining, Materials and Petroleum Engineering, Chiang Mai, Thailand, Nov. 2013.
[109] S.J. Neethling and J.J. Cilliers, ‘Grade-recovery curves: A new approach for analysis of and predicting from plant data’, *Minerals Engineering*, vol. 36–38, pp. 105–110.
[110] David V. Bubenick and Charles N. Faulstich Jr., ‘Evaluation of an Automated Sorting Process for Post-Consumer Mixed Plastic Containers’, EPA, Washington, DC, Sep. 1993.
[111] A. J. Gesing and R. Wolanski, ‘Recycling Light Metals from End-of-Life Vehicles’, *Journal of Materials*, vol. 53, no. 11, pp. 21–23, 2001.

[112] P. B. Schultz and R. K. Wyss, 'Color Sorting Aluminium Alloy Scrap for Recycling', *Plating and Surface Finishing*, vol. 87, pp. 62–65, 2000.
[113] Boyd R. Davis, Amjad Javaid, and E. Essadiqi, 'Final Report on Scrap Management, Sorting and Classification of Aluminum'. Dec. 2003.
[114] Adam Minter, 'Where America Recycles', *The Atlantic*, Dec. 2008.
[115] Olympus, 'Scrap Recycling with XRF – Sort More, Sort Faster, and Increase Your Profits'. https://www.olympus-ims.com/en/applications/scrap-recycling-xrf-sort/ (accessed May 02, 2020).
[116] David B. Spencer, 'The High-Speed Identification and Sorting of Nonferrous Scrap', *Journal of Materials*, vol. 57, no. 4, pp. 46–51, Apr. 2005.
[117] Thermo Fisher Scientific - BE, 'PGNAA and PFTNA Technology'. https://www.thermofisher.com/be/en/home/industrial/cement-coal-minerals/cement-coal-minerals-learning-center/cement-analysis-production-information/pgnaa-pftna-technology.html (accessed May 03, 2020).
[118] Salvador Guirado, Francisco J. Fortes, Luisa M. Cabalín, and Javier J. Laserna, 'Effect of Pulse Duration in Multi-Pulse Excitation of Silicon in Laser-Induced Breakdown Spectroscopy (LIBS)', *Applied Spectroscopy*, vol. 68, no. 9, pp. 1060–1066, Sep. 2014.
[119] A. Kramida, Y. Ralchenko, J. Reader, and NIST ASD Team, 'NIST Atomic Spectra Database (version 5.7.1)'. 2019, Accessed: May 04, 2020. [Online]. Available: https://physics.nist.gov/asd.
[120] Tristan O. Nagy, Ulrich Pacher, Hannes Pöhl, and Wolfgang Kautek, 'Atomic Emission Stratigraphy by Laser-Induced Plasma Spectroscopy: Quantitative Depth Profiling of Metal Thin Film Systems', *Applied Surface Science*, vol. 302, pp. 189–193, 2014.
[121] J. A. Aguilera and C. Aragón, 'Characterization of a laser-induced plasma by spatially resolved spectroscopy of neutral atom and ion emissions. Comparison of local and spatially integrated measurements', *Spectrochimica Acta Part B*, vol. 59, pp. 1861–1876, 2004.
[122] Cécile Fabre and Bernard Lathuilière, 'Relationships between growth-bands and paleoenvironmental proxies Sr/Ca and Mg/Ca in hypercalcified sponge: A micro-laser induced breakdown spectroscopy approach', *Spectrochimica Acta Part B*, vol. 62, pp. 1537–1545, 2007.
[123] Fatemeh Rezaei, *Plasma Science and Technology - Progress in Physical States and Chemical Reactions*. 2016.
[124] M. Burger, M. Skočić, and S. Bukvić, 'Study of self-absorption in laser induced breakdown spectroscopy', *Spectrochimica Acta Part B*, vol. 101, pp. 51–56, 2014.
[125] R. Yi, L. Guo, X. Yang, J. Li, X. Zeng, and Y. Lu, 'Investigation of the self-absorption effect using spatially resolved laser-induced breakdown spectroscopy', *Journal of Analytical Atomic Spectroscopy*, vol. 31, no. 4, pp. 961–967, 2016.
[126] Sathish K. Konidala, Govindarao Kamala, and Sravani Koralla, 'Laser Induced Breakdown Spectroscopy', *Research Journal of Pharmacy and Technology*, vol. 9, no. 1, pp. 91–100, Jan. 2016.
[127] Thermo Fisher Scientific - BE, 'Specification Sheet: Niton XL2 Plus XRF Analyzer'. https://www.thermofisher.com/document-connect/document-connect.html?url=https%3A%2F%2Fassets.thermofisher.com%2FTFS-Assets%2FCAD%2FDatasheets%2Fniton-xl2-plus-specification-sheet.pdf&title=U3BlY2lmaWNhdGlvbiBTaGVldDogTml0b24gWEwyIFBsdXMgWFJGIEFuYWx5emVy (accessed May 22, 2020).
[128] S. Anas Boussaa, A. Kheloufi, N. Boutarek Zaourar, and S. Bouachma, 'Iron and Aluminium Removal from Algerian Silica Sand by Acid Leaching', *Acta Physica Polonica A*, vol. 132, pp. 1082–1086, 2017.
[129] Joseph R. Davis, *Alloying: Understanding the Basics*. ASM International, 2001.
[130] Aaiysha F. Khursheed, 'Automobiles and Light-Duty Trucks: Industry Profile', EPA, NC, USA, Dec. 2000.

[131] Clarence H. Lorig and Holger Gruner, ‘Mineral processing’, *Encyclopaedia Britannica*. https://www.britannica.com/technology/mineral-processing/Dewatering (accessed May 23, 2020).
[132] Subodh K. Das, ‘Aluminum Recycling in a Carbon Constrained World: Observations and Opportunities’, *JOM*, vol. 63, no. 8, pp. 137–140, Aug. 2011.